FACIES AND DIAGENESIS OF THE UPPER DEVONIAN PALLISER FORMATION, FRONT RANGES OF THE SOUTHERN ROCKY MOUNTAINS, ALBERTA AND BRITISH COLUMBIA

by

DONALD CHARLES KAYLOR

Department of Geological Sciences
McGill University, Montréal

April, 1988

A thesis submitted to
the Faculty of Graduate Studies and Research
in partial fulfillment of the requirements
for the degree of
Master of Science.

DIAGENESIS OF THE PALLISER FORMATION, SOUTHERN CANADIAN ROCKIES

SHORT TITLE:

DIAGENESIS OF THE PALLISER FORMATION,

SOUTHERN CANADIAN ROCKIES

ABSTRACT

The Famennian Palliser Formation is a thick carbonate ramp unit dominantly composed of subtidal mudstones and wackestones, with lesser peloidal grainstones. The percentage of micritic lithotypes increases westward.

Three main types of dolomites are recognized. (1) Early planar dolomites fill burrows and replace micrite, have heavier oxygen and carbon isotopes, higher Ca/Mg ratios and dull, uniform cathodoluminescence. They likely precipitated as protodolomites in a shallow, subtidal marine environment, and underwent neomorphism during shallow burial diagenesis. Nonplanar dolomites (2 & 3) formed after microstylolitization. They have lighter carbon isotopes, generally lighter but variable oxygen isotopes, lower Ca/Mg ratios, and variable cathodoluminescence. (2) Replacive nonplanar dolomites pervasively replaced limestones as shown by relict (ghost) fabrics. (3) White sparry nonplanar dolomites precipitated in secondary voids and fractures in dolostones. Replacive nonplanar dolostones formed during deep burial diagenesis and uplift, with white sparry dolomites occurring simultaneously or soon after. White sparry dolomites also occur in primary and secondary voids in limestones, but their timing not known. Stylolitization occurred both before and after nonplanar dolomitization.

Sulfide mineralization occurs in nonplanar dolostones at the Munroe-Alpine-Boivin section, B.C. and the Oldman River section, Alberta. Sulfides are syn- to post-replacive nonplanar dolomite and syn- to pre-white sparry dolomite.

RÉSUMÉ

La Formation Palliser d'âge Famennien est une unité épaisse de plate-forme à carbonates principalement composée de mudstones et wackes soustidals, et de quelques grainstones peloïdes. Le pourcentage de lithotypes micritiques augmente vers l'ouest.

Trois principaux types de dolomites ont été reconnus. (1) Des dolomites précoces planes remplissent des terriers et remplacent la micrite, ont des isotopes de l'oxygène et du carbone relativement lourds, des proportions Ca/Mg relativement élévées, ainsi qu'une cathodoluminescence terne et uniforme. Les dolomites non-planes (2 & 3) se sont formées aprés la micro-stylolitisation. Elles ont des isotopes du carbone plus légers, des niveaux d'isotope de l'oxygène variables mais généralement plus légers, des proportions Ca/Mg plus basses ainsi qu'une cathodoluminescence variable. (2) Les dolomites non-planes de replacement ont remplacé les calcaires de façon envahissante comme le montre les fabriques de relique (fantômes). (3) Des dolomites non-planes, blanches et cristallines ont précipité dans les cavités et fractures secondaires des dolomies. Les dolomites non-planes de remplacement se sont formées durant la diagénèse d'enfouissement profond et de remontée, alors que les dolomites cristallines blanches sont apparues simultanément ou tôt après.

Les dolomites cristallines blanches se retrouvent aussi dans les cavités primaires et secondaires des calcaires, mais leur temps de formation est inconnu. La stylolitisation est apparue à la fois avant et après la dolomitisation non-plane.

Une minéralisation en sulfures se retrouve dans les dolomies non-planaires de la section Munroe-Alpine-Boivin (C.-B.) et à la section Oldman River en Alberta. Les sulfures sont syn- à post-dolomite non-plane de remplacement et syn- à pré-dolomite cristalline blanche.

TABLE OF CONTENTS

LIST of FIGURES

LIST of TABLES

LIST of PLATES

ACKNOWLEDGEMENTS

I wish to express my appreciation for the patience and understanding displayed by my thesis supervisor, Dr. Eric Mountjoy. His guidance, knowledge, and criticisms greatly improved this thesis. Many ideas followed up during the course of this study originated with Prof. Mountjoy, as his detailed and varied background in Rocky Mountain geology was invaluable.

Esso Minerals Canada, which provided financial and technical support for two field seasons (1984 and 1985), plus additional expenses, is gratefully acknowledged. Dr. John A. McDonald and George de Mille were particularly helpful during the initial phases of this study. Guido diLeandro supplied samples collected by Esso field parties.

The staff of the Institute of Sedimentary and Petroleum Geology (G.S.C.) in Calgary, especially Dr. Helmut Geldsetzer, was very helpful, providing desk space, field equipment, and scientific guidance.

Dr. Colin Stearn of McGill provided helpful suggestions and identified the stromatoporoids. Dr. Tim Marchant of Amoco Canada Petroleum Company identified 'The Lone Foram'. Other suggestions and information came from Bill Styan and Dr. Les Eliuk, both of Shell Canada Resources Ltd. and Dr. Frank Stoakes of Stoakes-Campbell Geoconsulting Ltd. Richard Yates of McGill was extremely helpful with all matters concerning drafting and photography, especially plate preparation. Dr. K.C. Lohmann and David Dettman of the University of Michigan ran the stable isotope analyses. Tariq Ahmedali of McGill provided technical advice and supervised the x-ray fluorescence analyses. Keith Mountjoy gave able assistance in the Rockies during the summer of 1985.

Gordon Gibson of Vancouver supplied the author with samples and descriptive notes from the Munroe-Alpine-Boivin zinc occurrences which he mapped as part of his M.Sc. thesis at the University of British Columbia. This aided in the early focussing of this study.

Fellow students proved to be excellent sounding boards (boreds?) for innumerable ideas, some workable, some not, as well as providing invaluable moral support and fun times at T.H. and the O.D.! Special thanks go to my office-mates, Roland Dechesne and Daniel Lebel (Dan expertly translated the abstract into French). I also appreciate the help given by Andre Chow, Ed Dalton, Manda Halim-Dihardja, Carl Hughson, Hans Machel, Jeanne Paquette, and Qing Hairuo.

McGill University and the Department of Geological Sciences are acknowledged for financial support provided through teaching assistantships (4), the Carl Reinhardt Award (1986) and the M.H. Beatty Award (1986). The Canadian Society of Petroleum Geologists is thanked for the Petroleum Geology Graduate Scholarship granted to the author in 1985. Additional funds came from the National Sciences and Engineering Research Council grant #A2128 to E.W. Mountjoy and from the 'carbonate research fund'. Alberta Recreation and Parks personnel permitted me to camp and collect in their beautiful mountain parks.

Most importantly, I wish to thank my wife, Ida Delli Colli, for her love and compassion (and proof-reading). She has made my work, and my life, more rewarding.

CONTRIBUTIONS TO ORIGINAL KNOWLEDGE

The occurrence of several types of dolomites in the Palliser Formation has not been reported previously. These distinct populations were delineated using petrographic observations and stables isotopes. Beales (1953) discussed only the dolomitic mottling and did not described the various dolomite textures. However, the early marine origin for early planar dolomite is essentially similar to that proposed by Beales (1953). Recent developments in the study of modern and ancient dolomites have been included to confirm Beales' (1953) proposals.

Ch. 1 INTRODUCTION

1.1 PURPOSE

The name for the Palliser Formation was derived from the Palliser Range, which was, in turn, named after Captain John Palliser (1807-1887), an Irish geographer and explorer who led the Palliser British North American Expedition in Canada's west from 1857 to 1860 (Spry 1963).

The Famennian Palliser Formation is an extensive, thick carbonate unit exposed in the Front and Main Ranges of the Canadian Rocky Mountains (Plate 1a) from which a peculiar colour and texture mottling has long been noted (Plate 1c). One main aim of this study is to explain the occurrence of this fabric. In the subsurface, Palliser equivalents locally contain commercial quantities of hydrocarbons and sulphur. In addition, there have been several base metal occurrences reported from Palliser outcrops in Alberta and British Columbia. Despite the economic potential of this unit, relatively few detailed studies have been done on the Palliser Formation (see 1.3).

Initiated jointly by Esso Minerals Canada and the Geological Survey of Canada, this study describes several major, recurring lithofacies common to many Palliser field sections in the southern Canadian Front Ranges. Rare, but potentially economically important lithofacies, e.g., stromatoporoid boundstones, are also detailed. The depositional environments are inferred from the rock fabrics and relationships.

Diagenesis, universally recognized as a major process in shaping the fabric of rock units, has been studied in detail, especially the multiple stages of dolomitization, including dolomitic mottling, that were recognized locally. These stages are especially important in relation to hydrocarbon accumulations (e.g., see Halim-Dihardja 1986) and base metal mineralization. The different phases of dolomitization are described, and possible origins are discussed. A generalized paragenetic sequence for the Palliser Formation, based on petrographic and field observations, and geochemical analyses, is presented.

1.2 METHODS of STUDY

The field areas for this project were located in the Front Ranges of the Canadian Rocky Mountains (Figures 1 and 2). All field work was carried out during the summers of 1984 and 1985. In addition to notes and samples collected during these field seasons, Esso Minerals Canada provided over 500 thin sections collected by their field parties from twenty-three sections (see Appendix Three). The author visited six of these twenty-three sections, as well as four additional sections (#24, 25, 26, and 27, Figure 2). The Munroe-Alpine-Boivin section (#24) was examined to augment data from notes and samples provided by Gordon Gibson of Vancouver.

Approximately one hundred and ninety 75×50 mm thin sections were cut for facies and diagenetic study. Geochemical methods (see 3.4 and Appendix Two) included staining thin sections with mixtures of alizarin red-S and potassium ferricyanide, x-ray fluorescence, and carbon and oxygen isotope analyses. Study of thin sections using cathodoluminescence revealed many 'hidden' characteristics of diagenetic phases, such as growth banding or patchy distribution (qualitatively) of minor and trace elements.

Plate 1

<u>General field aspects</u>

a. Hummingbird Creek section (#27). Larger arrow at horizon of stromatoporoid mounds. Smaller arrow at Morro/Costigan contact. Overlying units are Mississippian <M>.

b. Closer view of the Morro<M>/Costigan<C> contact, showing approximately 5 m of section, Hummingbird Creek (#27). 210 m above base of Palliser Formation.

c. Two-dimensional view of burrow-mottling. Bedding-plane surface above lens cap, cross-section below. Morro Member, Loder Peak (#02). 10 m above base. 5 cm lens cap.


M
a
C
M
b
c

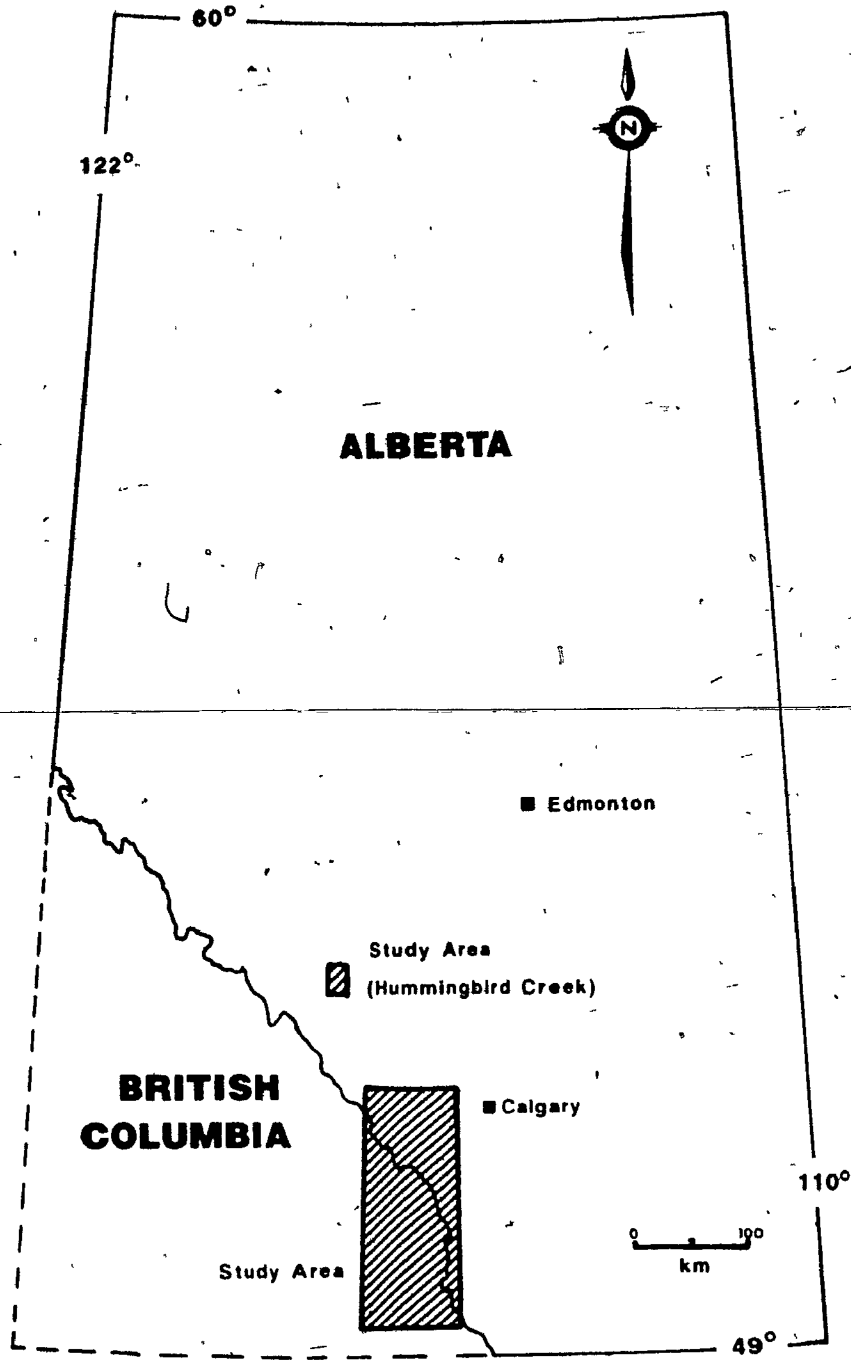

Figure 1: Study areas, Alberta and British Columbia

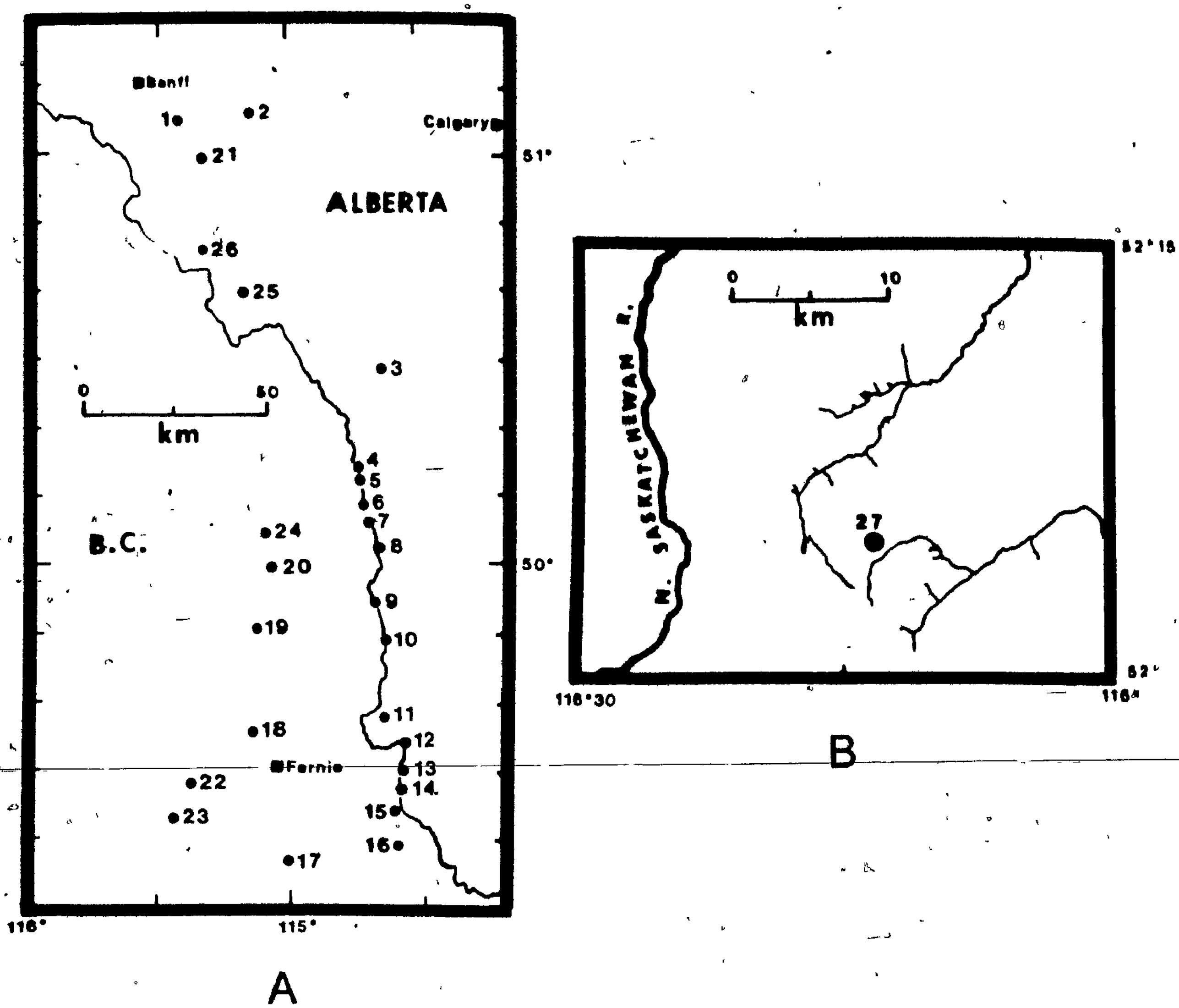

Figure 2: Detail of the study areas shown in Figure 1. For precise locations of sections, see Appendix Three.

01 WHITEMAN GAP
02 LODER PEAK
03 MT. HEAD
04 MT. FARQUHAR
05 LOST CREEK
06 OLDMAN RIVER
07 MT. LYALL
08 CACHE CREEK
09 MT. ERRIS
10 RACEHORSE
11 CROWSNEST PASS
12 MT. COULTHARD
13 PEECHEE
14 MT. DARRAH
15 MT. BORSATO
16 FLATHEAD
17 CHINA WALL
18 THREE SISTERS
19 MT. FRAYN
20 PHILLIPS PEAK
21 SPRAY LAKES
22 BULL RIVER
23 WARDNER
24 MUNROE-ALPINE-BOIVIN
25 MT. INDEFATIGABLE
26 MT. MURRAY
27 HUMMINGBIRD CREEK

1.3 PREVIOUS STUDIES

Stratigraphic sections of the Palliser Formation have been measured and briefly described in numerous early field studies, especially by the Geological Survey of Canada (e.g., Beach 1943; de Wit and McLaren 1950; Fox 1951, 1954; and McLaren 1955). Beach (1943) first proposed the name Palliser Formation for the carbonates overlying the Fairholme Group and underlying the Exshaw Formation in the Bow Valley area of Alberta. De Wit and McLaren (1950) divided the Palliser into a lower Morro Member, a thick-bedded, mottled and micritic sequence of limestones and dolomite, and the upper, thinner-bedded Costigan Member which is less mottled, more argillaceous, and more fossiliferous.

Fox (1951, 1954) related a personal communication from R. de Wit in which the dolomitic mottling is ascribed to pre-lithification percolation of fluids through more permeable "algal colonies". Beales (1953) modified and expanded upon this idea. The mottling was, in part, suggested to be due to the presence of "worm tubes" (or burrows). Sea water influx during early diagenesis along permeable pathways was suggested to be the agent of dolomitization.

Beales (1954, 1956) described, in some detail, the facies occurring in the Palliser. A close correlation between Palliser rocks and the Recent Bahamian calcareous sands was suggested.

Maurin (1972, 1982) briefly described the small stromatoporoid-mud buildups in the Palliser Formation at Hummingbird Creek. Holter (1977) described the Oldman River lead-zinc occurrence in southwestern Alberta. Geldsetzer (1982) has described the Palliser from the mountain areas north of Jasper National Park. Styan (1984) provided a description and interpretation for a Palliser section at Jura Creek, Alberta.

N.E. B.C.	N.W. Alta. & B.C.	N. Central Alta.	Mountain Outcrops	S. Central Alta.	S. Alta. & W. Sask.
Besa River Fm.	Exshaw Fm.	Exshaw Fm.	Exshaw Fm.	Exshaw Fm.	Exshaw / Bakken Fm.
	WABAMUN Grp.	WABAMUN Grp.	PALLISER Fm.	WABAMUN Grp.	WABAMUN Grp.
	Kotcho Fm.	Big Valley Fm.	Costigan Mem.	Big Valley Fm.	Three Forks Fm.
	Tetcho Fm.	Stettler Fm.	Morro Mem.	Stettler Fm.	Potlach Fm.
	Trout River Fm.	Graminia Fm.	Sassenach Fm./ U. Alexo Fm.	Graminia Fm.	Crowfoot Fm.

Figure 3: Simplified stratigraphy and nomenclature for the Famennian and parts of the Frasnian and Tournaisian stages, Western Canada Sedimentary Basin. Modified from Styan (1984).

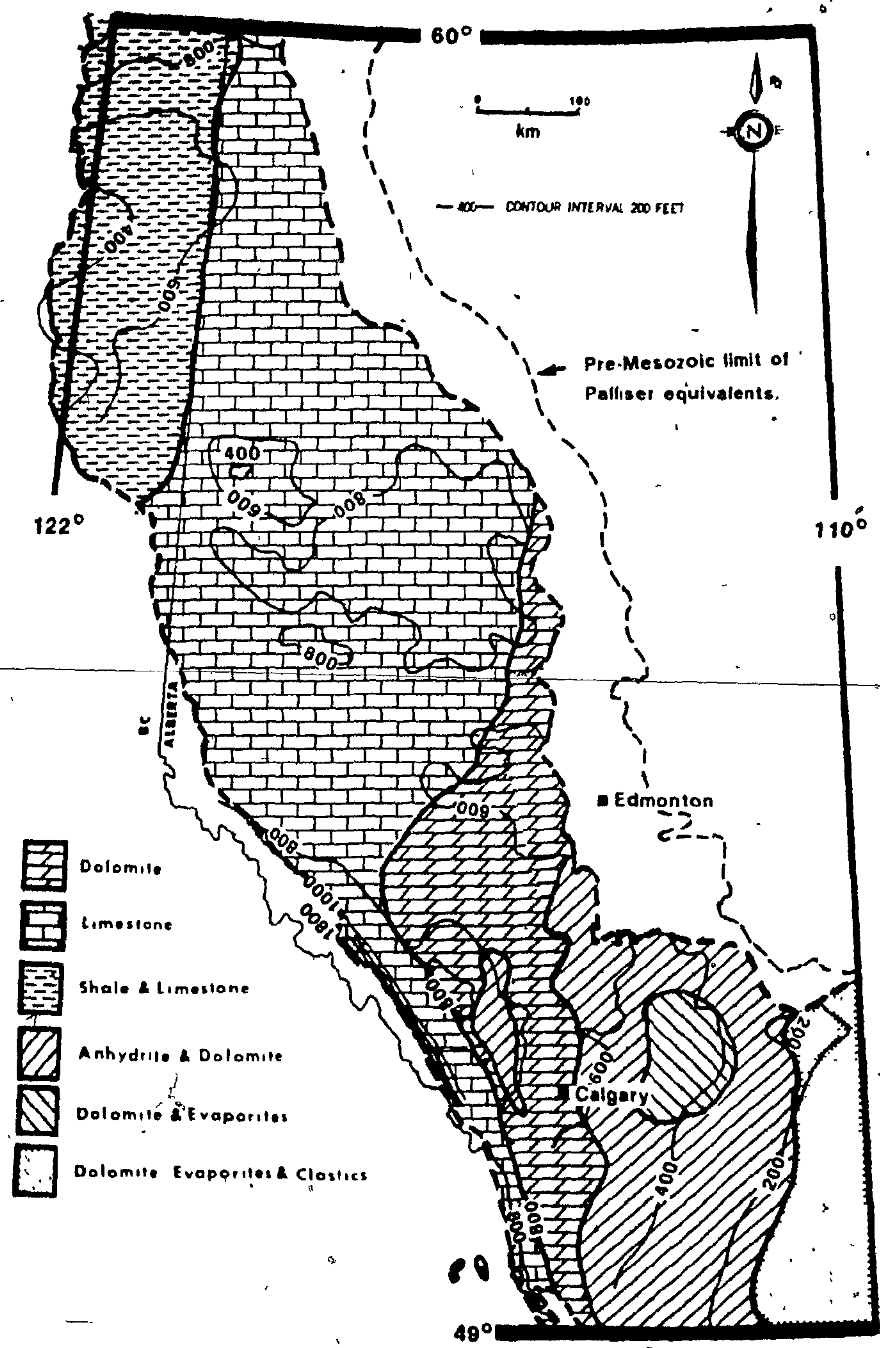

Figure 4: Isopach and lithofacies distribution of the Palliser Formation and its equivalents. Modified from Belyea (1964).

There are several studies on the Wabamun Group (Figure 3), the subsurface equivalent of the Palliser Formation; Wonfor and Andrichuk (1956) in the Stettler area; Sutterlin (1958) in southern and central Alberta; Andrichuk (1960) in west-central Alberta; Halim-Dihardja (1986) in the Tangent, Normandville, and Eaglesham oil fields area (west-central Alberta); Eliuk and Hunter (1987) in the Limestone-Burnt Timber gas fields area (southern Foothills); Halbertsma and Meijer-Drees (1987) in north-central Alberta; and Stoakes in the Tangent oil field (west-central Alberta).

In addition, Nishida et al. (1985) and Nishida (1987) described and illustrated stromatoporoid-algal buildups from the Normandville oil field in north-central Alberta. Leslie (1953) and Sonnenfeld (1964) had earlier mentioned briefly the existence of these buildups. Stearn et al. (1987) further elaborated on these stromatoporoid "patch reefs" and similar faunal assemblages worldwide.

1.4 GEOGRAPHIC DISTRIBUTION and REGIONAL VARIATION

The Palliser Formation and its equivalents occur throughout the Western Canada Sedimentary Basin (Figure 3). In the subsurface of Alberta and northeastern British Columbia, the Palliser equivalent is the Wabamun Group, in western Saskatchewan and the United States, it is the Three Forks Formation, and the Qu'Appelle Group in southeastern Saskatchewan.

The distribution of the major lithofacies of the Palliser and its equivalents (based mostly on subsurface data and on a non-palinspastic base in the thrust-fold belt) are illustrated in Figure 4. In the study area, the Palliser is mostly limestones and dolomitic limestones. Northwest, there is an increase in open marine shales, especially in the upper part, the Kotcho Formation in British Columbia. In southeast Alberta, the Wabamun Group changes from dominantly marine limestones and replacement dolostones to evaporitic anhydrite and salts. Eastward into Saskatchewan (Potlach and Three Forks Formations), there is an increase in anhydrite and halite, and finally, terrigenous clastics (Qu'Appelle Group).

In general, the Palliser and its equivalents (Figure 4) gradually thin towards the east and southeast. The thickest sections occur in thrust sheets in the Front and Main Ranges of the Rocky Mountains of Alberta and British Columbia. In southern Alberta the Palliser Formation is typically about 240 m thick in the Foothills and 300 m thick in the Front Ranges (Stewart 1960). Geldsetzer (1982) reported that the Palliser is 530 m thick at Mt. Hannington on the British Columbia-Alberta border south of the Peace River Arch. One of the thickest Palliser sections, at 660 m, occurs in the Bull River Valley of southeastern British Columbia (Gibson 1981).

The Palliser Formation is exposed along uplifted thrust slices in the Front and Main Ranges of the Canadian Rocky Mountains. These thrust blocks have been displaced eastward relative to the North American craton during the Columbian and Laramide orogenies in Cretaceous time. Numerous sections of the Palliser have been tectonically thickened or thinned. For example, the Crowsnest Pass section is in part duplicated along several small faults (McClay and Insley 1986) and the base of the Palliser is missing where the formation was carried on (and truncated by) the Lewis Thrust, overriding Jurassic and Cretaceous clastics in the High Rock Range.

Fault repeats in the Palliser may be difficult to recognize, due to the monotonous, thick sequences of similar carbonates.

1.5 FRASNIAN STAGE

In Frasnian time, a broad shelf sea, deepening towards the west and northwest, was established in western Canada, covering most or all of Alberta and British Columbia and extending eastward to Manitoba.

Fairholme Group

In the study area, the uppermost Frasnian is represented by the Fairholme Group which consists of carbonates and shales and is correlatable with the Woodbend and lower Winterburn Groups of the Alberta Plains. The upper Fairholme, or Southesk Formation carbonates contains local buildups developed on platforms (Mountjoy 1965, 1967; Workum 1978; and others).

1.6 FAMENNIAN STAGE

During the Famennian, tropical, marine conditions occurred throughout much of western Canada (Belyea 1964).

Sassenach Formation

In the southern Rockies, the Sassenach is predominantly silty carbonates and calcareous or dolomitic siltstones. In the upper Sassenach, small scale cross-bedding, asymmetric ripples, fenestral fabrics and soft-sediment deformation (Belyea and McLaren 1956; McLaren and Mountjoy 1962; Mountjoy and Geldsetzer 1981; Styan 1984) are indicative of shallow and agitated water deposition.

The Sassenach Formation unconformably overlies the upper Fairholme in parts of the study area. McLaren and Mountjoy (1962) correlated the Sassenach of the Jasper region with the upper part of de Wit and McLaren's (1950) Alexo Formation.

The Sassenach/Alexo is absent in the mountain areas between the Peace River Arch and the northern part of Jasper National Park (Geldsetzer 1982) where the Famennian Palliser unconformably overlies the upper Frasnian.

Palliser Formation

In the southern Rockies, the Palliser Formation is a thick carbonate succession of mottled dolomitic limestones. De Wit and McLaren (1950) divided the Palliser into a thick lower Morro Member and an upper, thinner Costigan Member.

Morro Member

The Morro Member is grey-weathering, cliff-forming, massive-bedded, micrite-rich and generally sparsely fossiliferous. The lower Morro Member was deposited as the Upper Devonian sea continued to transgress over the Sassenach/Alexo, causing a deepening of depositional environments. Towards the top of the Morro Member, some sections show evidence of shallowing (Styan 1984; this study), including fenestral fabrics and algally laminated muds.

Costigan Member

The Costigan Member is grey to rusty weathering, thinner-bedded, argillaceous, micritic, and more fossiliferous. It is usually more recessive than the underlying Morro Member (Plate 1b). The Costigan Member represents a deepening from the underlying Morro Member. In most Palliser sections, deeper water deposition continued to the top of the Palliser, although at Hummingbird Creek, the top of the Costigan Member represents very shallow water deposition (stromatolites, fenestrae, polygonal mud crack horizons, and rip-up clasts).

In most sections, the Palliser Formation overlies the Sassenach/Alexo conformably and gradationally (Belyea and McLaren 1956; Belyea 1964; Mountjoy and Geldsetzer 1981; this study). However, Styan (1984), based on brecciation at the top of the Alexo and shallow water facies (algal laminites, evaporite-dissolution breccias) in the basal Palliser near Canmore, Alberta, suggested that transgressive Palliser sediments unconformably overlie regressive, shallow water, Alexo strata. Belyea and McLaren (1956) described the Alexo-Palliser contact as gradational in the Bow River Valley.

Sartenaer (1969), on the basis of rhynochellid brachiopods, assigned an early and middle Famennian age to the Palliser (his upper Basilcorhynchus and lower Gastrodetoechia zones). An early and middle Famennian age was also suggested by Lethiers (1981) from a study of ostracods. Geldsetzer (1982) reported conodont and miospore study results that also indicate early and middle Famennian ages. Raasch (1987) suggested there are nine distinct faunal zones in the Famennian of western Canada and informally correlates the Palliser Formation with the "middle Famennian". Raasch (1987) also suggested that faunal breaks separate the Sassenach ("lower Famennian") Formation from the Morro Member of the Palliser, the Morro Member from the Costigan Member, and the Costigan Member from the overlying Exshaw Formation ("upper Famennian"). Supposedly, these faunal breaks indicate a time gap in deposition.

1.7 UPPER FAMENNIAN(?)/TOURNAISIAN STAGE

Exshaw Formation

The black, fissile shales of the Exshaw Formation directly overlie the Palliser Formation throughout the mountain outcrop belt. Warren (1937) defined the Exshaw and suggested that it was latest Devonian in age. Later, Crickmay (1952 and 1956), Belyea (1955) and others considered the Exshaw to be Mississippian in age based on fossils and the sharp lithologic change from the Palliser.

Warren and Stelck (1950) suggested that the Palliser-Exshaw contact is disconformable and erosional, even though they found no faunal discontinuity between the two formations and they considered the Exshaw to be of latest Devonian age. McLaren (1955) also suggested that the Palliser-Exshaw contact is an unconformity, at least between the Bow and Athabasca Rivers. Kutney (1960) considered it to be disconformable.

Macqueen and Sandberg (1970) suggested that the Exshaw Formation is both Devonian and Mississippian on the basis of conodonts taken from several sections, including the type section at Jura Creek. They described a thin, phosphatic sandstone bed occurring at the base of the Exshaw at Jura Creek as a "basal lag" and considered the Palliser-Exshaw contact to be unconformable. Harker and McLaren (1958) also mentioned a basal sandstone in the Exshaw, and believed the contact to be disconformable. Crickmay (1956) had previously described the contact at Jura Creek and had suggested that there was little or no break in deposition across the Devonian-Mississippian boundary. Styan (1984) also described the contact at Jura Creek as continuous.

Geldsetzer (1982) reported that, in the central to northern areas of the Canadian Rockies, the Exshaw yielded middle Tournaisian age miospore assemblages (versus middle Famennian or older fossils for the Palliser), indicating the presence of at least a disconformity above the Palliser. However, the level within the Exshaw from which the miospores were collected was not reported. Geldsetzer (1982) also reported finding a "fossil hash" or sandstone unit at the Palliser-Exshaw contact in the same area. He therefore suggested that some uplift and erosion occurred before Mississippian deposition. As mentioned in the previous section, Raasch (1987) suggested that at least part of the Exshaw Formation is Famennian in age.

In the Jasper region, the Exshaw has a basal quartz sand and is locally missing, resulting in Banff directly overlying Palliser. This suggests local relief and small islands, indicating the presence of an unconformity at the top of the Palliser. The Exshaw contains some plant fragments, suggesting that it may have been deposited in shallow, anoxic water (Mountjoy 1960).

Ch. 2 LITHOFACIES and ALLOCHEMS

Introduction

This chapter describes lithotypes and rock-forming constituents. The geographic distribution of the major lithotypes is discussed. Burrowing, one of the most common outcrop features, is treated extensively because of its important relationship to dolomitization (see 3.2). Non-skeletal and skeletal components are listed in the order of their abundance, with peloids, intraclasts and echinoderm fragments the most common allochems.

2.1 LITHOTYPES

2.1.1 Mudstones and Wackestones

Subtidal mudstones and wackestones

Subtidal mudstones and wackestones are commonly burrowed and non-laminated (Plate 2a). Echinoderms, brachiopods and peloids are the most common allochems, along with gastropods, ostracods, calcispheres, nautiloids, and bryozoans. These lithotypes weather light to dark grey in outcrop and are often colour-mottled due to the differential weathering of dolomite-filled burrows (Plate 2b). Fresh surfaces are medium to dark brown. These rocks are usually massive bedded. Most of the mudstones and wackestones in the Palliser were deposited subtidally in a quiet, open to partially restricted environment.

Intertidal to supratidal mudstones and wackestones

Intertidal to supratidal laminated, non-burrowed mudstones and peloidal wackestones occur at Hummingbird Creek. They weather light to medium brown and are light brown to olive-brown on fresh surfaces. They are thinner bedded than the burrowed subtidal mudstones and wackestones and are composed of micrite and very fine micritic peloids (see 2.3.1.1) with some calcispheres. Stromatolitic laminations (Plate 2e), rare square- and rectangular-shaped pores, polygonal desiccation cracks and spar-filled fenestral porosity indicate intertidal to low supratidal conditions.

The restricted fauna suggests elevated salinities. Spar-filled cavities with right-angled corners (Plate 2c) are interpreted to be pseudomorphs after evaporitic anhydrite and/or halite. These features are rare and were found only in unfossiliferous mudstones from the Costigan Member at Hummingbird Creek. The rectangular to square voids have been geopetally(?) in-filled by fine micritic calcite, and subsequently by coarser, clear sparry calcite. The 'geopetal' tops of the fine calcite may occur parallel or at high angles to bedding. However, tilted examples are all oriented in the same quadrant (i.e., 0-180° and not 270-360°).

Budai et al. (1987, Figure 8, p.916) illustrated gypsum blade molds partially filled by dolomite silt, with the remaining pore volume occluded by calcite cement. They suggested that the dolomite may have been present in the gypsum as solid inclusions, and formed an internal sediment after dissolution of the gypsum.

Mud cracks (Plate 2f) are indicative of periodic wetting and desiccation of the sediment. Fenestrae (Plate 2d) occur as flattened to irregular, bedding-parallel, cement-filled pores. Pores are filled with blocky, mosaic calcite spar, with minor occurrences of early, isopachous calcite fringe cement. The fenestrae occur in mudstones and finely peloidal grainstones. These rocks may contain calcispheres, peloids, micro-cavings of cohesive micrite chunks and algal laminations (stromatolites).

Bedding-parallel fenestral porosity, along with other intertidal to supratidal features, suggests frequent drying, although Shinn (1983) cautioned that fenestrae can occur in any peritidal environment (the area from just above the highest tides to just below the lowest tides), but most commonly occurs in high intertidal to supratidal environments. Fenestrae may be caused by sediment shrinkage or gas expansion (Shinn 1968a).

Plate 2

Lithotypes and associated features

a. Mudstone, Morro Member, Mt. Frayn (#19). 224 m below top of Palliser Formation. 1 mm scale bar.

b. Water-washed outcrop of burrow-mottled fossiliferous wackestone (containing echinoderm, brachiopod, and nautiloid fragments), Morro Member, Mt. Indefatigable (#25). 80 m above base. 5 cm lens cap.

c. Evaporite casts in laminated mudstone. Casts are filled by blocky mosaic calcite and internal sediment(?). Costigan Member, Hummingbird Creek (#27). 270 m above base. 1 mm scale bar.

d. Fenestral porosity in peloidal wackestone. Pore space occluded by blocky mosaic calcite cement. Morro Member, Hummingbird Creek (#27). 180 m above base. 1 mm scale bar.

e. Domal stromatolite, Costigan Member, Hummingbird Creek (#27). 290 m above base.

f. Bedding-plane view of mud cracks in laminated mudstone unit, Costigan Member, Hummingbird Creek (#27). 280 m above base. 5 cm lens cap.

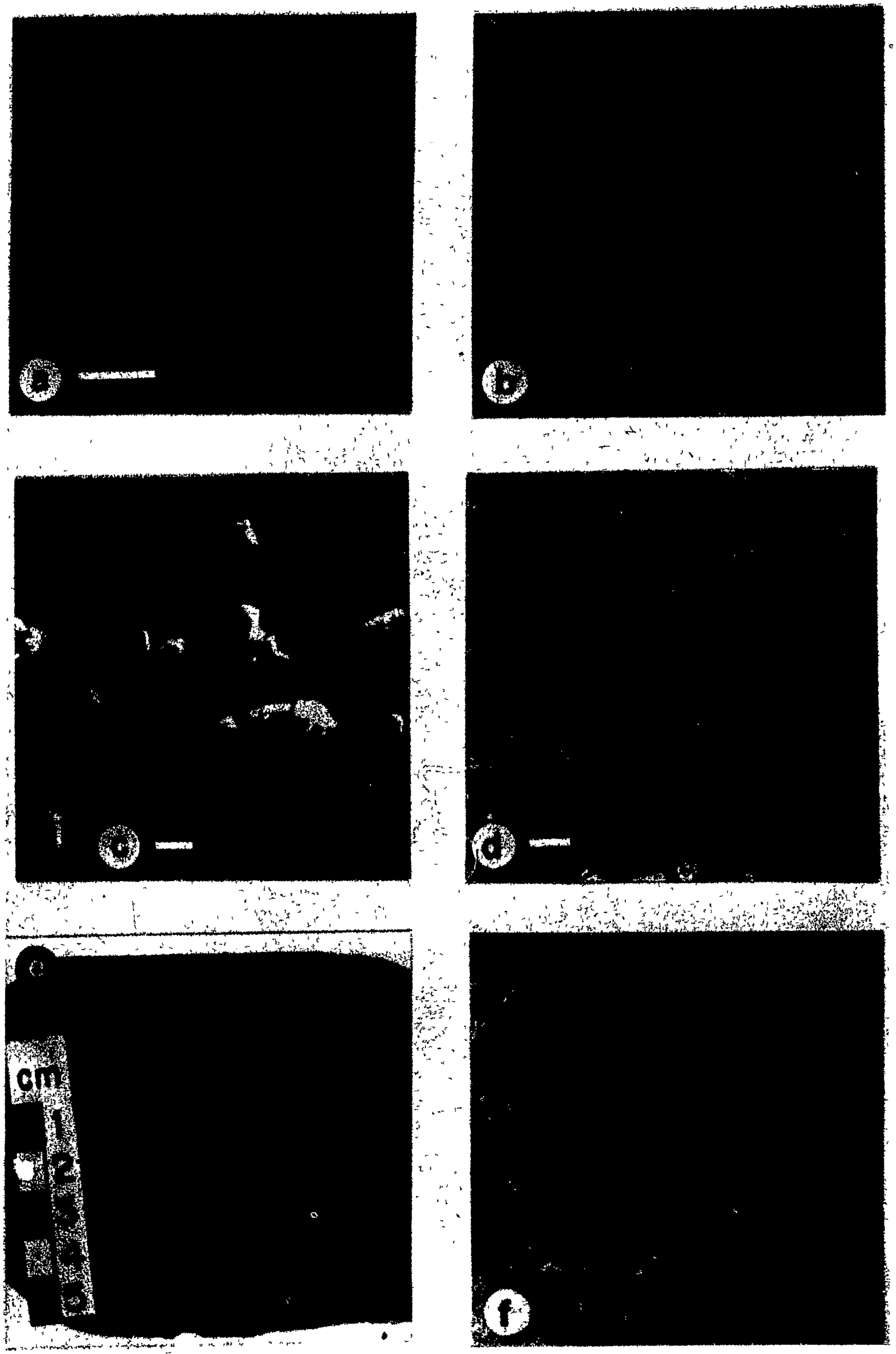
a
b
c
d
e
cm
1
2
f

2.1.2 Packstones

Packstones may be rich in shelly fossils (especially ostracods, brachiopods, gastropods, and echinoderms), peloids and/or intraclasts (Plate 3a). Packstones are commonly burrowed and non-laminated. They weather medium to dark grey and are often colour-mottled due to the differential weathering of the burrow-dolomite.

Many packstones have been highly affected by pressure solution. Some of these packstones may have been deposited with a greater percentage of micrite (e.g., as a wackestone) than is now present. Compaction may increase packing through reduction of porosity in the micrite, or through chemical solution. Micrite may have been more susceptible to pressure solution than grains due to its high surface area to volume ratio, or because of a relatively high argillaceous content (Wanless 1979). An echinoderm-packstone that occurs in many sections at the top of the Palliser Formation is a possible example of such a rock type (Plate 3b).

Shinn and Robbin (1983) noted a similar process occurring in their artificial compaction experiments. Wackestones of Recent sediments became packstones after compaction. Shinn and Robbin (1983) noted that both physical and chemical compaction had occurred.

2.1.3 Grainstones

Grainstones occur at all sections of the Palliser Formation. The most common types are peloidal (Plates 3c,d, 6a) and/or echinodermal grainstones. Intraclasts and shell fragments are also common (Plate 6b). Grain size usually ranges between 25 and 1000 μm. Grainstone units are usually non-laminated and may or may not be burrowed. Occasionally, cross-stratification and scour-and-fill structures occur. Commonly, they are in beds from 10 cm to 1 or 2 m thick and weather light to medium grey. Patches of finely peloidal grainstone that occur in mudstones from the Costigan Member at

Hummingbird Creek are laminated, weather tan or light olive-brown, unburrowed, and contain filled fenestral porosity (Plate 3e).

Blocky mosaic calcite is the most common cement (Plates 6c, 9b). Skeletal components are often destructively micritized through the action of micro-boring organisms (see 3.1.2.2).

2.1.4 Boundstones

Stromatoporoid boundstones

Stromatoporoid boundstones are rare in the Palliser Formation and were only observed at Hummingbird Creek and Crowsnest Pass. In situ tabular to lamellar stromatoporoids occur in isolated patches or in well defined lens-shaped mounds (as at Hummingbird Creek, Plate 1a). Stromatoporoids also occur at Racehorse, Flathead, and Mount Darrah.

Stromatoporoids, 1 to 5 cm thick, grow over (bind), and are overlain by mudstones or wackestones (Plate 4). Locally, minor shelter porosity is developed and is filled by geopetal sediment and blocky mosaic calcite spar and/or white sparry dolomite.

Stromatolite boundstones

Cryptalgal laminations of peloidal muddy carbonate boundstones occur infrequently in the Palliser. These laminations may be planar, wavy or domed-up into laterally-linked hemispherical forms (Plate 2e). Large stromatolite mounds (up to 1 m in diameter) are present at Hummingbird Creek. Stromatolitic rocks often display fenestral porosity which is filled by blocky mosaic calcite spar (Plate 2d).

Finely laminated dolostones with occasional hemispherical structures that occur at the base of some Palliser sections are interpreted as being dolomitized stromatolitic units although there is now no evidence of fenestral fabrics or peloidal muds.

Plate 3

Lithotypes, continued

a. Packstone with echinoderm and shell fragments, and peloids, Costigan Member, Peechee (#13). 16 m below top of Palliser Formation. 1 mm scale bar.

b. Echinoderm packstone, possibly formed through pressure solution, Alpine (#24). 1 mm scale bar.

c. Negative print of peloid-intraclast grainstone. Large fragments are intraclasts, pore space is filled by blocky mosaic calcite. Hummingbird Creek (#27). 200 m above base. 1 cm scale bar.

d. Peloidal grainstone with blocky mosaic calcite cement. Note large intraclast in centre of photograph. Hummingbird Creek (#27). 195 m above base. 1 mm scale bar.

e. Patches of algal peloid grainstone in a fenestral peloid wackestone, Morro Member, Hummingbird Creek (#27). 180 m above base. 0.5 cm scale bar.

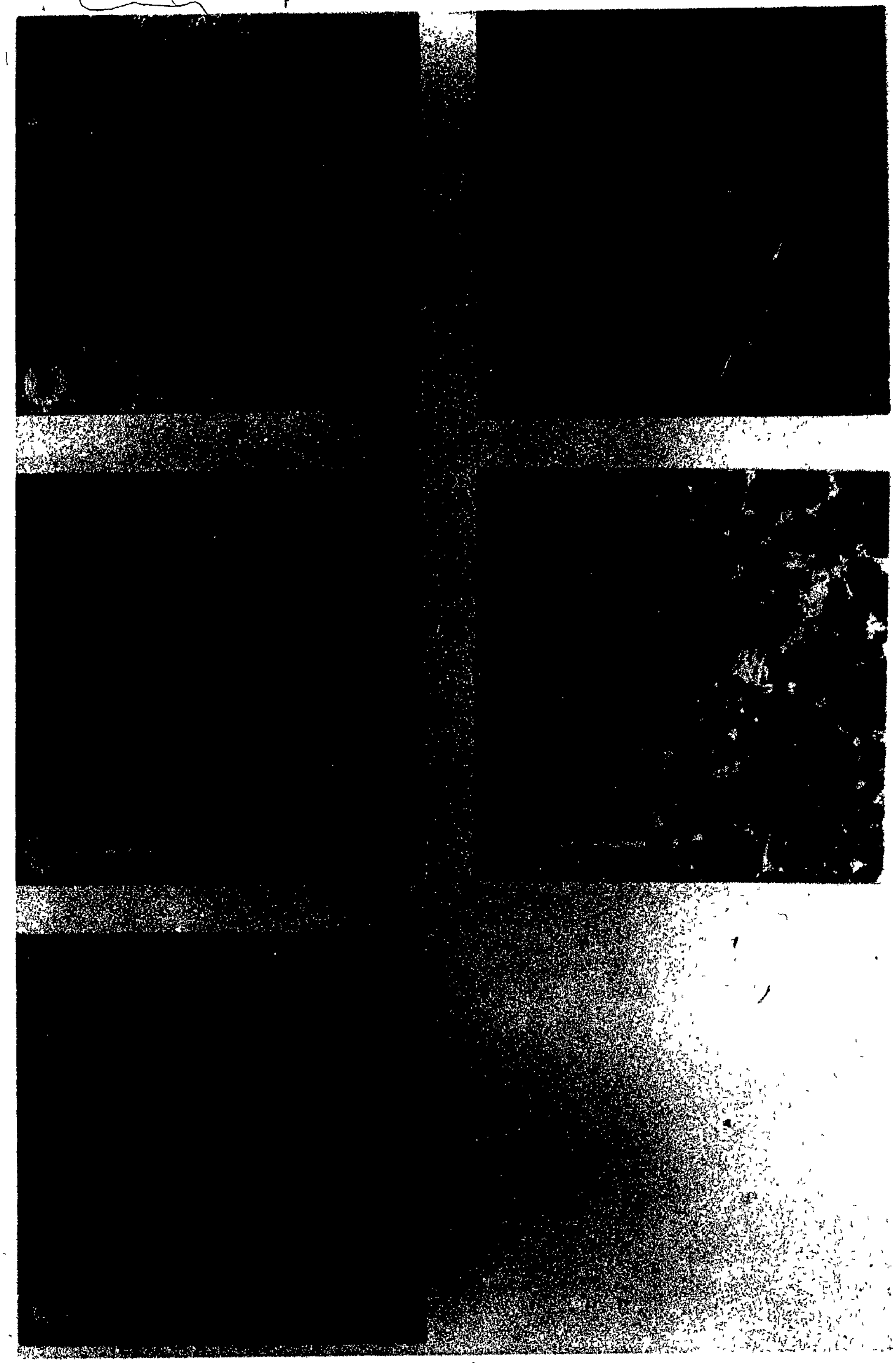

Plate 4

Stromatoporoid boundstones, Morro Member Hummingbird Creek (#27)

a. Tabular stromatoporoid. 157 m above base of Palliser Formation. 6 cm lens cap.

b. Tabular stromatoporoid. 159 m above base. 5 cm lens cap.

c. Negative print of tabular stromatoporoid (Stylostroma sp.). 158 m above base. 1 cm scale bar.

d. Detail of 4c, normal (positive) print. 1 mm scale bar.

e. Labechiid stromatoporoid (Rosenella sp.?). 159 m above base. 1 mm scale bar.

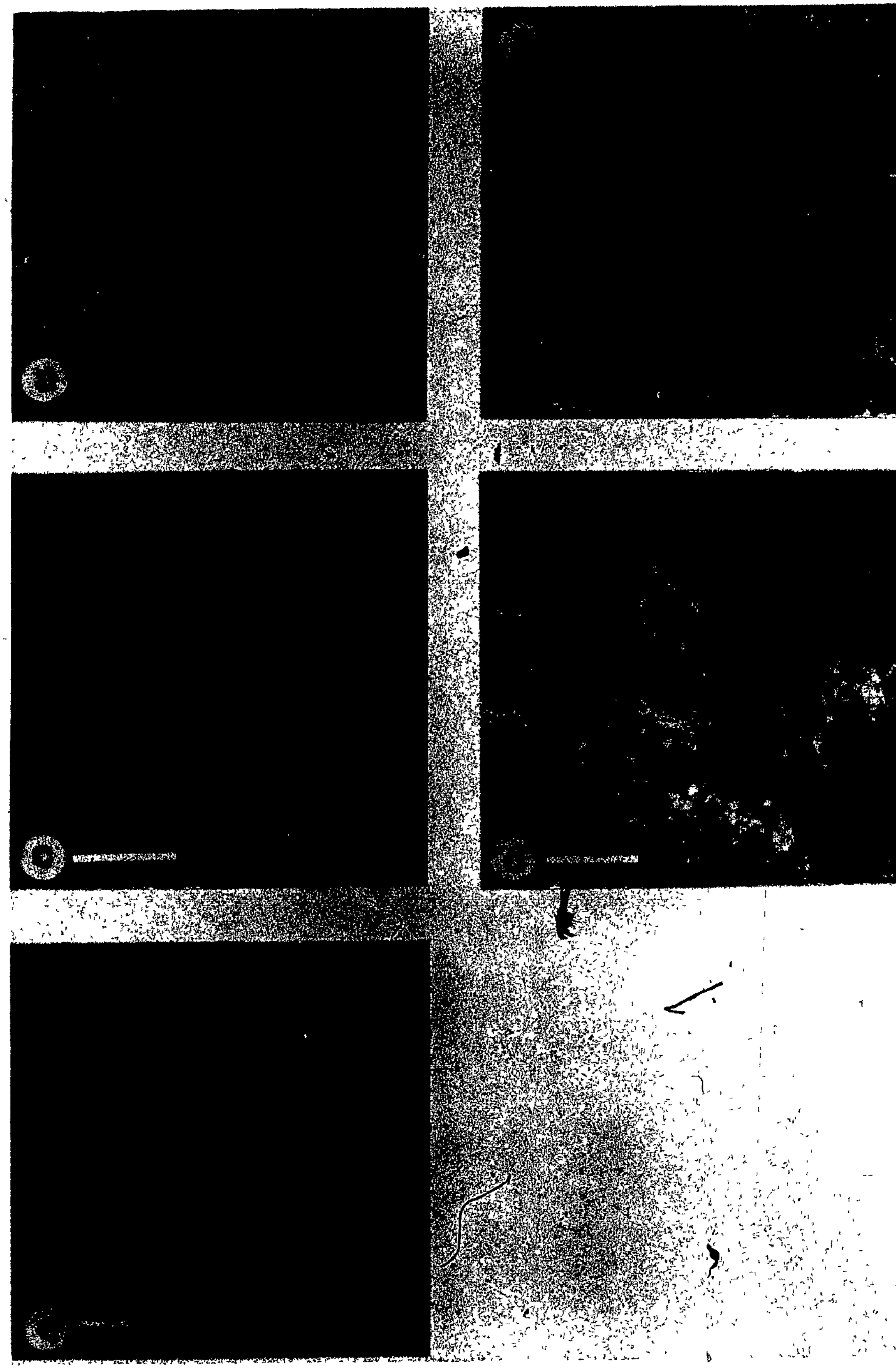

2.1.5 Occurrence of Main Lithotypes

The occurrence and distribution of the main lithotypes (Table 1 and Figures 5a, 5b, and 5c) are based on the classification of 496 samples from the Palliser Formation, following the scheme of Dunham (1962). These samples were collected as part of a regional study of the Palliser Formation conducted jointly by Esso Minerals Canada and the Geological Survey of Canada. Esso crews took samples (for geochemical analyses), usually at 8 m intervals, throughout the vertical extent of the Palliser at twenty-three locations (see Appendix Three).

The samples were taken without regard to their lithology, therefore, for the purposes of this study, this sampling technique is considered to be random with respect to rock type and the data can be treated statistically. Samples that are completely dolomitized (≈ 3%) or otherwise recrystallized are not included in the results shown below.

On the basis of this sampling and classification procedure, about 34% of the samples are mudstones, 30% are wackestones, 21% are packstones, and 15% are grainstones. The most commonly occurring lithotype in the Palliser Formation is a fossiliferous mudstone, containing echinoderm and some shell fragments as grains. The next most common rock type is a sparsely to moderately fossiliferous wackestone.

Dunham's (1962) classification used an arbitrary boundary at 10% grain content to separate mudstones from wackestones, while packstones and grainstones are distinctly different, being grain-supported. Many micrite-rich samples lie close to the 10% cutoff, either being a fossiliferous mudstone or a sparse wackestone. Considered together as a micritic limestone with fossil fragments and peloids, they are the dominant rock type (Figures 5a, 5b, and 5c).

Field sections can be grouped to show variations in the aerial distribution of the lithotypes (Table 1 and Figures 5b, and 5c). The southwestern group, west of the Elk River in

British Columbia (sections 18, 19, 20, 22, and 23; Figure 5b), has a strong predominance of mudstones. The eastern group, along the Alberta - British Columbia border and mostly in the Rundle and Lewis thrust sheets (sections 1 to 17 and 21; Figure 5c), contains a greater proportion of fossiliferous wackestones and also a higher percentage of peloid/fossil packstones.

TABLE 1
Geographic Distribution of Lithotypes

	Sections 1 - 23	18,19,20, 22, & 23	1 - 17 & 21
mudstones	34.5%	72.3%	20.1%
wackestones	30.2%	10.2%	37.9%
mudstones + wackestones	64.7%	82.5%	58.0%
packstones	20.6%	8.8%	25.1%
grainstones	14.7%	8.8%	17.0%
number of samples	496	137	359

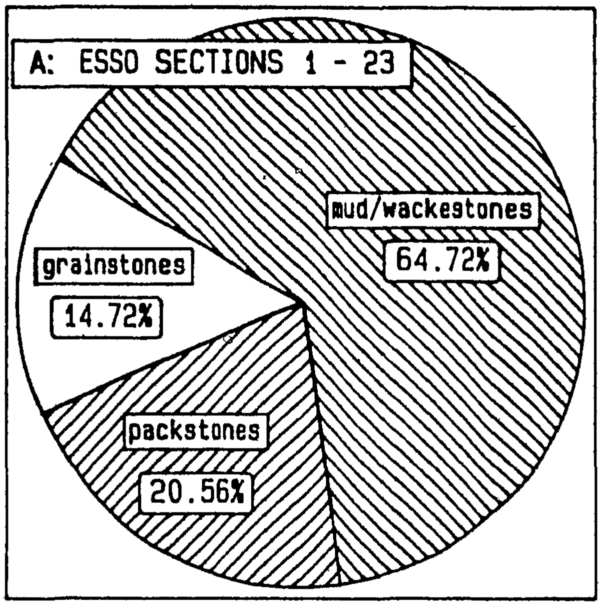

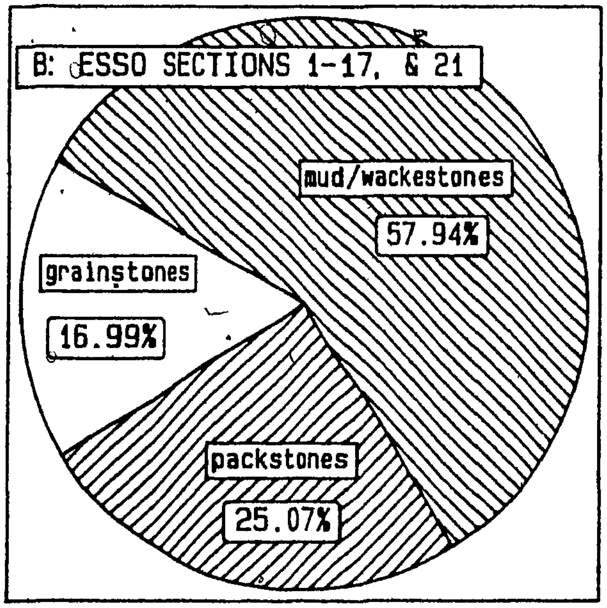

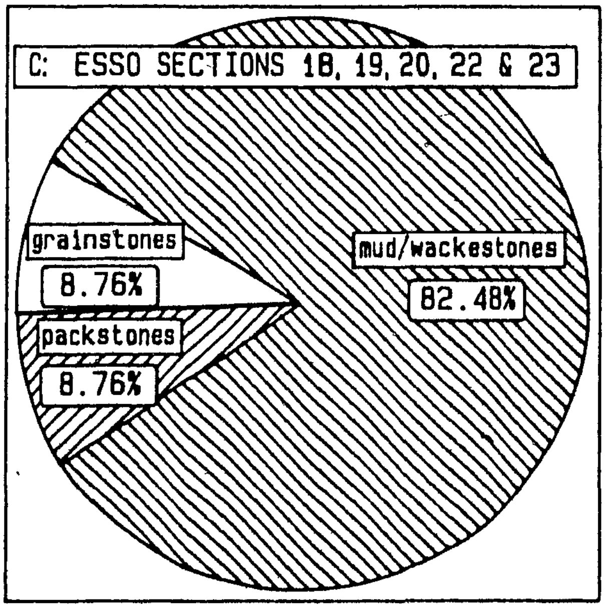

Figure 5: Occurrence of major lithotypes: a) In all 23 Esso Minerals Canada sections (#1 - 23); b) In EMC sections 1-17, and 21, west of the Elk River; c) In EMC sections 18, 19, 20, 22, and 23, Rundle and Lewis thrust sheets.

2.2 BURROWING

A major macroscopic feature of the Palliser Formation is the conspicuous colour-mottling seen in weathered outcrops (Plates 1b, 2b, 5a,b). The mottling is caused by the differential weathering of dolomite versus the mostly micritic calcite host-rock (Beales 1953). The mottles tend to weather to a lighter colour and to stand in relief relative to the micrite often imparting an extremely rough surface to weathered outcrops (Plate 5a). The mottles are commonly light tan or light grey to white in outcrop, but are occasionally dark grey and are darker than the groundmass. Colour-mottling may also be due to the differential dolomitization of successive beds, leading to interbedded dolomite (dolostone) and limestone.

Tube-shaped mottles are oriented both vertically and horizontally and are generally 1 to 5 cm long and 0.5 to 1 cm in diameter. In some sections, mottles are largely unaffected by later burial and compaction of the surrounding muds, while others appear to have been moderately deformed. This may indicate varying degrees of early induration of the mottle and/or the surrounding sediment (which is usually micrite). The mottles are commonly straight and tubular but may display widenings or branchings (Plate 5c) and may be interconnected or isolated. The majority of these tubular mottles are interpreted to be the burrowing traces of a Devonian infauna that have been selectively dolomitized as compared to the surrounding micrite as suggested by Beales (1953).

Burrows are almost invariably filled with early planar dolomite crystals (see 3.2.1.1), with or without minor amounts of intercrystalline calcite (Plate 5c, 8e,f). Burrow-filling dolomite composes 95 to 99% by volume of individual burrows. The dolomite crystals range in size from 30 to 120 µm in their longest dimension, and are generally about 70 µm.

A brown stain that occurs locally along the edge of some burrows might represent impurities (clays? organics?) that were present in the burrow and excluded during displacive growth of the dolomite, or the remnant of a wall-lining of the burrow, e.g., an organic mucus-like coating used to stabilize the burrow (Ekdale et al. 1984). Virtually no other internal structures, layering, or biogenic textures of any kind are visible in the burrow-dolomite studied. Rarely, the crystal size of the dolomite coarsens towards the top of the burrows; usually, the size of rhombs is consistent throughout.

In rare examples, undolomitized lime peloids and blocky mosaic calcite cement fill burrows in mixed wackestone/peloid grainstones (Plate 5d). In some of these samples, there are partially dolomitized (early planar dolomite) circular patches of peloid grainstone surrounded by wackestone (Plate 5e). These represent burrow-fillings in an intermediate stage between undolomitized (example above) and completely dolomitized burrow-fillings. In the Palliser Formation, the vast majority of burrow-fillings are dolomite (or dolomitized).

In some rare examples, echinoderm fragments (not dolomitized) are present in dolomitized burrows (Plate 5f).

Plate 5

Burrowing textures

a. Bedding surface view of burrow-mottling showing rough texture, Costigan Member, Hummingbird Creek (#27). 252 m above base of Palliser Formation. 5 cm lens cap.

b. Cross-sectional view of burrow-mottling, Morro member, Hummingbird Creek (#27). 130 m above base. 5 cm lens cap.

c. Negative print of burrow-mottling in mudstone. Note micrite-replacive dolomite rhombs surrounding some burrows. Percentage of dolomite decreases away from burrows. Morro Member, Crowsnest Pass (#11). 117 m above base. 1 cm scale bar.

d. Peloids and blocky mosaic calcite in undolomitized burrow, Whiteman Gap (#01). 208 m above base. 1 mm scale bar.

e. Partially dolomitized burrow with calcite peloids concentrated near bottom, Loder Peak (#02). 64 m above base. 1 mm scale bar.

f. Echinoderm fragment in dolomitized burrow, Spray Lakes (#21). 192 m above base. 1 mm scale bar.

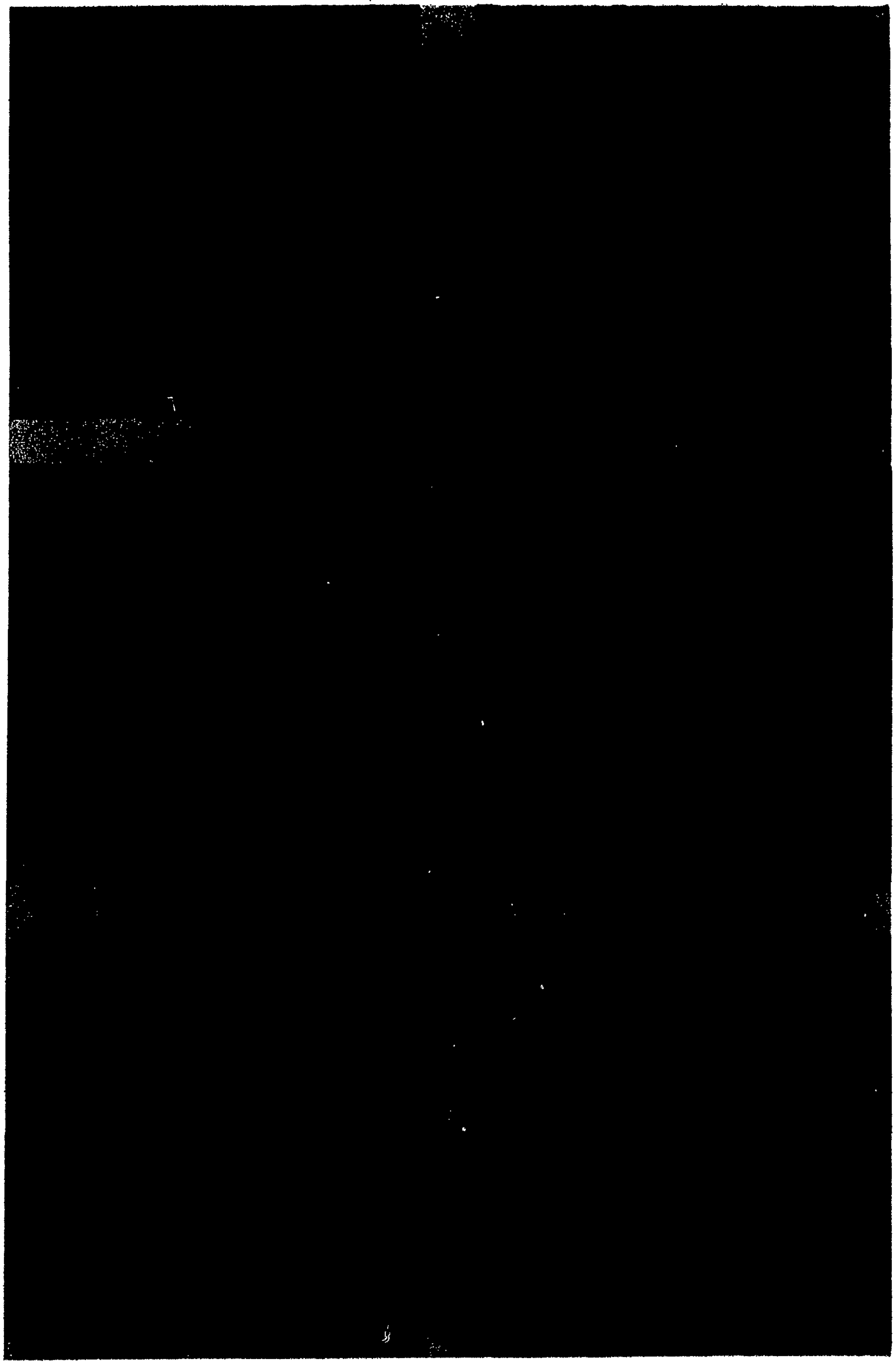

2.3 NON-SKELETAL ALLOCHEMS

2.3.1 Peloids - Introduction

The term peloid is non-genetic and denotes rounded grains composed mainly of featureless crypto- or micro-crystalline carbonate mud (micrite).

Peloids occur in all field sections and are present at all stratigraphic levels. They are the most abundant type of allochem. Peloids vary from completely micritic to containing some traces of skeletal (echinoderm fragments, calcispheres) or detrital (quartz silt) material as do modern peloids or pellets. Peloids range in size from 25 to 1000 µm and exceptionally up to 4000 µm. Generally, rocks containing smaller peloids are better sorted than those containing larger peloids. Peloids are rounded to sub-rounded, and the sphericity is usually low to moderate, but is locally high. Their cross-sectional form is elongate, oval, irregular or round. They occur in both micrite-rich rocks and grainstones. Peloids are commonly the dominant grain in grainstones. Textures range from indistinct, merged or clotted fabrics to grains with distinct outlines.

Three varieties of peloids were recognized, although their wide distribution, variety of forms and their usually featureless nature (by definition) makes interpretation of their genesis difficult. The three types are 1) algal, 2) fecal, and 3) micritizational.

2.3.1.1 Algal Peloids

Fine, featureless micrite peloids, 25 to 35 µm in diameter, are found in association with planar fenestral porosity, calcispheres and thin shelled ostracods in mudstones (Plate 3e). Faint planar or slightly undulose laminations are also commonly present. In thin section, these laminations are composed of either these tiny peloids or light-coloured bands of micrite up to 100 µm thick. The peloids are indistinct and often merge together, but are in general spherical and well sorted. These peloids are interpreted as originating as 1) fine fecal pellets (uniformity of size and shape) trapped by growing algae, similar to stromatolite formation, or 2) as algally clotted or precipitated micrite particles (peloids). Local, irregular patches of peloid grainstone (on the scale of millimetres to a few centimetres) may occur in non-bioturbated mudstones which show no evidence of winnowing wave or current action. Algally controlled clotting or precipitation of micrite is a possible explanation for the occurrence of these peloids. Alternatively, the entire mudstone fabric may actually be composed of merged pellets originally deposited as a fecal-pellet grainstone that was in part bound by algae. Compaction then destroys most of the grainy texture, only locally preserving distinct grains which were indurated early.

An algal origin for the peloids is supported by the rock type (fenestral, laminated mudstone with thin crusts) and its close association with stromatolite mounds and facies interpreted to represent high intertidal to supratidal environments at Hummingbird Creek. In addition, calcispheres are relatively numerous, suggesting that algal growth was intimately associated with the formation of this rock (and peloid) type.

Similar, well sorted, round magnesium calcite peloids have been interpreted by Macintyre (1985), on the basis of their micro-texture ("a euhedral, dentate microcrystalline rim around a dense core of interlocking sub-microcrystalline crystals") and occurrence ("the best-developed peloidal textures occur in restricted microcavities") to have originated by "repeated nucleation around centers of growth". Although some Palliser peloids do occur in shelter porosity or similar protected cavities, most do not. Microcavities play no role in the preservation of the peloidal texture in the fenestral example described above. These fenestra do not contain peloids, geopetally or otherwise. The peloids, which locally project into fenestral cavities, are part of the muddy matrix.

Therefore, Macintyre's (1985) model of precipitation and settling of peloids in microcavities, similar to the origin suggested for pyrite framboids by Honjo (1965), does not appear to apply to the majority of Palliser peloids.

2.3.1.2 Fecal Pellets

Fecal pellets are recognized by their uniform shape and size (well sorted). They are well rounded and may have rod-like, oval, or spherical shapes. Roughly spherical micritic particles may have other origins (e.g., micritized echinoderm fragments) and are harder to identify as fecal pellets. Rod or oval-shaped peloids (Plate 6a) are more strongly suggestive of a fecal origin if their shape is not due to compaction.

The shape, lack of internal texture and "gregarious" occurrence (Flugel 1982) of these peloids makes a fecal origin a strong possibility. It is, however, difficult to exclude an intraclastic, micritizational (see below), or even precipitational origin for many of these grains.

Potential pelleting organisms that are preserved include brachiopods, ostracods, gastropods and echinoderms. Numerous soft-bodied organisms capable of pelleting lime mud were probably present but have not been preserved. The degree of sediment reworking is, in part, shown by the ubiquity of the burrows which are responsible for much of the colour mottling in the Palliser Formation.

2.3.1.3 Micritized Grains

Micritized grains (Bahamite peloids of Flugel 1982) are common. Beales (1958) proposed the term Bahamite for "granular limestones that closely resemble the present day deposits of the interior of the Bahama Banks, as described by Illing (1954)".

Some micritized grains were skeletal fragments that were subjected to micro-boring by endolithic algae or fungi. These borings were subsequently in-filled by micrite. It is not known if this micrite is detrital or precipitated _in situ_ through biological action. A spectrum of textures is produced, ranging from micrite envelopes on grains (relatively thin, centripetally-deposited micrite rims) to completely structureless micrite masses, which are therefore peloids. This process is referred to as "micritization" (Bathurst 1966, 1975) and is discussed further in 3.1.2.2.

2.3.2 Intraclasts

Virtually all aggregate grains are intraclasts as they are cemented and sub-angular to well-rounded; no lobate grapestones were noted. Induration is indicated by truncation of primary features, such as peloids at the edge of the intraclasts.

Intraclastic aggregate grains are common especially in peloid grainstones but also occur in micrite-rich rocks. These intraclasts are probably derived from previously deposited peloid grainstones. This may indicate shifts in the energy of the depositional environment, causing peloidal sediments to be eroded and, relatively quickly, redeposited as a peloidal-grainstone intraclast. Locally, peloid-grainstone intraclasts are themselves the grains that form a later generation intraclast, indicating that at least three generations were possible.

Intraclasts were derived from all of the rock types that occur in the Palliser Formation, ranging from fossiliferous or peloidal wackestones and packstones, to mudstones and grainstones. In grainstones, they are often the largest grains present and may be twenty-five to fifty times greater in size than the mode, ranging up to 1 cm in their longest dimension (Plate 6b, also 3c,d).

The relative scarcity of angular and sub-angular intraclasts indicates either sufficient time or energy during transport to cause rounding, or a relatively low degree of induration of the parent sediment, or both.

Plate 6

Non-skeletal allochems

a. Peloidal grainstone, rod-shaped grains may be fecal pellets. Also contains intraclasts, micrite envelopes and blocky mosaic calcite cement. Hummingbird Creek (#27). 195 m above base of Palliser Formation. 1 mm scale bar.

b. Large wackestone intraclast in echinoderm-peloid grainstone, Morro Member, Flathead (#16). 136 m below base. 0.5 mm scale bar.

Calcite cements

c. Fringe <F> and blocky mosaic <B> cements in peloidal grainstone, Morro Member, Hummingbird Creek (#27). 195 m above base. 0.1 mm scale bar.

d. Syntaxial overgrowth <S> on an echinoderm fragment. Overgrowth occurred after minor micritization, Crowsnest Pass (#11). 276 m above base. 0.25 mm scale bar.

e. 4d under crossed nicols.

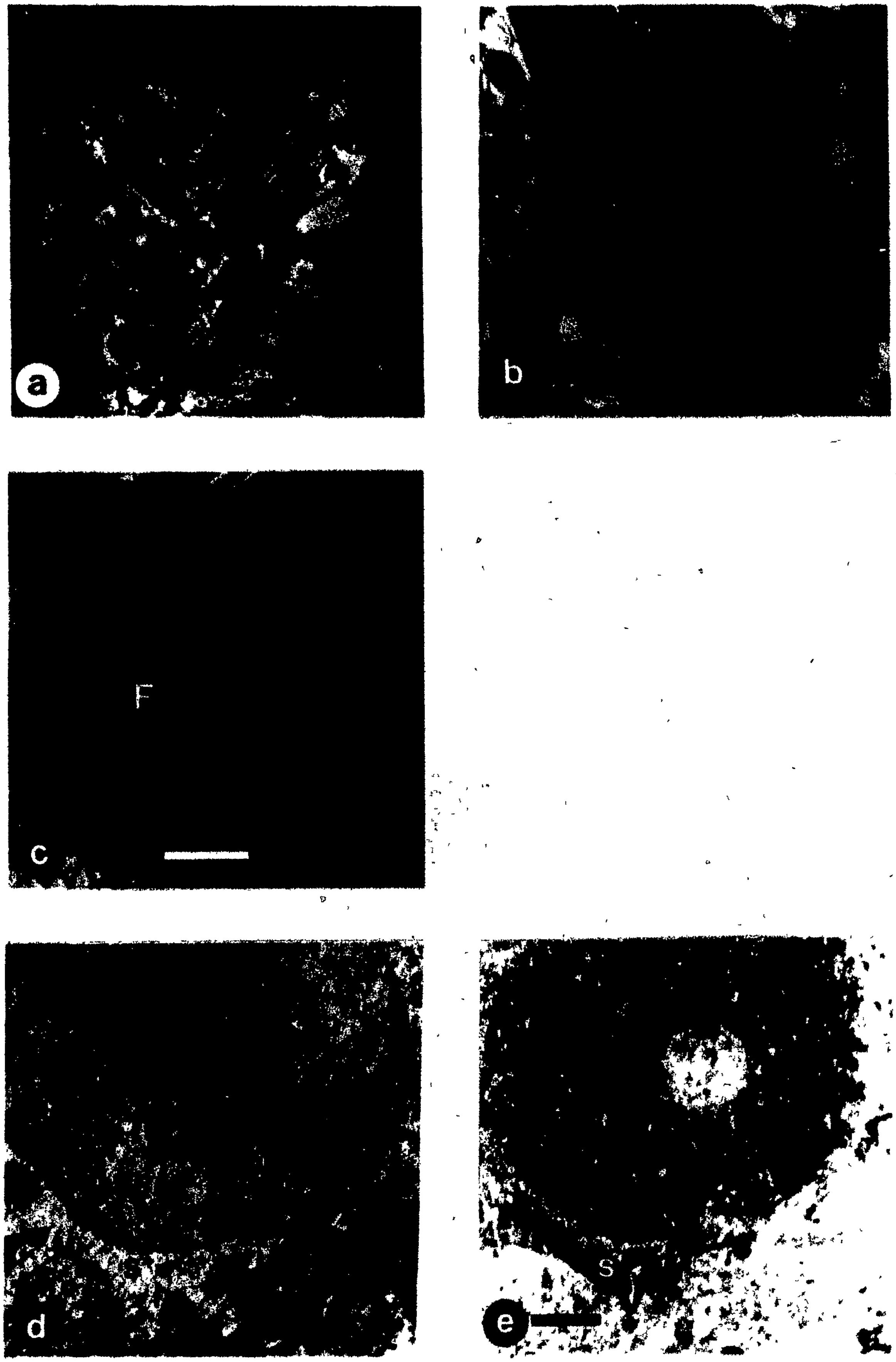
a
b
F
c
d
S
e

Some angular to sub-angular mudstone or peloidal wackestone intraclasts occur in rudstones from Hummingbird Creek. These tabular rip-up clasts were derived from semi-cohesive mud that probably did not experience much transport. Rip-up clasts are associated with a mud-flat facies containing desiccation cracks and fenestral porosity; they were chips eroded from the mud polygons during storms.

2.4 SKELETAL COMPONENTS

Echinoderm fragments, especially crinoid columnals and plates, are the most common skeletal grain (Plate 6b,d,e). They are the third most abundant allochem, behind peloids and intraclasts. Echinoderm spines also occur locally.

The majority of echinoderm fragments are low-Mg calcite and contain abundant crystals of microdolomite (see 3.2.1.2). Some fragments are partially replaced by silica or completely replaced by nonplanar dolomite (see 3.2.2).

Brachiopods occur at all stratigraphic sections and at all levels, both as fragments and as articulated shells up to 4 cm long. Fibrous-parallel wall structures are preserved, locally with punctae or pseudo-punctae.

Ostracods are common, with whole ostracods averaging about 1 mm long. Along with calcispheres, ostracods are usually the only fossils present in mudstones that are interpreted to represent restricted environments.

Calcispheres occur in samples from most field sections. They are spherical, thin-walled and range from 60 to 200 μm in diameter. The walls are micritic (calcite) and are 5 to 10 μm thick. However, this thickness may include external micritic coatings. Locally, calcispheres have a fringe, up to 50 μm thick, of prismatic, radially oriented calcite crystals.

Gastropods are not abundant but occur at all sections. They occur both in low-spired (turbiform) and high-spired forms up to 5 cm in length. Shells are not well preserved and usually occur as molds filled with mosaic calcite or locally, nonplanar dolomite, or as micrite envelopes.

Rare straight nautiloid fragments up to 10 cm long occur in fossiliferous packstones and wackestones (Plate 2b).

Planar to hemispherical stromatolites and domal stromatolite mounds are evidence of the growth of algae (Plate 2e). Planar or wavy lamellar forms appear in thin section as indistinct clottings of peloids or bands of alternating lighter and darker micrite, and are often associated with fenestral porosity, calcispheres and quartz silt. Stromatolites occur in units interpreted to have been deposited in a variety of depositional environments, ranging from the subtidal to the high intertidal (based on fossil assemblages, sedimentary structures, etc.). At Hummingbird Creek, stromatolites (individual mounds up to 1 m across) in the upper Costigan Member which are closely associated with mud cracks, fenestral mudstones and rip-up clasts, probably formed in the high intertidal environment.

Except for stromatolites, clear evidence of algae is rare. Some encrusting forms of algae (possibly codiacean) occur. A very similar, but nodular form also occurs, as do rare dasycladacean algae.

Calcispheres may be algal remains. Rupp (1967) and Marszalek (1975) have noted similarities between calcispheres and the reproductive structures of modern dasycladacean algae in the subfamily Acetabulariae.

Stromatoporoids are rare, occurring in micrite- and peloid-rich rocks from the Morro Member at Hummingbird Creek, Crowsnest Pass, Racehorse, Flathead, and Mount Darrah. Stromatoporoids form boundstones at Hummingbird and Crowsnest. The growth form is tabular with a 1 to 5 cm thick coenosteum, though, locally, turbinate or hemispherical stromatoporoids occur. Stromatoporoids may be partially to completely silicified with concomitant destruction of textures.

Stearn (1987) identified the stromatoporoids collected from Crowsnest Pass as the labechiids Stylostroma sp. and Labechia palliseri. At Hummingbird Creek (Plate 4), the labechiid stromatoporoids Stylostroma sp. and Rosenelia sp. were collected, as well as the clathrodictyid stromatoporoid Clathostroma sp. The stromatoporoids from Racehorse, Flathead, and Mt. Darrah are labechiids. According to Stearn (1987), this assemblage correlates with the lower Famennian Cheiloceras zone of Sartenaer (1969) and the Famennian-2 age of Lethiers (1981).

Branching **bryozoans** are rare; several fragments were noted in the Costigan Member. They are solid, tabular or flattened, branching forms with polygonal zooecia.

Only one **foraminiferid** test was noted in seven hundred thin sections examined. It occurs in a peloid grainstone from the Costigan Member, Racehorse section (EMC 10: Figure 2a or Appendix Three). The planispiral test is approximately 350 μm in diameter. Dr. T.R. Marchant (personal communication, 1987) tentatively identified the poorly preserved specimen as belonging to the genus Septatournayella (Family Tournayellidae).

Ch. 3 DIAGENESIS

Introduction

The importance of diagenetic alteration in sedimentary rocks is universally acknowledged. Carbonates are particularly susceptible to diagenetic changes and overprinting, which may completely obscure the original depositional fabric.

This chapter includes descriptions and discussion of calcite and dolomite diagenesis. Calcite diagenesis includes all cementation, mechanical and chemical compaction, and alteration affecting calcite components. Dolomite diagenesis is treated separately due to its special characteristics and includes all processes of alteration to, or precipitation of, the mineral dolomite.

3.1 CALCITE DIAGENESIS

3.1.1 Calcite Cements

Included are all calcite phases that have precipitated *in situ* after deposition of the sediment. Peloids are excluded although some may have had a precipitational origin (see 2.3.1). Most calcite cement phases do not display banding or zoning, indicating homogeneous growth.

3.1.1.1 Fringe cement

Fringe calcite cement occurs as the first pore lining in some limestones. The fringe is usually isopachous and occurs as an intraparticle (intrafossil) cement or interparticle cement in grainstones (Plate 6c). It is rare and, when present, usually occludes less than 10% of the available pore space. The crystals are 10 to 25 μm long (perpendicular to pore wall) and 4 to 25 μm wide and are stubby (equant) to prismatic. The thickness of the fringe varies from 10 to 30 μm.

3.1.1.2 Blocky mosaic cement

Blocky mosaic cement is the most common type, occurring in all stratigraphic sections and at all levels. It occurs as an intrafossil or interparticle cement and usually occludes all available pore space in limestones. The roughly equant crystals range in size from 50 to 3000 μm. This cement occurs after the fringe cement or directly on pore walls (Plate 6c, also 3c,d, 5d, 9b). In one sample from Hummingbird Creek, this cement displayed a series of growth stages or bands (visible as banded cathodoluminescence, see 3.4.2).

3.1.1.3 Syntaxial overgrowth cement

Syntaxial overgrowths occur in optical continuity on single crystal echinoderm fragments and are always the first phase of cement. Overgrowths are up to 500 μm thick. A few overgrowths contain oriented microdolomite inclusions; most do not.

Syntaxial overgrowths appear to have formed before grain-to-grain pressure solution (see 3.1.3.2) occurred. In many grainstones where most grains (peloids and rounded peloidal intraclasts) have contacts indicative of moderate to extensive grain-to-grain pressure solution (e.g, Plate 8b), some echinoderm fragments with syntaxial overgrowths have 'normal' point contacts (e.g., Plate 6b). Evidently, syntaxial overgrowths prevented closer packing from occurring during mechanical compaction or grain-to-grain pressure solution.

Perkins (1985) has found syntaxial overgrowths on echinoderm fragments in Holocene, submarine-cemented beachrock, indicating that such cements may form very early from marine fluids without any meteoric influence.

3.1.1.4 Poikilotopic cement

Coarsely crystalline poikilotopic calcite cements occur in some dolostones. They are late stage and usually occlude any remaining pore space. They are present at Hummingbird Creek, Mt. Indefatigable, Munroe-Alpine-Boivin, and Oldman River sections. Dolomite crystals seem to float in the calcite, but these crystals are probably in contact with dolomite out of the plane of the thin section. A single poikilotopic calcite cement crystal may continue for a centimetre or more through several individual pores, which must be interconnected to explain the crystal continuity.

Poikilotopic calcite cement may occur as the last pore-filling after planar and/or nonplanar dolomite (Plate 11e,f).

3.1.1.5 Coarse blocky cement

Coarse blocky calcite cement is a volumetrically minor phase but occurs in many sections. Equant calcite crystals up to 5 mm in size occur as a late-stage filling after nonplanar dolomite, sulfides, and quartz. It occurs in solution-enlarged voids (Plate 12b) but is otherwise similar to fracture-filling calcite (see 3.1.1.6). This cement occurs in fractured or brecciated rocks and postdates stylolite formation. In brecciated units, blocky to idiotopic, equant calcite crystals surround (and partially replace?) limestone and dolomite clasts. It occurs in mineralized rocks in a fault zone at Oldman and in partially brecciated rocks of the stromatolitic mudstones of the upper white unit at Hummingbird Creek.

3.1.1.6 Fracture-filling calcite cement

Calcite in fractures occurs in all sections and at all stratigraphic levels. Some fractures may contain both calcite and nonplanar dolomite. Fractures range in thickness from less than 20 μm to more than 50 cm. Generally, this calcite is coarsely crystalline, equant, and non-ferroan. Two ferroan fracture-filling calcite examples were noted, both from the Costigan Member, one from the Oldman section, and the other from Crowsnest Pass.

Rarely, fracture-filling calcite has precipitated in optical continuity with an echinoderm fragment and its syntaxial overgrowth (Plate 7a,b). At Munroe-Alpine-Boivin, some late calcite-filled fractures contain native sulphur as the last phase. Tectonic fractures may have more than one stage of opening and calcite in-filling (Plate 7c).

3.1.1.7 Stylolite calcite

Stylo-precipitated calcite was observed at Hummingbird Creek. The fibrous calcite is up to 3 cm thick perpendicular to the trend of the stylolites (Plate 7d). These stylolites are parallel or sub-parallel to bedding and occur in fenestral, laminated mudstones.

3.1.2. Micrite

3.1.2.1 Diagenesis of micrite

Most micrite has been neomorphosed to microspar (4 to 31 μm), and rarely, to pseudospar (greater than 31 μm); terms and size ranges were defined by Folk (1965). The most common size range for micrite is 3 to 6 μm (Plate 9c), putting it on the boundary between true mud (<4 μm) and microspar. Folk (1965) suggested that 'normal' micrite is deposited as 1 to 3 μm carbonate needles and then undergoes neomorphism and becomes 1 to 3 μm subequant polyhedra, but that most microspar is coarser than 10 μm.

Locally, small (up to 1 cm) early-cemented micritic nodules formed in mudstones and wackestones. These nodules show less evidence of mechanical and chemical compaction than does the surrounding limestone, and are unaffected by wispy microstylolites which deflect around the exteriors of the nodules.

3.1.2.2 Micritization of allochems

Skeletal components are often micritized. This process, described by Bathurst (1966, 1975), occurs when endolithic algae or fungi bore into substrates for food or protection. These borings are subsequently in-filled by micrite, either detritally or through biologically-controlled precipitation. This results in centripetally-deposited (destructive) micrite rims or complete micritization of grains.

In grainstones, echinoderms tend to be centripetally micritized. In muddy rocks, however, echinoderms are either unaltered or have thin, centripetal, micrite coatings, which could be algal. Non-destructive micritization is identified by the preservation of the outer form of the grain, and the sharp, smooth contact with the micritic coating. Destructive micritization produces a micrite-grain boundary that is irregular and not sharp. 'Intermediate' micritization stages are easily recognized in echinoderm fragments. Preservation of the single-crystal structure, as patches in the mostly micritic grain, is diagnostic (Plate 7e,f, 8a and Figure 6).

Kobluk and Kahle (1978) described centrifugal micrite coats or "constructive micrite envelopes", as opposed to centripetal or "destructive micrite envelopes". They suggested that constructive envelopes develop when endolithic (boring) algal filaments grow on the exterior of carbonate grains. The filaments die and may be quickly calcified. If water energies are low enough, these filaments may be preserved. The mud-rich rocks in which centrifugal (constructive) micrite rims developed indicate a quiet depositional environment. Such coats will not form in constantly agitated waters and will be subordinate or non-existent in periodically agitated waters.

Plate 7

Calcite cements, continued

a. Calcite-filled fracture in peloidal grainstone. Note that some calcite has precipitated in optical continuity (syntaxially <S>) with echinoderm fragment, Morro Member, Hummingbird Creek (#27). 195 m above base of Palliser Formation. 0.25 mm scale bar.

b. 7a under crossed nicols.

c. Calcite-filled fracture in mudstone showing at least two stages of opening and filling, Alpine (#24). 0.5 mm scale bar.

d. Negative print of fibrous calcite precipitate along stylolite in fenestral, laminated peloidal wackestone, Hummingbird Creek (#27). 180 m above base. 1 cm scale bar.

Micritization

e. Intermediate stage in formation of peloid from bio-fragment. Arrow points to small unmicritized patch of echinoderm grain which is in optical continuity with larger unmicritized patch. Morro Member, Spray Lakes (#21). 49 m above base. 0.5 mm scale bar.

f. 7e under crossed nicols.

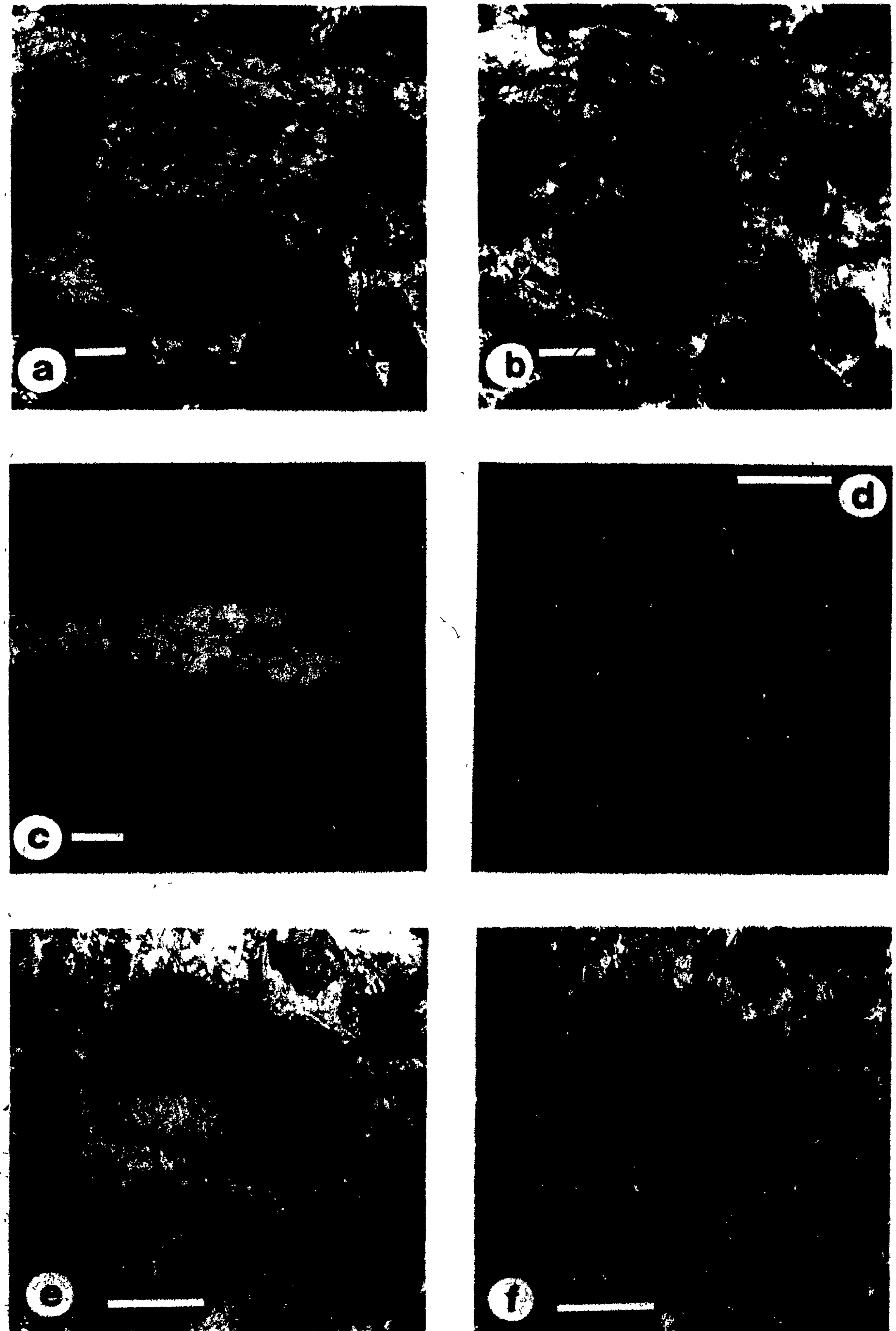
a
b
c
d
e
f

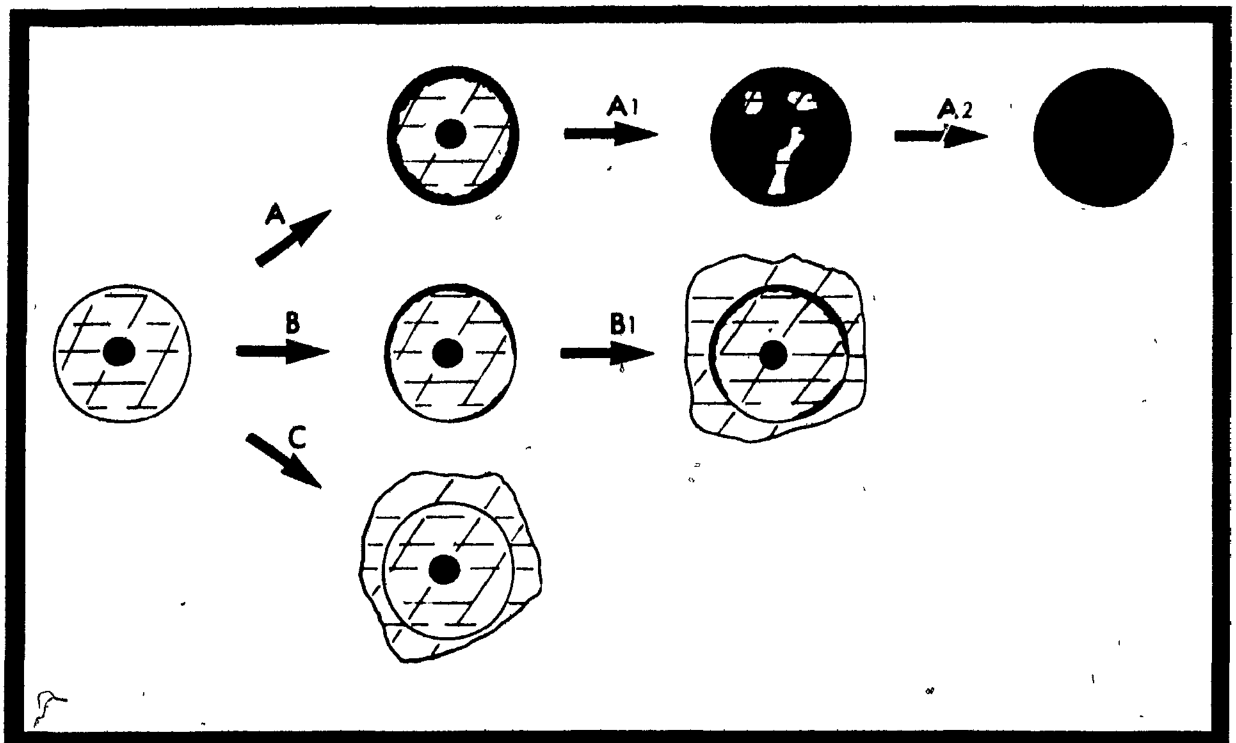

Figure 6: Possible diagenetic pathways for echinoderm fragments.
Path A - thick rim of micritization. A_1 - intermediate stage of micritization. A_2 - complete micritization. Results in a peloid.
Path B - thin and/or partly discontinuous rim of micritization. B_1 - syntaxial overgrowth.
Path C - syntaxial overgrowth, no micritization.

Micritization occurred before the formation of syntaxial calcite overgrowths on echinoderm fragments (Plate 6d,e, and Figure 6). Echinoderms that suffered extensive micritization did not develop overgrowths due to the destruction of their single crystal structure. Grains that developed only a thin envelope tend to have overgrowths. Echinoderm fragments are the most commonly micritized grains. Some shell fragments (brachiopods? and ostracods) have also been micritized.

Rarely, the grain was dissolved after the formation of the micrite envelope. This left a thin micrite band that preserved the form of the original skeletal grain (Plate 6a), although crushed envelopes also occur. The interiors are usually filled with blocky calcite cement, but some envelopes from Hummingbird Creek were first filled by geopetal micrite. Most of the orientations of these geopetal fillings agree with the facing direction determined in outcrop, however, some were rotated 90° or 180°, indicating very early grain dissolution, micrite infilling and later reworking. This must have occurred before significant induration and/or burial, again indicating that the micritization process occurred very early on the sea floor. Possibly, some early sea floor cementation of the micrite envelope helped to preserve its delicate form during rotation.

Determination of the organisms responsible for microboring is difficult as individual tubules are not distinct. Where vague tubules are visible, they seem to have diameters of about 6 to 10 μm. According to Bathurst (1966, 1975), this would indicate algal rather than fungal activity. However, Friedman et al. (1971) suggested that fungal borings may range up to several hundreds of μm in diameter. The scale of the boring is definitely too small for sponges, ostracods or pelycypods. Bacteria may bore carbonate substrates, but their cell diameters are generally 2 to 3 μm although they range up to 10 μm (Friedman et al. 1971)

Ekdale et al. (1984) suggested that photosynthesizing organisms bore into substrates to escape from the rigours of the physical environment while fungi are chiefly searching for food, and therefore attack organic-rich substrates. Calcite crinoid columnals were probably not a rich source of nutrients, again suggesting that the majority of borings in fragments from the Palliser were caused by endolithic algae.

Swinchatt (1969) indicated that modern algal boring commonly takes place in water depths of less than 15 to 18 m on the Great Barrier Reef, Australia and less than 12 m on the Florida Shelf and Bahama Banks. Although boring by photosynthetic algae would be restricted to the photic zone, bacteria, fungi, and heterotrophic algae may be active in very deep water, so that the presence of borings cannot be used as a bathymetric indicator (Friedman et al. 1971). In addition, bored grains may experience transport into deeper water. However, Budd and Perkins (1980) found that different boring morphologies were bathymetrically zoned (analogous to trace macrofossil facies), with some borings occurring at 530 m water depth in Puerto Rican shelf and slope sediments.

3.1.3 Limestone Compaction

3.1.3.1 Mechanical compaction

Evidence for mechanical compaction comes mainly from crushed micrite envelopes and shells, especially ostracods and brachiopods. Mechanical compaction may be responsible for some of the clotted or merged texture of peloid wackestones.

3.1.3.2 Grain-to-grain pressure solution

Grain-to-grain pressure solution (Figure 7a) occurred locally in grainstones (and some packstones). Grain-to-grain pressure solution will only occur where grains are free to move relative to each other, as in uncemented grainstones under non-hydrostatic pressure (Chanda et al. 1983).

Grain-to-grain pressure solution is indicated by concave-convex or sutured contacts between grains (Plate 8b). Intergranular cement was not affected by the grain-to-grain pressure solution, suggesting that it did not form until after this style of pressure solution ceased. Very little or no insoluble material accumulated at grain-grain contacts.

3.1.3.3 Microstylolites

Microstylolites are low amplitude wispy pressure-solution seams. Wanless (1979) referred to the formation of such features as non-sutured seam solution and suggested that it occurs in limestones containing "significant" amounts of platy, insoluble minerals (e.g., clays, platy silt). Microstylolites commonly coalesce to form swarms (Figure 7b), sometimes termed horsetails.

Microstylolites occur in all sections and at all stratigraphic levels. They tend to occur in darker, more argillaceous micritic limestones, but often occur with through-going (or high-amplitude) stylolites in the same sample. Dark brown opaque material (clays?), quartz silt and dolomite rhombs are commonly concentrated along these seams. The clays and the silt are insoluble cumulates; the dolomite may be a cumulate or a precipitate (see 3.2.4).

3.1.3.4 Stylolites

Through-going stylolites (Plate 8c,d) occur throughout the Palliser Formation in most rock types. The majority are approximately bedding parallel, indicating that they were caused by burial pressures while other stylolites are at moderate to high angles to bedding, suggesting a later, tectonic origin.

Column and socket suturing (Figure 7c) is most pronounced when two different rock types interpenetrate or when resistant grains such as echinoderm fragments, are present. The height of individual columns (which equals the minimum thickness of rock removed along this stylolite) varies up to 10 cm.

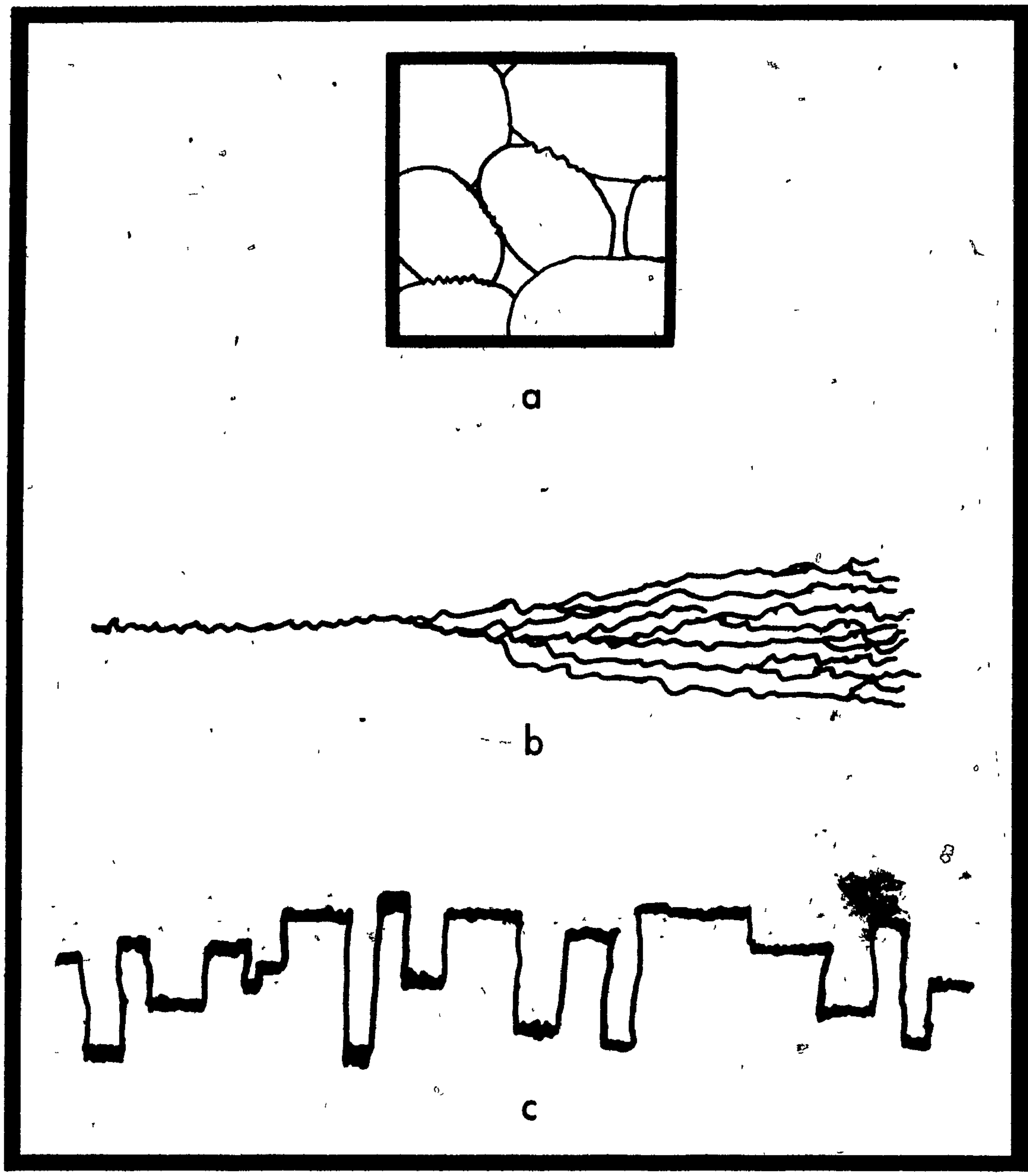

Figure 7: Styles of pressure solution. (a) Grain-to-grain pressure solution. (b) Microstylolite seam swarm. (c) High amplitude stylolite.

Plate 8

Micritization, continued

a. Two partially micritized echinoderm fragments in packstone, Crowsnest Pass (#11). 208 m above base of Palliser Formation. 0.25 mm scale bar.

Pressure solution

b. Grain-to-grain pressure solution in a peloidal grainstone, Morro Member, China Wall (#17). 2 m above base. 0.25 mm scale bar.

c. High amplitude stylolite cutting tabular stromatoporoid boundstones, Morro Member, Hummingbird Creek (#27). 160 m above base. 5 cm lens cap.

Planar dolomite

d. Early planar dolomite in a peloidal wackestone cut by a stylolite, Morro Member, Hummingbird Creek (#27). 130 m above base 0.5 mm scale bar.

e. Burrow-filling early planar dolomite in mudstone, Morro Member, Crowsnest Pass (#11). 117 m above base. 1 mm scale bar.

f. Edge of burrow shown in 8e. Note micrite-replacive rhombs <arrows> outside burrow. 0.25 mm scale bar.

Insoluble cumulates may include clays, quartz silt, dolomite, and pyrite. Precipitates include calcite, dolomite and possibly pyrite. At Munroe-Alpine-Boivin, thick (up to 1 cm) deposits of black organic matter (carbonaceous? kerogenous?) with associated pyrite were noted along stylolites in partially dolomitized mudstones. This dark, opaque material might represent hydrocarbon residue which migrated along the stylolite after expulsion from its source bed.

Where a contact is evident, stylolites always cut microstylolites; the reverse relationship does not occur, therefore stylolites appear to have formed after microstylolites.

3.2 DOLOMITE DIAGENESIS

Introduction

The classification of dolomite (Figure 8) follows the scheme of Gregg and Sibley (1987). On this basis, various categories and sub-categories of dolomite are recognized (Figure 9 and Table 2).

Planar and nonplanar are the two major modifying terms applied to dolomite phases. The terms unimodal and polymodal are used to described the crystal size distribution. Gregg and Sibley (1984, 1987) suggested that dolomite with planar intercrystalline boundaries formed below a "critical roughening temperature"; nonplanar boundaries indicate formation above this temperature. This critical temperature was suggested to be around 50°C. They further suggested that a unimodal size distribution likely indicates a single nucleation event on a homogeneous substrate (e.g., micrite), while a polymodal distribution may be formed by a single nucleation event on a polymodal substrate or multiple nucleation events on a unimodal or polymodal substrate.

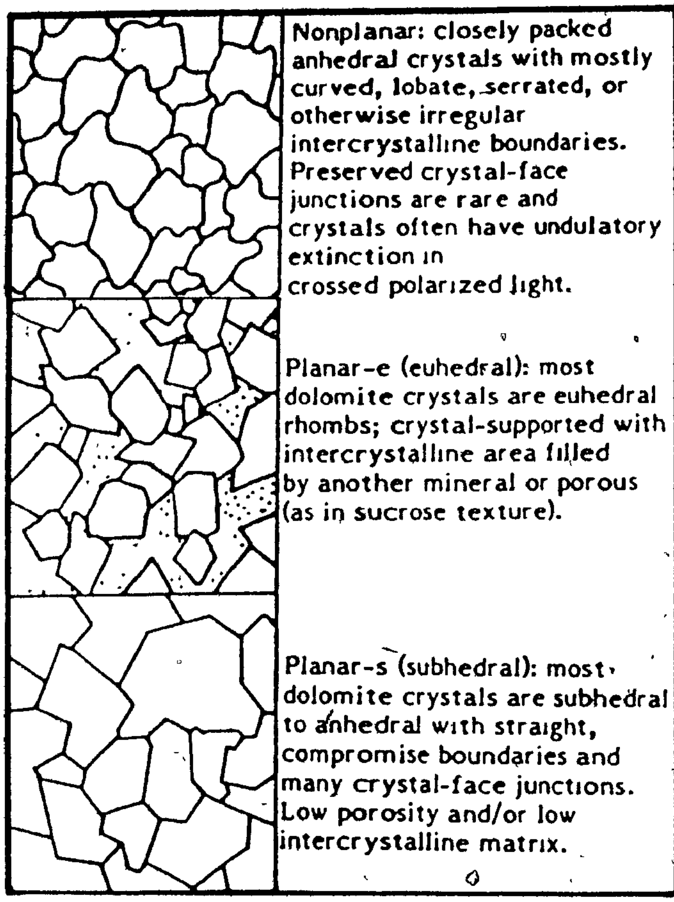

Figure 8: Planar and nonplanar dolomite textures, from Gregg and Sibley (1987).

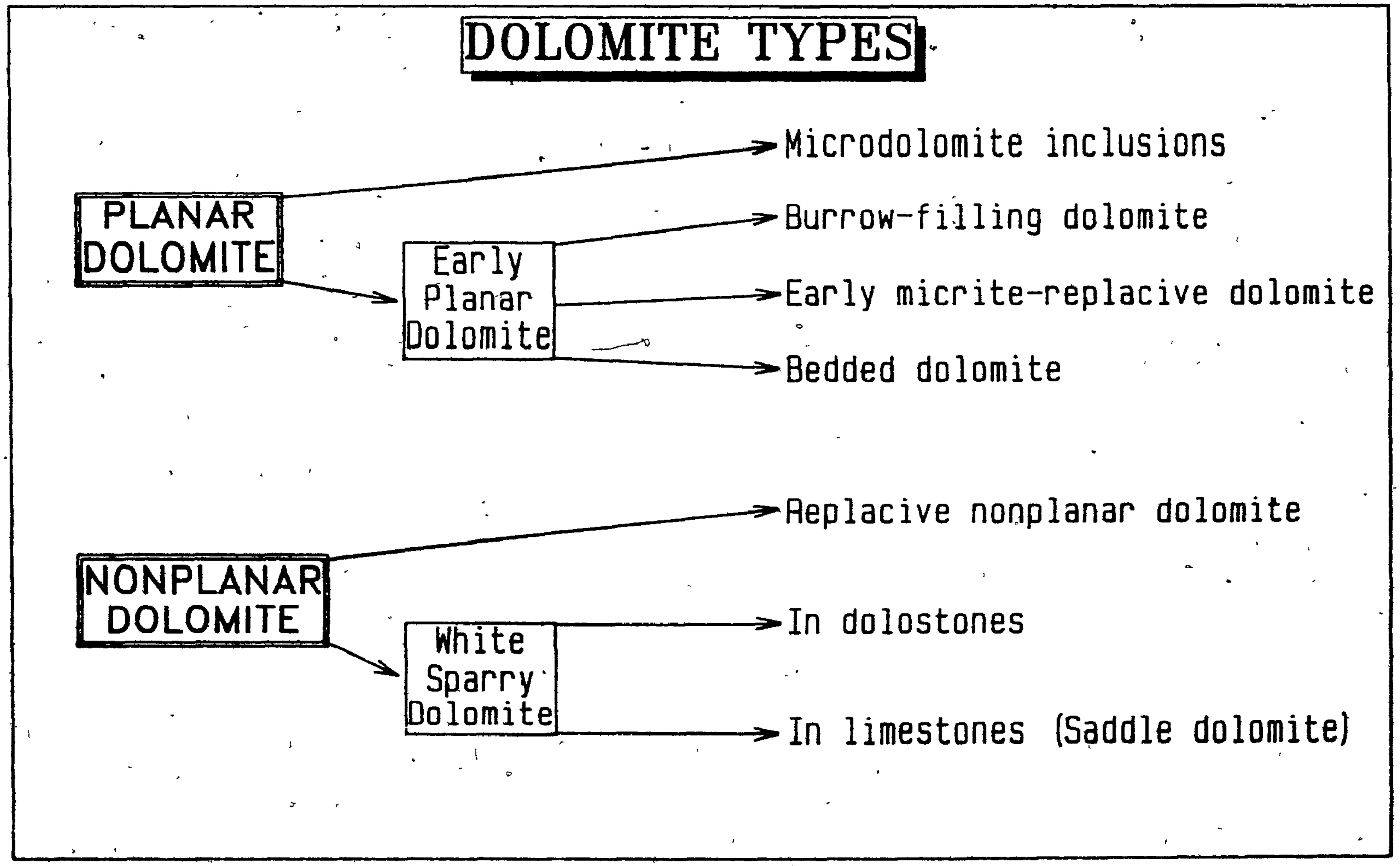

Figure 9: Dolomite classification scheme used in this report.

TABLE 2
Summary of Dolomite Characteristics

<u>Microdolomite Inclusions</u>
Euhedral. 4-15 μm. Unimodal. Clear rhombs.
Occurrence: in echinoderm fragments.

<u>Early Planar Dolomite</u>
Euhedral to subhedral. 30-75 μm. Unimodal. Often cloudy-centred, clear-rimmed.
CL: uniform, dull, orange-red (locally with thin, brighter rim).
XRF: Ca/Mg= 1.143-1.193, mole%Ca= 53.34-54.39.
Isotopes: $\delta^{18}O$= -5.1, $\delta^{13}C$= +0.3; n= 8.
Not banded. No ghosts.
Occurrence: Fabric selective, burrow-filling dolomite, early micrite-replacive dolomite, bedded dolomite, in peloids, rarely in micritic and chert nodules.

<u>Replacive Nonplanar Dolomite</u>
Anhedral to subhedral. 50-300 μm. Usually polymodal, locally unimodal. Inclusion-rich. Dark-coloured in hand specimen ('euhedral' replacive nonplanar dolomite is lighter grey).
CL: medium to bright, reddish-orange, uniform (locally with minor banding).
XRF: Ca/Mg= 1.060-1.111, mole%Ca= 51.46-52.63.
Isotopes: $\delta^{18}O$= -13.9, $\delta^{13}C$= -0.2; n= 8.
Not banded. Ghosts of fossils, peloids, fractures, microstylolites.
Occurrence: Pervasively replaces whole units.

<u>White Sparry Dolomite</u>
Includes: Saddle dolomites in dolostones and limestones.
Anhedral to euhedral. 50 μm to 1 cm. Unimodal or polymodal. Numerous inclusions (less than replacive nonplanar dolomite). White to greyish in hand specimen.
CL: dull to bright, reddish-orange to orange, banded or patchy or uniform.
XRF: Ca/Mg= 1.112, mole%Ca= 52.90.
Isotopes: in dolostones: $\delta^{18}O$= -12.6, $\delta^{13}C$= -0.3; n= 9; (plus two with light carbon: $\delta^{13}C$= -15.2 & -14.1); in limestones: $\delta^{18}O$= -6.0, $\delta^{13}C$= -0.1; n= 3.
Banding common (in inclusion density and Fe content).
Occurrence: fractures, solution-enlarged voids, primary voids, and possibly along stylolites.

Isotopes - average of δ^{18}Oxygen & δ^{13}Carbon; per mil (PDB); n= number of samples.
CL - cathodoluminescence.
XRF - results of x-ray fluorescence analyses.
Ca/Mg - ratio of calcium to magnesium in dolomite.
mole%Ca - mole percentage of calcium in dolomite.

Planar dolomite crystals have straight boundaries. Rocks with a high percentage of pore space or another phase between the dolomite crystals are planar-e (euhedral). Densely packed planar dolomite are planar-s or -a (subhedral or anhedral), but still have a high proportion of straight intercrystalline boundaries.

Nonplanar dolomite refers to all dolomites with anhedral, curved or irregular crystal boundaries and sweeping or undulose extinction patterns. Nonplanar dolomite crystals have roughened edges and a paucity of preserved crystal faces (when in contact with other nonplanar dolomite crystals).

3.2.1 Planar Dolomite

In this study, planar dolomite is subdivided into microdolomite inclusions and early planar dolomite. Based on occurrence, early planar dolomite is divided into 1) burrow-filling dolomite, 2) early micrite-replacive dolomite, and 3) bedded dolomite. In a given sample the crystal size of planar dolomite is usually unimodal, but may locally be polymodal.

3.2.1.1 Early planar dolomite

Early planar dolomite is characterized by euhedral to subhedral rhombs ranging from 30 to 175 μm with a mode at about 70 μm. Early planar dolomite rhombs may be cloudy-centred, clear-rimmed, or have a more or less homogeneous distribution of inclusions. Fabrics vary from planar-e to planar-s in dolomite mottles and planar-e in limestones (Plate 8d,e,f). Dolomite mottling may reflect control by burrows (burrow-filling dolomite) or small-scale interbedding of dolostone (bedded dolomite) and limestone (Plate 9a). A dolomite mottle is defined as any small area of rock, surrounded by limestone, that contains more than 75% dolomite (and is therefore a dolostone). Mottles are usually 95% or more early planar dolomite. Mottles with planar-e texture contain minor amounts of intercrystalline calcite (micrite?). Surrounding the mottles, there may be a transition zone, containing scattered dolomite rhombs, generally 0.5 to 2 cm wide, in which the amount of dolomite decreases with increasing distance from the mottle into the limestone (Plate 8f, also 5c). These transitional dolomite rhombs (planar-e) tend to be larger and better formed than the mottle-rhombs possibly due to a lack of competition for space with other dolomite crystals during growth. Scattered (planar-e) transitional dolomite is termed early micrite-replacive dolomite because it clearly replaced micrite while the precursor to mottle dolomite (void? micrite? grains?) is more problematic. Mottle dolomite may have replaced micrite or some coarser material that originally filled these mottles (Plate 5d,e).

Early micrite-replacive dolomite is not always associated with mottles. Early micrite-replacive dolomite may be scattered throughout a mud-rich limestone or replace the micritic peloids in grainstones (Plate 9b). Early planar dolomite occurs in early-formed micritic nodules (see 3.1.2.1). The percentage of early planar dolomite in the nodules is the same or slightly less than in the surrounding limestones. Microstylolites have residually concentrated the dolomite around the nodule, but the nodules themselves (including the dolomite) are unaffected, suggesting that they formed early.

Early planar dolomite also occurs in chert in argillaceous wackestones from the upper Costigan Member, Hummingbird Creek and Mt. Indefatigable (Plate 9d). At both localities, the chert occurs in discrete zones in nodular, bedded-nodular, and bedded forms. Locally, the chert preserves fine detail, including fossils, peloids, and a relatively uncompacted grainstone texture (Plate 9e), from the limestones it has replaced. Pervasive microstylolitization has concentrated early planar dolomite surrounding the chert, but has not affected the disseminated early planar dolomite contained within.

Plate 9

Planar dolomite, continued

a. Weathered hand specimen showing bedded and burrow-filling early planar dolomite <D>, Hummingbird Creek (#27).

b. Early planar dolomite replacing wackestone intraclasts in grainstone. Cement is blocky mosaic calcite, Costigan Member, Crowsnest Pass (#11). 276 m above base of Palliser Formation. 0.5 mm scale bar.

c. Small calcite-filled fracture cutting early planar dolomite rhomb in wackestone. Micrite has been neomorphosed to microspar. Morro Member, Hummingbird Creek (#27). 159 m above base. 0.025 mm scale bar.

d. Early planar dolomite <e.g., arrow> in early-formed chert nodule. Microstylolites concentrate early planar dolomite in the surrounding micrite (not shown), but do not occur in the chert nodule, indicating that some early planar dolomite formed before chert, which in turn formed before microstylolites. Costigan Member, Mt. Indefatigable (#25). 343 m above base. 0.5 mm scale bar.

e. Nodule preserving relatively uncompacted grainstone fabric, therefore chert formed early, before any pressure solution. Costigan Member, Hummingbird Creek (#27). 214 m above base. 0.5 mm scale bar.

f. Planar microdolomite inclusions in echinoderm fragment. Note similar crystallographic orientation of rhombs. Costigan Member, Crowsnest Pass (#11). 276 m above base. 0.05 mm scale bar.

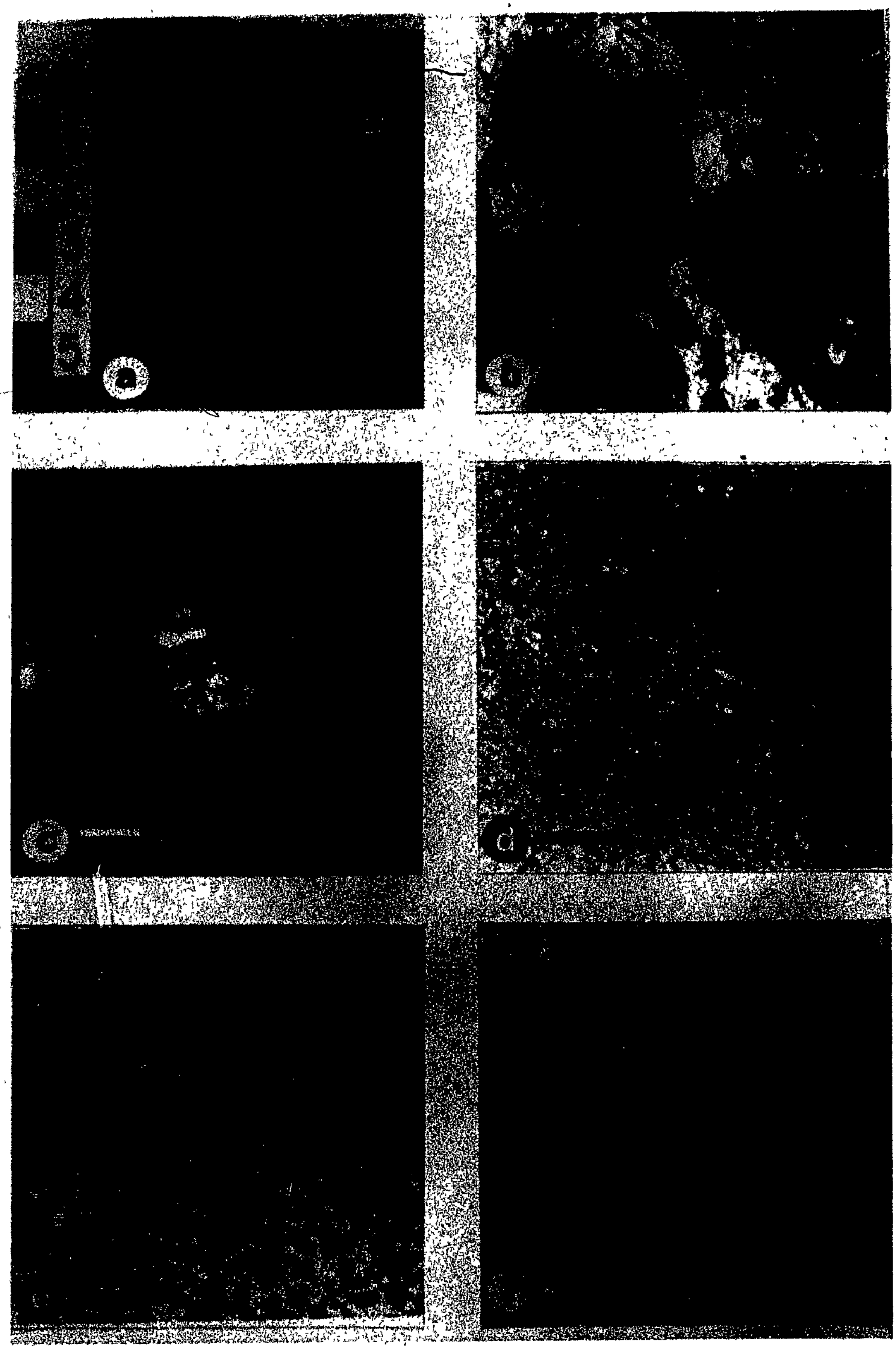

Early planar dolomite is ubiquitous, occurring at all measured sections, at all stratigraphic levels, and in virtually every lithotype, but is most common in micritic rocks types. The only units that do not contain early planar dolomite are the completely replacive nonplanar dolostone, such as at Oldman River, Munroe-Alpine-Boivin, and Mt. Indefatigable.

3.2.1.2 Microdolomite inclusions

Microdolomite inclusions occur in echinoderm fragments and rarely in syntaxial overgrowths on these fragments. They vary between 4 and 15 μm in size, are euhedral (planar-e) and are all crystallographically oriented within single echinoderm fragments (Plate 9f). Microdolomite inclusions occur at all field sections and at most stratigraphic levels.

Lohmann and Meyers (1977) suggested that the oriented dolomite rhombs exsolved from the echinoderm crystal lattice during the transformation of the originally high-Mg calcite to present-day low-Mg calcite mineralogy. They suggested that microdolomite inclusions may be used as a general criterion for identifying carbonate phases that formerly were high-Mg calcite.

3.2.2 Nonplanar Dolomite

In this study, nonplanar dolomites are subdivided into replacive nonplanar dolomites and white sparry dolomites. Replacive nonplanar dolomites have pervasively replaced limestones as shown by preserved primary textures. White sparry dolomites are primary precipitates which fill voids in dolostones and limestones, similar to Gregg and Sibley's (1987) nonplanar cements. Most examples of white sparry dolomite would fit the definition for saddle dolomites. The best examples of 'classic' saddle dolomites occur as late stage cements in pore spaces, where the curved crystal faces and/or cleavages, and systematic, strongly sweeping extinction (Radke and Mathis 1980; and others) are well developed. The useful, descriptive term saddle dolomite is retained because of its wide usage. Anywhere white sparry dolomites nucleated and grew in competition with other nonplanar dolomites, the euhedral saddle form did not develop, resulting in an anhedral mosaic. These anhedral crystals locally grade into true saddle dolomites. While the two terms are used almost synonymously, white sparry dolomite is more general, and saddle dolomite refers to euhedral crystals.

Nonplanar dolomite may have a polymodal or unimodal size distribution. However, replacive nonplanar dolomite is usually polymodal. Nonplanar dolomite is generally coarser than planar dolomite found in the Palliser Formation. Most nonplanar dolomites are nonferroan, however, at Oldman River, both white sparry and replacive nonplanar dolomites are ferroan. Elsewhere, white sparry dolomites locally contain thin ferroan bands.

3.2.2.1 Replacive nonplanar dolomite

Dolostone composed of replacive nonplanar dolomite formed through replacement of limestone. This anhedral dolomite ranges from 50 to 300 μm and larger. The extinction pattern is usually undulose, but is locally sweeping (Plate 10).

Replacive nonplanar anhedral dolomite is usually brown to black in hand specimen, is very inclusion-rich and is usually nonferroan (ferroan at Oldman River). Ghosts of allochems (especially echinoderm columnals) are preserved in the nonplanar dolomite. Also preserved as ghosts are the outlines of shells (especially gastropods and brachiopods), fractures, microstylolites (Plates 12e, 13c), and possibly peloids. Most allochems are replaced nonmimically by a mosaic of crystals that preserve the outline of the grain (Plate 10c,d), but locally, echinoderm fragments are replaced mimically by a single crystal (Plate 10e). Replacive nonplanar anhedral dolomite occurs at most field sections, most commonly at the base of the Palliser Formation, but dolomitized units may occur higher up as well (Mt. Indefatigable and Munroe-Alpine-Boivin).

A subcategory of replacive nonplanar dolomite was recognized where significant intercrystalline porosity (or a non-dolomite mineral filling porosity) is present. This appears to be a very local phenomenon. Euhedral, planar crystals probably developed due to a lack of competitive growth with other nonplanar dolomite crystals (Gregg and Sibley 1987). Intercrystalline boundaries between adjacent dolomite crystals are nonplanar. This 'euhedral' replacive nonplanar dolomite (Plate 10e) tends to be coarser than the truly anhedral replacive nonplanar dolomite and finer than the saddle dolomite (which has curved, or nonplanar, crystal forms) with which it is associated. Crystals range up to 2 mm in size. In hand specimen, euhedral replacive dolomite is an intermediate colour between dark replacive nonplanar dolomite and white saddle dolomite. Its grey colour is due in part to internal inclusions and in part to intercrystalline material which may be black and opaque, especially at Munroe-Alpine-Boivin. Ghost textures occur, although they are less common and less distinct than those occurring in the anhedral replacive nonplanar dolomite.

Euhedral replacive nonplanar dolomite can be distinguished from coexisting saddle dolomite by a lack of inclusions bands forming euhedral outlines (i.e., growth bands), the presence of ghost textures, a darker (lesser) cathodoluminescent response (see 3.4.2), and planar 'dolomite/other-phase' boundaries (versus curved dolomite/other boundaries for saddle dolomite). The euhedral and anhedral replacive nonplanar dolomite types have the same colour and intensity of cathodoluminescence.

Replacive nonplanar dolomite can locally be demonstrated to have formed before white sparry dolomite (Plate 11a,b), but in many examples the timing is ambiguous, and the two phases may have formed concurrently.

Plate 10

<u>Nonplanar dolomite</u>

a. Replacive nonplanar dolostone, Morro Member, Alpine (#24). 0.5 mm scale bar.

b. 10a under crossed nicols.

c. Nonmimically dolomitized echinoderm fragment (ghost) in replacive nonplanar dolostone. Microstylolites, which are not visible in photograph, wrap around ghost, while a stylolite <at arrow> cuts through. This suggests that microstylolites formed while the rock was still limestone, and stylolites formed after dolomitization. Morro Member, Alpine (#24). 0.25 mm scale bar.

d. 10c under crossed nicols.

e. Mimically dolomitized (by single crystal) echinoderm fragment, wrapped (not cut) by microstylolites, replacive nonplanar dolostone, Morro Member, Mt. Murray (#26). 0.5 mm scale bar.

f. Dark grey clasts of replacive nonplanar dolomite in white sparry dolomite. Stylolites occur in replacive dolomite but do not cut white sparry dolomite. Sphalerite is concentrated in replacive nonplanar dolomite at edges of clasts and in 'euhedral' replacive nonplanar dolomite (light grey) around clasts. Morro Member, Munroe (#24).

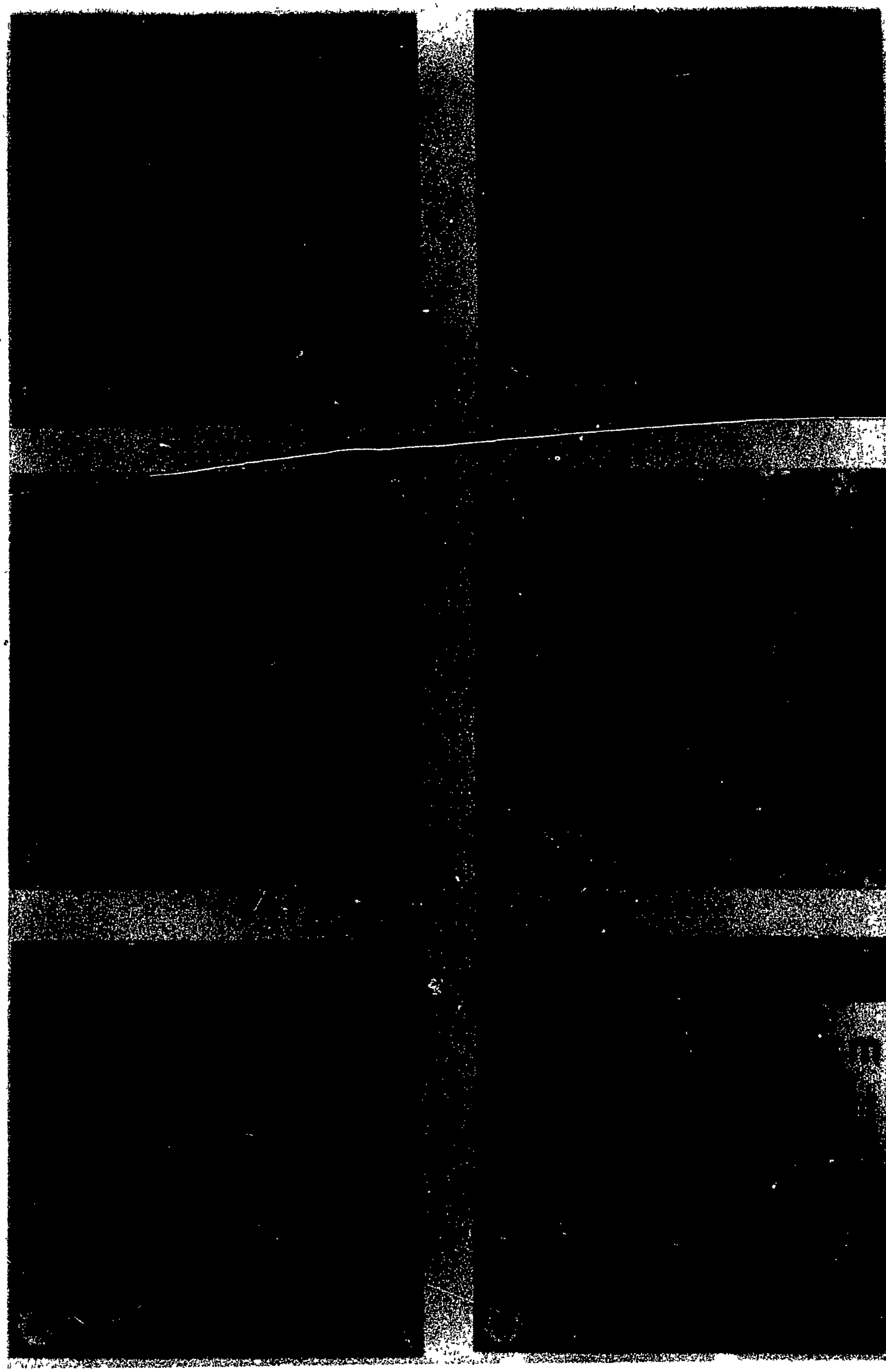

Plate 11

Nonplanar dolomite, continued

a. Replacive nonplanar dolomite clasts <R> surrounded by white sparry dolomite <W>. Sphalerite <S> is concentrated at edges of clasts. Arrow points to stylolite which does not cut white sparry dolomite. Same sample as 10f, Morro Member, Munroe (#24). 1 mm scale bar.

b. 11a under crossed nicols.

c. Inclusion density banding in white sparry dolomite occurring in irregular cavity in replacive nonplanar dolostone. Note that some intercrystalline boundaries are planar. Morro Member, Alpine (#24). 0.25 mm scale bar.

d. Inclusion density banding in white sparry dolomite occurring in peloidal wackestone, Morro Member, Crowsnest Pass (#11). 0.5 mm scale bar.

e. White sparry dolomite crystal <D> in growth cavity formed in massive crystalline sphalerite <S>. Poikilotopic calcite cement <C> occludes remaining pore space. Morro Member, Alpine (#24). 0.5 mm scale bar.

f. 11e under crossed nicols.

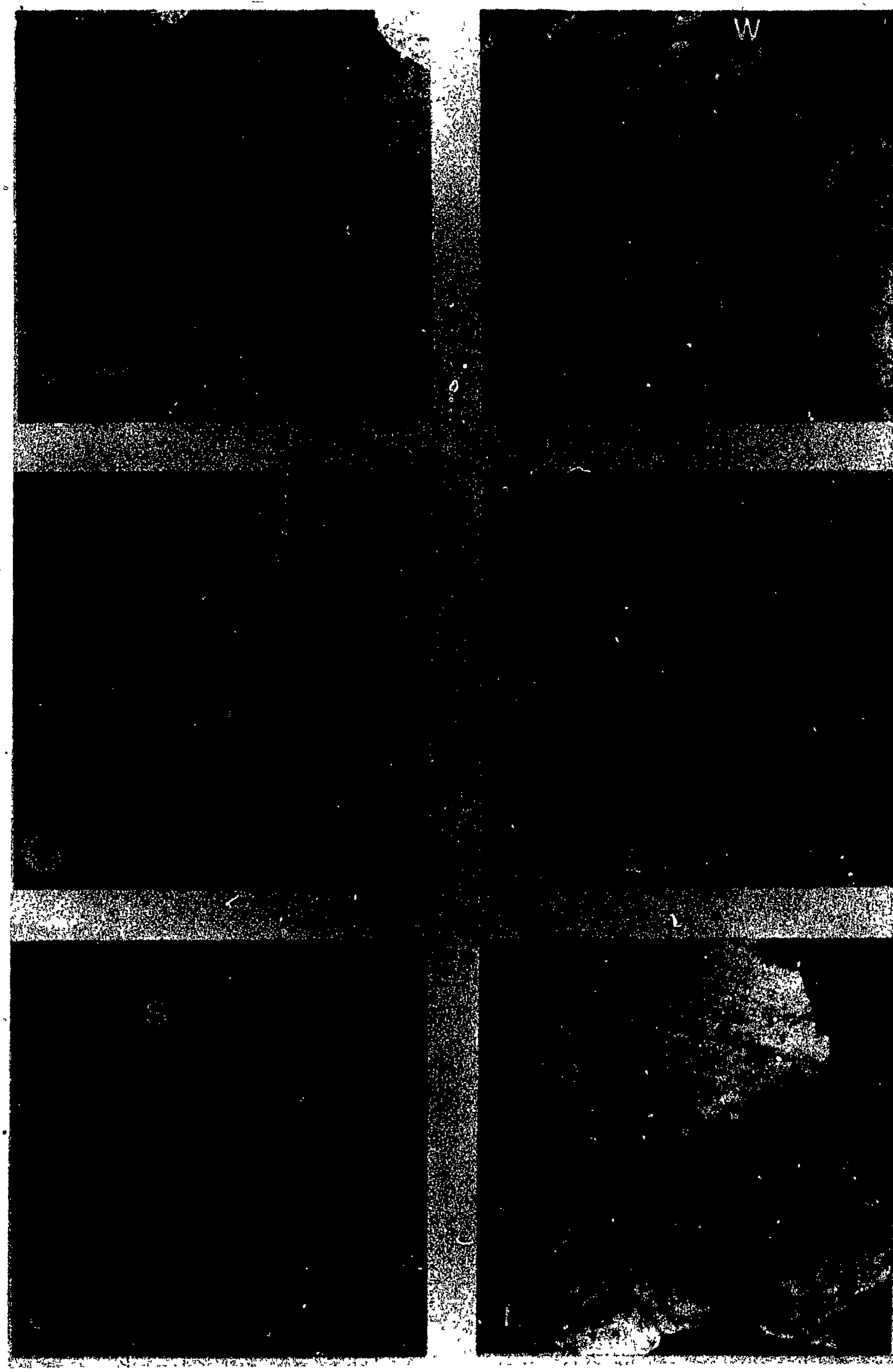
W

3.2.2.2 White sparry dolomite

White sparry dolomites are volumetrically minor but occur locally at all sections and stratigraphic levels. They display strong, systematically sweeping extinction, anhedral or curved crystals and cleavage traces, and pore-filling (cement) textures. Individual crystals range from 100 µm to 1 cm or more in length. Crystals may be nonferroan, ferroan, or mostly nonferroan but containing thin ferroan bands. Banding due to changes in inclusion density is common (Plate 11c,d). This banding, parallel to growth faces, indicates changes in pore fluids during crystal growth and demonstrates the pore-filling nature of this dolomite. White sparry dolomites are inclusion-rich, but less so than replacive nonplanar dolomite, and are usually white in hand specimen, although some ferroan saddle dolomite is grey-blue. Ferroan sparry dolomite is associated with sulfide mineralization at Oldman River.

White sparry dolomite occurs as a white, sparry fracture-filling and in primary and secondary voids. It in-fills irregular cavities in dolostones (Plates 12e,f, and 13) and cavities formed during the growth of sphalerite (Plate 11e,f). In limestones, white sparry dolomite occurs locally in geopetals in gastropod molds, in shelter porosity under tabular stromatoporoids (Plate 12a), solution-enlarged voids (Plate 12b) and as a minor interpeloidal cement (along with blocky mosaic calcite cement) in some grainstones (Plate 12c,d).

3.2.3 Dolomite and Fracturing

Some fractures in limestones contain dolomite. Fracture-filling, nonplanar dolomite with undulose extinction is volumetrically minor but occurs in most sections. Fracture-filling dolomite is probably void-filling (white sparry dolomite). Banding is not present in all cases, and some nonplanar dolomite in fractures may be a replacement of calcite and would therefore be replacive nonplanar dolomite.

Pure dolomite fracture-fillings are rare and most fractures also contain blocky calcite, which, based on petrographic observations, is usually later than the dolomite.

3.2.4 Dolomite and Pressure Solution

3.2.4.1 Dolomite and microstylolites

Dolomite rhombs may be concentrated along the length of wispy microstylolitic seams. This dolomite is usually identifiable as early planar dolomite, and in most cases, similar dolomite occurs scattered throughout the sample, indicating that the dolomite is a (micro)stylo-cumulate. Locally, dolomite of less certain affinity occurs along microstylolites in otherwise undolomitized limestones. This dolomite might be a stylo-precipitate.

Microstylolites that occur in replacive nonplanar dolostones at Munroe-Alpine-Boivin, Mt. Indefatigable, and Oldman River appear to predate the dolomitization. The microstylolites wrap or deflect around the dolomitized ghosts of echinoderm fragments that occur locally in the dolostones (Plates 13c, 10c,d,e). There is now little or no difference (just colour and/or inclusion density) between the "matrix" replacive nonplanar dolomite and the replacive nonplanar dolomitized echinoderm fragments. The consistent exclusion of echinoderms by microstylolites is best explained if it occurred while the rock was still limestone and the echinoderm fragments could act as resistant fragments. In limestones, resistant echinoderm fragments are not cut by microstylolites. Microstylolites do not cross-cut white sparry dolomite and are cut by fractures containing white sparry dolomite. Therefore microstylolitization predated nonplanar dolomitization. However, it is possible that in some cases microstylolites formed after the replacive nonplanar dolomitization.

Plate 12

Nonplanar dolomite, continued

a. Negative print of white sparry dolomite <W> in shelter cavity beneath tabular stromatoporoid (Stylostroma sp.), Morro Member, Hummingbird Creek (#27). 158 m above base of Palliser Formation. 0.25 cm scale bar.

b. White sparry dolomite <W> lining solution-enlarged void in partially early planar dolomitized <E> wackestone <M>. Coarse blocky calcite <C> fills remaining void space. Alizarin red-S/potassium ferricyanide stained hand sample. Alpine (#24).

c. White sparry dolomite crystal <D> with dedolomite bands. In peloidal grainstone. Blocky mosaic calcite cement <C> occludes remaining pore space. Morro Member, China Wall (#17). 2 m above base. 0.5 mm scale bar.

d. 12c under crossed nicols.

Irregular cavities in dolostones

e. White sparry dolomite-filled irregular cavities in replacive nonplanar dolostone. Larger arrow points to dolomitized internal sediment(?) forming geopetal fabric. Smaller arrow points to ghosts of microstylolites. Morro Member, Mt. Indefatigable (#25). 91 m above base.

f. Detail of 12e. Replacive nonplanar dolomite <R> containing ghosts of echinoderm fragments <arrow>. Irregular cavities filled by white sparry dolomite <W>. 1 mm scale bar.

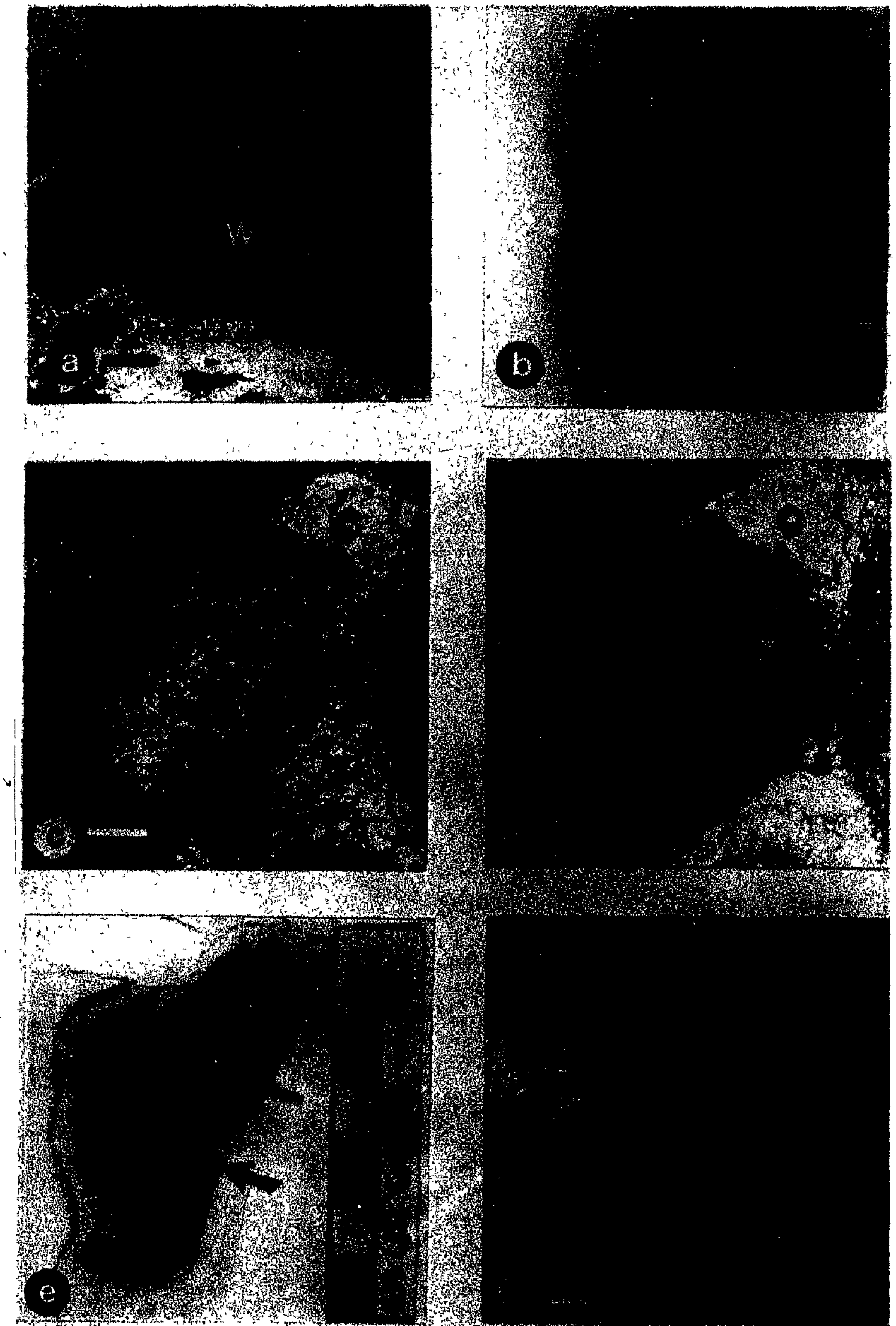
a
W
b
c
e

3.2.4.2 Dolomite and stylolites

Large, euhedral, ferroan dolomite rhombs with slightly to moderately undulose extinction (nonplanar?) occur along stylolites in rocks which do not otherwise contain similar rhombs, therefore, these rhombs are not likely to be a stylo-cumulate. Rather, this dolomite appears to be a stylo-precipitate which grew from fluids that migrated along the stylolite surface. Since these rhombs precipitated in situ, they would be considered as white sparry dolomite.

One sample (from Hummingbird Creek) was noted where dolomite clearly is a stylo-precipitate (or a replacement(?) of a stylo-precipitate, but not a stylo-cumulate) in a space opened along a stylolite surface. White, sparry nonplanar dolomite occurs along a high amplitude stylolite that cuts through this sample that is 90% early planar dolomite.

Stylo-cumulates of dolomite (both planar and nonplanar) are common in partially dolomitized limestone. Stylolites cut through replacive nonplanar dolostone, indicating a phase of total, replacive dolomitization prior to at least the latest stage of stylolite formation. In the example from Hummingbird Creek cited above, primary(?) nonplanar dolomite precipitated along the surface of a stylolite, and is therefore syn- to post-stylolitization.

In several dolostone samples from Munroe-Alpine-Boivin and several from Mt. Indefatigable, stylolites cut through white sparry dolomite that is filling voids in replacive nonplanar dolostones. Also from Munroe-Alpine-Boivin, a sample from the Morro Member dolostone unit contains clasts(?) of dark replacive nonplanar (and grey 'euhedral' replacive nonplanar, see 3.2.2.1) dolomite which are cut by stylolites and are surrounded by white sparry dolomite. The stylolites end abruptly at the boundaries of the clasts and do not cut through the white sparry dolomite (Plates 10f, 11a,b). In some cases, a single stylolite appears to continue through two clasts that are separated by sparry dolomite. Therefore, there is a phase of white sparry dolomite that locally postdates stylolites. Stylolites were not seen cutting fracture-filling white sparry dolomite such as that occurring at Oldman River.

3.2.5 Irregular Cavities in Dolostones

Irregular cavities occur in the Morro Member at Mt. Indefatigable, Mt. Murray, and Munroe-Alpine-Boivin (Plates 12e,f, 13). White spar fills these irregular cavities which occur in replacive nonplanar dolostones. These structures are approximately bedding-parallel, up to 1 cm thick and generally 5 cm or less wide, and commonly display smooth, curved or flat, geopetal bases. The cavity-filling spar consists mostly of white sparry dolomite and locally, later white poikilotopic calcite cement. The white sparry dolomite locally contains thin ferroan bands. The host rock or matrix consists of dark grey-brown nonplanar dolostone containing ghost textures of fossils (Plate 12f), indicating a replacement origin. Swarms of microstylolites also appear to be ghost textures (Plates 12e, 13c). Stylolites cut both replacive and white sparry dolomites.

At Munroe-Alpine-Boivin, these irregular cavities were described by Gibson (1981) as fenestrae. However, this term is often associated with a synsedimentary origin, and is not used. Some of these irregular, tepee shaped, spar-filled cavities resemble, in some aspects, stromatactis. Bathurst (1982) defined stromatactis using five major criteria; (1) irregular, sheet-like masses of sparry calcite (interpreted to have been marine cements) with or without layered, geopetal, internal sediment, (2) smooth, flat or undulose bases, (3) irregular, digitate roofs without visible support, (4) occurrence in swarms with sub-horizontal floors, (5) and local interconnections to form a three-dimensional anastomosing or reticulate structure.

Plate 13

Irregular cavities in dolostones, continued

a. Outcrop view of irregular cavities, Morro Member, Alpine (#24). 5 cm lens cap.

b. Weathered hand sample showing irregular cavities. Lighter grey replacive nonplanar 'host' rock, darker grey geopetal replacive nonplanar dolomite, and white sparry dolomite. Morro Member, Alpine (#24).

c. Thin section showing irregular cavities. Ghosts of microstylolites <arrow> wrap around echinoderm ghosts, Morro Member, Mt. Murray (#26).

d. Hand sample displaying 'pull-apart' irregular cavities, Morro Member, Alpine (#24).

e. Hand sample showing irregular cavities. Note darker replacive nonplanar dolomite which appears to have collapsed from the roofs of the cavities, but did not flatten out into geopetal. Morro Member, Alpine (#24).

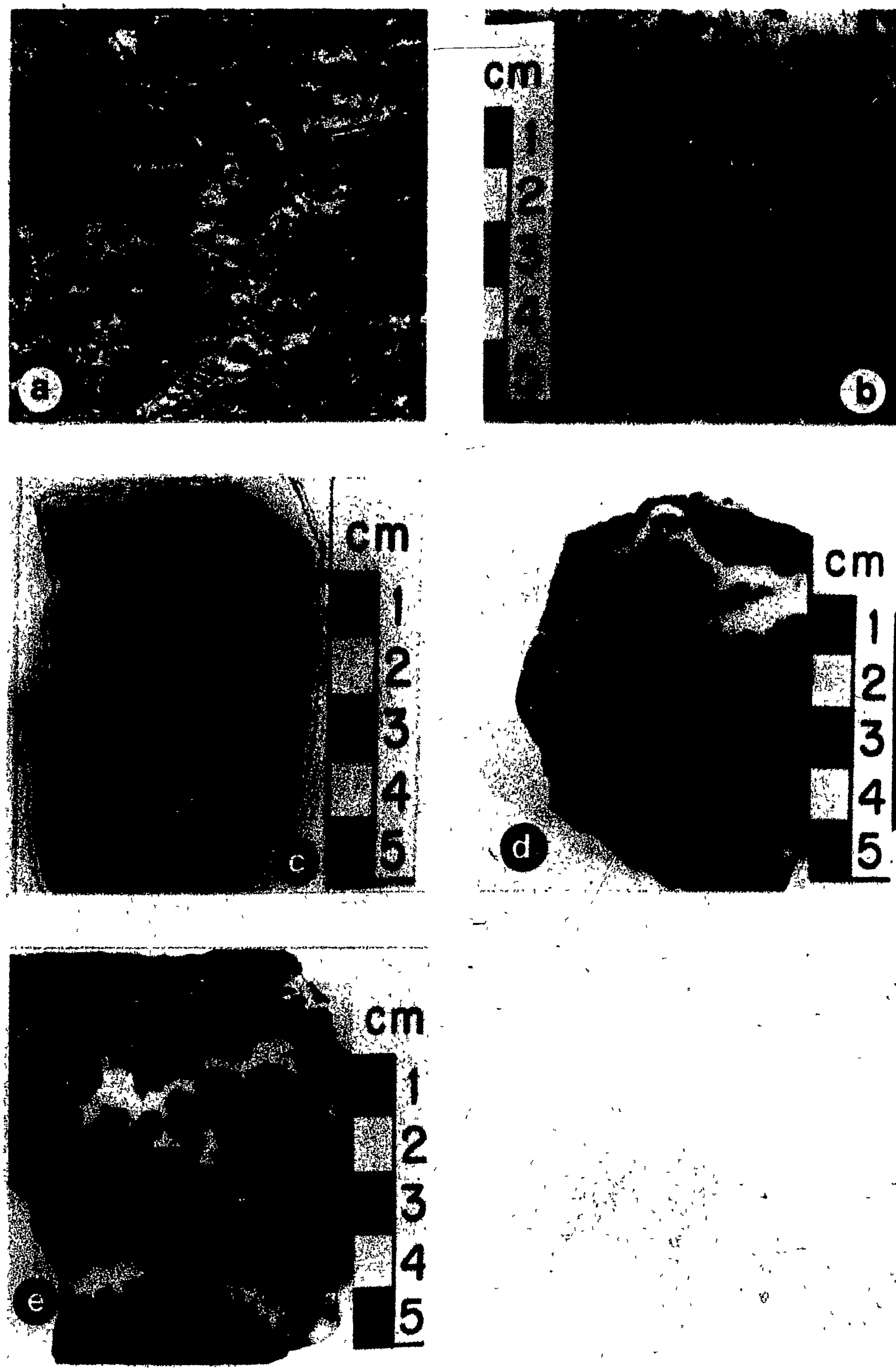
a
cm
1
2
3
4
5
b
cm
1
2
3
4
5
c
cm
1
2
3
4
5
d
cm
1
2
3
4
5
e

Many workers consider Bathurst's (1982) third criteria, the digitate roof, as one of the most important. Bathurst (1982) interpreted this fabric to be indicative of erosion of overlying micrite and is an important feature of classic stromatactis localities such as the Devonian red mud mounds and the Carboniferous Waulsortian mud mounds of Belgium (E.W. Mountjoy, personal communication, 1987). Similarly shaped cavities with irregular, but not digitate roofs may have origins that are different and must therefore be distinguished from true stromatactis. Irregular cavities in the Palliser have irregular or tepee-shaped roofs which are not digitate (Plates 12e,f, 13) and are therefore not stromatactis. However, some form of dolomitized, presumably internal, geopetal sediment is present, the cavity bases are roughly bedding-parallel, the tops are irregular and often tepee-shaped, and the cavities are commonly interconnected. Possibly, the originally limestone host sediments were all or mostly micrite (sparsely fossiliferous mudstones) since so few allochems ghosts were seen in the dolostones containing these structures. A micritic host rock has been reported in most studies of stromatactis. These similarities suggest that the origin of the irregular cavities may be comparable in some respects to stromatactis, and thus may have formed during early submarine diagenesis.

However there is no evidence of banded, isopachous submarine cements in these cavities. Possibly, such cement textures have been obliterated by dolomitization. Since no analogue for these cavities was found in any limestone section, it is possible that they formed during dolomitization of the limestone precursor in the burial environment (see Chapter 4). Partial solution of limestone during dolomitization might have created a semi-interconnected cavity network. Loosened material might have settled down (either before or after dolomitization) to form the flat, geopetal bases or pull-apart structures (Plate 13d). This collapsed material did not always flatten out, and in some samples appears to mimic the shape of the roof (Plate 13e). White sparry dolomite occluded the remaining pore space, possibly precipitating when all the 'available' limestone had been replacively dolomitized. The similar isotopic compositions of the replacive nonplanar and white sparry dolomites (see 3.4.4) provides support for this hypothesis. The negative $\delta^{18}O$ values also supports the burial hypothesis. The cavity distribution may have been controlled by bedding-parallel inhomogeneities, pre-existing porosity, or dissolution of a specific limestone component (fossil?).

3.2.6 Dedolomitization

Dedolomitization (von Morlott 1847) is the replacement of dolomite by calcite, although many studies have since used the term to refer to the replacement of dolomite by other minerals. Dedolomitization only occurs locally in several sections. Dedolomitization fabrics include thin bands of calcite or a reddish-brown stain (iron oxides and hydroxides) that occur in dolomite rhombs (Plate 12c,d). Dedolomitization, though rare, appears to be more common in nonplanar versus planar dolomite.

The distribution and thickness of the iron stained bands in dedolomites closely resembles that of ferroan bands in nonplanar dolomites. The predominance of dedolomitization in nonplanar dolomite may result from a high divalent iron content relative to the low-iron planar dolomite (based on potassium ferricyanide staining).

Numerous workers (e.g., Evamy 1963; Folkman 1969; Katz 1971; Al-Hashimi and Hemingway 1973; Frank 1981) noted the occurrence of iron oxides and/or hydroxides as dedolomitization products (with or without calcite) and suggested that ferroan dolomite was unstable during surface weathering. Al-Hashimi and Hemingway (1973) suggested that this instability might result from crystal lattice disordering caused by the Fe^{2+} ion.

Dedolomitization may be due to the influence of surface processes such as weathering, with the percentage of dedolomitization increasing towards both present-day surfaces (e.g., Al-Hashimi and Hemingway 1973) and ancient unconformities (e.g., Schmidt 1964), or to the flow of meteoric waters undersaturated with respect to calcite and supersaturated with respect to dolomite, possibly due to gypsum dissolution (Back et al. 1981). Dedolomitization may also occur in the deep burial environment (Budai et al. 1987). Experimental studies, such as that by de Groot (1967), have indicated that high water flow rates and low pCO_2 levels promote dedolomitization.

3.3 MINERALIZATION

Introduction

Base metal occurrences in the Palliser Formation have been reported from three areas, the Oldman River (#06) lead-zinc occurrence (Holter 1977), the Munroe-Alpine-Boivin (#24) zinc occurrence (Gibson 1981), and a galena showing at Whiteman Gap (#01) (Geldsetzer et al. 1986). The mineralization at Oldman and Munroe-Alpine-Boivin is related to the formation of replacive and/or white sparry dolomite, and sparry calcite.

3.3.1 Oldman River (#06)

The Oldman River lead-zinc occurrence (Holter 1977) is located on Mount Gass, on the east side of the High Rock Range, near the headwaters of the Oldman River, southwestern Alberta, near the British Columbia border. The upper 76 m of the Palliser Formation are exposed above the Lewis Thrust, overlying Lower Cretaceous non-marine clastics of the Kootenay Formation. Sulfides (in order of abundance: pyrite, galena, sphalerite) are localized around two high-angle, east-west tear faults and a lower-angle intersecting fault, interpreted to be a splay of the Lewis Thrust (Holter 1977).

Plate 14

<u>Features related to mineralization, Oldman River (#06)</u>

a. Banded sample displaying alternations of mineralogy. Dark basal band is sphalerite <S>, galena <G>, and nonplanar dolomite. Next is ferroan white sparry dolomite <W>, and then mixed ferroan white sparry dolomite and sphalerite, 1 mm scale bar.

b. Field location of sample shown in 14a, in footwall of thrust splay. Sample was positioned at level of 5 cm lens cap.

c. Negative print of mineralized sample. Clast (?) of replacive nonplanar dolomite <R> is rimmed by white sparry dolomite <W>, surrounded by fractured bands or crusts of sphalerite and galena (white) and ferroan white sparry dolomite (dark). Remaining pore space occluded by coarse blocky calcite (dark). 1 cm scale bar.

d. Detail of 14c. Fractured bands of sphalerite <S> and ferroan nonplanar dolomite <D>, in-filled by later sparry calcite <C>. 1 mm scale bar.

e. Gossan in hangingwall of thrust fault, and late, calcite-filled fractures, oriented approximately normal to the plane of the thrust. View looking west. Scale given by narrow-gauge rail tracks projecting from talus in middle foreground.

f. Edge of calcite-filled fracture (white). Grey, ferroan white sparry dolomite lines wall composed of ferroan replacive nonplanar dolomite. Some white sparry dolomite (grey in photograph) has been 'torn' from wall of fracture. 5 cm lens cap.

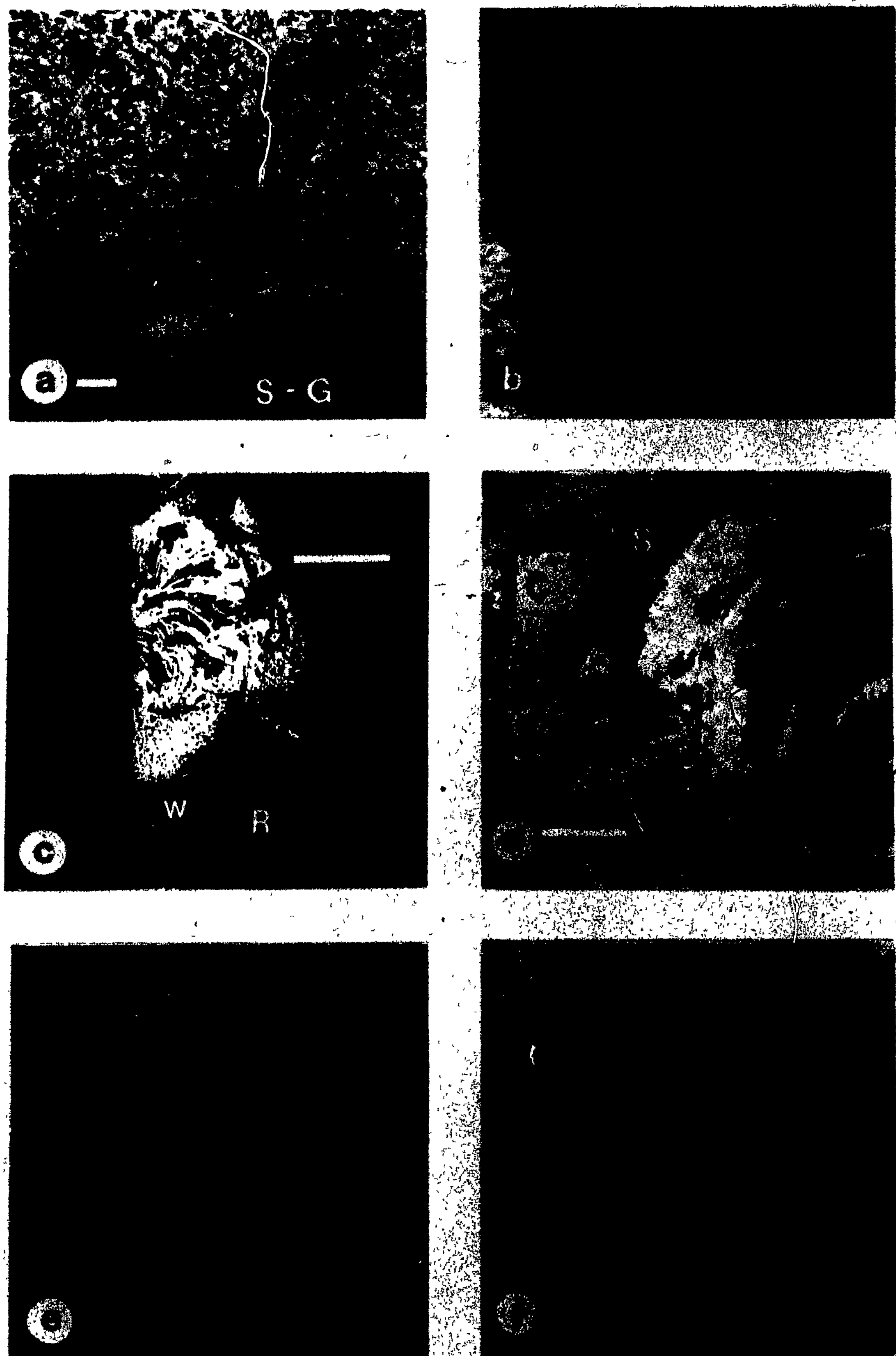
a
S - G
b
c
W
R

Sulfides are associated with nonplanar dolomite in, and surrounding, the fault intersections. Massive and disseminated sulfides occur as pods in the footwall of the thrust splay, below a limonitic fault gouge. There are also some pods of sulfide mineralization in the hangingwall. Some massive and disseminated sulfides occur with primary nonplanar dolomite and calcite along the thrust fault plane.

Thin bands of mixed white sparry dolomite and sphalerite alternate with bands of sphalerite-poor white sparry dolomite (Plate 14a,b). This mixing suggests that nonplanar dolomite and sphalerite were co-precipitating. The dolomite in the sphalerite-poor bands has uniform, medium reddish-orange cathodoluminescence while the dolomite in the sphalerite-rich bands has patchy medium and bright reddish-orange luminescence (Plate 16e). Locally, bands are fractured and distorted, as shown by brecciated sphalerite and dolomite 'crusts' (Plate 14c,d), and warped cleavages in galena. Holter (1977) reported fractured pyrite bands. The banded nature of the sulfides and ferroan white sparry dolomite suggests that they precipitated in open spaces that might have formed by the physical opening of fractures, or the chemical solution of wall rock, or a combination of both. However, no evidence of solution was found in the nearby, stratigraphically equivalent limestone section.

Surrounding the fault gouge is a zone of replacive nonplanar dolostone containing disseminated sulfides. The replacive nature of this dolomite is shown by rare ghost textures of fossil fragments. Some of the dolomite interpreted as being replacive has been coarsened to such an extent that no original textures (i.e., ghosts) are preserved.

Calcite-filled fractures range from millimetre- to metre-scale (Plate 14e). Most fractures are in the hangingwall, oriented approximately normal to the plane of the thrust fault (Holter 1977). These cut all diagenetic phases. Locally, coarse ferroan white sparry dolomite precipitated on the replacive nonplanar dolomite walls of the fractures (Plate 14f). In places, saddle dolomites are fractured and healed by non-ferroan, syntaxial white sparry dolomite. In isolated examples, euhedral pyrite occurs after saddle dolomites in fractures. In places, ferroan saddle dolomite is corroded and replaced by nonferroan, coarse, equant calcite which fills the majority of the volume of the fractures. Fractures containing calcite and ferroan white sparry dolomite, cut and are cut by, stylolites, indicating more than one phase of stylolitization. The younger stylolites may be tectonic.

In hand specimen, the sphalerite is dark brown; in thin section, it is colour-banded, usually with a darker centre and several lighter outer bands. Sphalerite may be disseminated or massive; individual crystals are anhedral to subhedral, and usually range from 0.5 to 1 mm, but locally range from a few micrometres to 4 mm. Pyrite occurs as anhedral masses. Galena occurs as disseminated or massive, subhedral to euhedral grains up to several centimetres in size.

As the mineralization appears to be localized by faulting related to the Laramide Orogeny, Holter (1977) suggested that it is constrained to be syn- to post-orogenic. Similarly, associated white sparry dolomite may also be syn- to post-orogenic. Along strike, the Lewis Thrust carries the Palliser Formation over the Campanian Belly River Formation, constraining the age of thrusting in the Front Ranges and Foothills to be younger than 74.5-84 Ma.

Holter (1977) suggested that the age of thrusting is much younger (by 100 to 250 Ma) than the minimum ages reported for the closest major intrusive events in the eastern Cordillera, ruling out a direct magmatic source for the mineralizing and dolomitizing fluids. This is not necessarily correct as complex, multiple-intrusion quartz monzonite batholiths with radiometric ages ranging from 45 to 111 Ma occur 100 km due west of Oldman (and 75 km west of Munroe-Alpine-Boivin), in the Lardeau, B.C. map-area (Reesor 1973). Other plutons in the same area have emplacement ages of 94 and 122 Ma (Höy and van der Heyden 1988). Archibald et al. (1983) reported Jurassic to mid-Cretaceous intrusives in and near the Kootenay Arc.

The interpretation that the mineralization is localized around late tectonic features has important implications for the understanding of the local paragenetic sequence and for regional exploration for lead-zinc deposits. In addition, there is a lack of published reports of dolomite (and Pb-Zn sulfides) in late, thrust-related fracture systems in the Canadian Rockies. For these reasons, it is important to consider other possible models. E. W. Mountjoy (personal communication, 1988) suggested an alternative whereby sparry dolomite, sphalerite, and galena may have been present in a fracture system of unknown affinity prior to thrusting. Remobilization of sulfides might have occurred when faulting "fortuitously" cut the mineralized unit. This sort of model could explain the unusual nature of the Oldman occurrence (i.e., its relationship to thrusting). However, Oldman is not unique. Geldsetzer et al. (1986) reported a galena show in a "shear zone" in the Morro Member near Whiteman Gap (#01). Further afield, Budai et al. (1987) noted dolomite in tectonic veins in the Madison Group (Mississippian) of the Wyoming and Utah Overthrust belt.

3.3.2 Munroe-Alpine-Boivin (#24)

The Munroe-Alpine-Boivin section (Gibson 1981) is located east of the Bull River near its headwaters in the Elk Provincial Forest in southeastern British Columbia. The geology has been mapped and briefly described by Gibson (1981).

Sphalerite mineralization occurs in the upper Morro Member in an overturned panel. The mineralization is confined to pods of dolostone, oriented parallel to bedding, composed mostly of dark, replacive nonplanar dolomite with patches of white sparry dolomite. Many of these pods are fault-bounded. Gibson (1981) interpreted the bedding-parallel patches to be fenestral porosity filled by white sparry dolomite, with late-stage sphalerite having precipitated last. These irregular cavities are discussed in 3.2.5. The only calcite components in the dolostones are poikilotopic cements that fill the pore space not occluded by white sparry dolomite, and late, completely cross-cutting, calcite-filled veins. Some differences from the Oldman River section are that pyrite only occurs in limestones, replacing micrite, there is no galena, and sphalerite does not occur in fractures.

Sphalerite is pale yellow to amber to greenish in colour. The colour is either uniform or slightly mottled, but is not banded. Sphalerite occurs as small, disseminated crystals or as large, coarsely crystalline masses. Individual crystal sizes range from 100 μm to 5 cm. Sphalerite, along with all other phases, is fractured and healed by sparry calcite. However, the fracturing is much less intense than it is at Oldman River.

Petrographic study of samples from Munroe-Alpine-Boivin indicates that sphalerite precipitated before the major period of in-filling by white sparry dolomite. Sphalerite only occurs in replacive nonplanar or 'euhedral replacive nonplanar' dolomite (see 3.2.2.1), and does not occur within the white sparry dolomite. Sphalerite mineralization is commonly associated with haloes of nonplanar dolomite that luminesces brighter than the surrounding replacive nonplanar dolomite (Plate 15d). This is similar to the relationship seen at Oldman River (Plate 16e). Locally, white sparry dolomite, followed by coarse, poikilotopic calcite, precipitated in cavities in large masses of crystalline sphalerite (Plate 11e,f).

Brecciated replacive dolostones provide a clue as to the timing of pervasive dolomitization with respect to mineralization. Clasts of replacive nonplanar and euhedral replacive dolomite are surrounded by white sparry dolomite (Plates 10f, 11a,b). Pressure solution seams which cut the replacive dolomite do not affect the white sparry dolomite. In addition, sphalerite occurs in the replacive nonplanar and euhedral replacive nonplanar dolomite, but not in the white sparry dolomite, suggesting that, at least locally, white sparry dolomite formed later than the replacive dolomite.

Sphalerite may have formed at the same time as the replacive dolomite, or have nucleated in intercrystalline spaces after this dolomite had formed. In either case, it predates the white sparry dolomite.

3.3.3 Local Paragenetic Sequences

An overall paragenetic sequence based on all sections is presented in Chapter Four. For comparison, the paragenetic sequences for Oldman River and Munroe-Alpine-Boivin are:

<u>Oldman River</u>

Limestones: 1) Early planar dolomite, 2) Microstylolites, 3) Fracturing + calcite, 3) Stylolites.

Dolostones: 1) Microstylolites (in precursor limestones), 2) Ferroan replacive nonplanar dolomite, 4) Galena, sphalerite, pyrite, and ferroan white sparry dolomite, 5) Nonferroan syntaxial white sparry dolomite, 6) Stylolitization, 7) Tectonic(?) fracturing + ferroan white sparry dolomite, minor pyrite, and calcite, 8) Tectonic(?) stylolitization.

<u>Munroe-Alpine-Boivin</u>

Limestones: 1) Early planar dolomite, 2) Microstylolites, 3) Solution void formation, 4) Sparry calcite, 5) White sparry dolomite, 6) Fracturing + calcite, 7) Stylolites, 8) Fracturing + calcite. ?) Pyrite occurs after early planar dolomite.

Dolostones: 1) Pressure solution (in precursor limestones), 2) Replacive nonplanar dolomite, 3) Stylolites, 4) Sphalerite, 5) Local brecciation, 6) White sparry dolomite, 7) Stylolites, 8) Poikilotopic calcite, 9) Fracturing + calcite.

3.4 GEOCHEMISTRY

Introduction

The results of chemical analyses are summarized in this section. Staining, cathodoluminescence, elemental distribution, and isotopic composition are important to the identification and understanding of various carbonate phases.

3.4.1 Staining

Staining with alizarin red-S/potassium ferricyanide solutions produced pink to red calcite, unstained dolomite, pale to medium blue ferroan dolomite, and, rarely, purple ferroan calcite.

Overall, ferroan calcites and dolomites are rare to absent, except at Oldman River and Munroe-Alpine-Boivin, where the majority of ferroan phases occur. At Munroe-Alpine-Boivin, the uppermost Costigan Member contains ferroan dolomite and calcite in partially dolomitized wackestones, packstones and mudstones, which weathers to a distinct orange-brown. The Oldman section contains ferroan primary nonplanar (white sparry) dolomite associated with the mineralization along fractures and faults cutting the upper Costigan, where the highly weathered gossan imparts a brownish-orange colour to the hillside. At both sections, most of the ferroan dolomite was nonplanar.

White sparry dolomites, especially saddle-types, locally have alternating ferroan/non-ferroan banding, suggesting changes in the chemistry of the pore fluids during precipitation. These iron-banded white sparry dolomites occur at Mt. Indefatigable, Oldman River, Munroe-Alpine-Boivin, China Wall and Crowsnest Pass.

3.4.2 Cathodoluminescence

Introduction

Observations of cathodoluminescence must be internally consistent so that the relative observations of luminescence (light versus dark, orange versus red, etc.) are useful. Figure 10 summarizes the classification of observed cathodoluminescent responses.

Five categories pertaining to the degree of luminescence are used in this report. (1) Non-luminescent means the phase is black, emitting no light in response to excitation. (2) Dark luminescence means a very faint response. The colour of the emitted light (e.g., dark red) can be determined with some difficulty. (3) Dull, (4) medium, and (5) bright are relative (and subjective) classifications of the intensity of the emitted light. Dull luminescence means the phase has an easily determined colour and stands out clearly against any non-luminescent phases.

Three textural categories are used to describe the distribution of the luminescence within single crystals or groups of crystals. (1) Uniform luminescence refers to an even, homogeneous distribution of colour and intensity. Uniform luminescence would indicate a homogeneous crystal, which therefore likely reflects formation under relatively uniform chemical conditions. (2) Banded luminescence refers to a distinct, sharp-edged alternation or change (usually in intensity) within individual phases. This is usually seen as an alternation of lighter and darker bands within, and parallel to the faces of, crystals. Luminescent banding may show the outlines of previous growth stages of crystals. Sequences of crystal growth bands can occasionally be correlated between crystals (cement stratigraphy: Meyers 1974). Banding indicates pore-filling growth (not replacement) under varying chemical conditions. (3) Patchy luminescence is a diffuse alternation or mottling of lighter and darker zones within single crystals or groups of crystals (i.e., cutting across crystal boundaries). Patchiness may indicate neomorphism and/or irregular incorporation of available ions during formation under variable chemical conditions. Possibly, some patchy luminescence may be caused by polishing irregularities on the surface of thin sections.

Results

Calcite

Most micrite is uniformly non-luminescent or dark or dull red luminescent (Plate 15b,c). Where neomorphism has coarsened micrite to microspar and pseudospar, the cathodoluminescence is slightly brighter and patchy. Calcite in fractures shows dull to medium, salmon-pink to red luminescence that is usually uniform but is locally patchy (some darker patches). Most calcite cements display uniform, dark to dull red cathodoluminescence. However, in one grainstone sample from Hummingbird Creek, some very coarse blocky mosaic calcite cement displays multiple cathodoluminescent bands, ranging from dull red to non-luminescent. Brachiopod shells are non-cathodoluminescent, with some thin darkly luminescent bands in some samples (Plate 15a).

Dolomite

Early planar dolomite displays uniform, dull orange-red luminescence (Plate 15c). Locally, early planar dolomite luminescence is patchy, or displays thin, brighter rims on individual rhombs, or is medium orange in colour.

Nonplanar dolomite exhibits the most variable cathodoluminescence; medium to bright reddish-orange, and uniform, patchy, or banded. Generally, the cathodoluminescence of replacive nonplanar dolomite is more uniform and slightly darker than that of coexisting white sparry dolomite (Plate 15e).

White sparry dolomite cathodoluminescence ranges from dull to bright, reddish-orange to orange, and is banded, patchy, or uniform. The best development of luminescent banding occurs in saddle dolomites in both dolostones (Plate 15e) and limestones (Plate 16a). However, white sparry dolomite in dolostones (<W> in Plate 16e) and limestones (Plate 16b) may be mostly uniform. The luminescence of white sparry dolomites in limestones is more orange and less bright than the luminescence of white sparry dolomites in dolostones. Also, patchy luminescence only occurs in white sparry dolomites in dolostones (upper part of Plate 16e). Very bright, orange to orange-yellow luminescing late-stage, white sparry dolomite heals fractures, forms syntaxial overgrowths on, and replaces nonplanar dolomite (replacive nonplanar and white sparry dolomites) in the Oldman River and Munroe-Alpine-Boivin sections (Plates 15d, 16c,d,e).

Sulfides

At Oldman, sphalerite crystals have non-luminescent cores with very bright yellow luminescent rims (Plate 16e). At Munroe-Alpine-Boivin, sphalerite has patchy, yellowish-green and very bright yellow cathodoluminescence (Plate 15e); the rims are usually bright yellow, like the sphalerite at Oldman River.

Some euhedral pyrite crystals from Munroe-Alpine-Boivin (Plate 15b) contain inclusions of small, euhedral, medium red-orange luminescing dolomite rhombs and irregularly shaped patches of dark red luminescing calcite (micrite?). These authigenic pyrite cubes occur in a partially dolomitized (early planar dolomite) mudstone. The amount and distribution of dolomite is similar in the pyrite and micrite, suggesting that the pyrite has replaced parts of the dolomitized limestone, but preserved patches of the early planar dolomite and micrite.

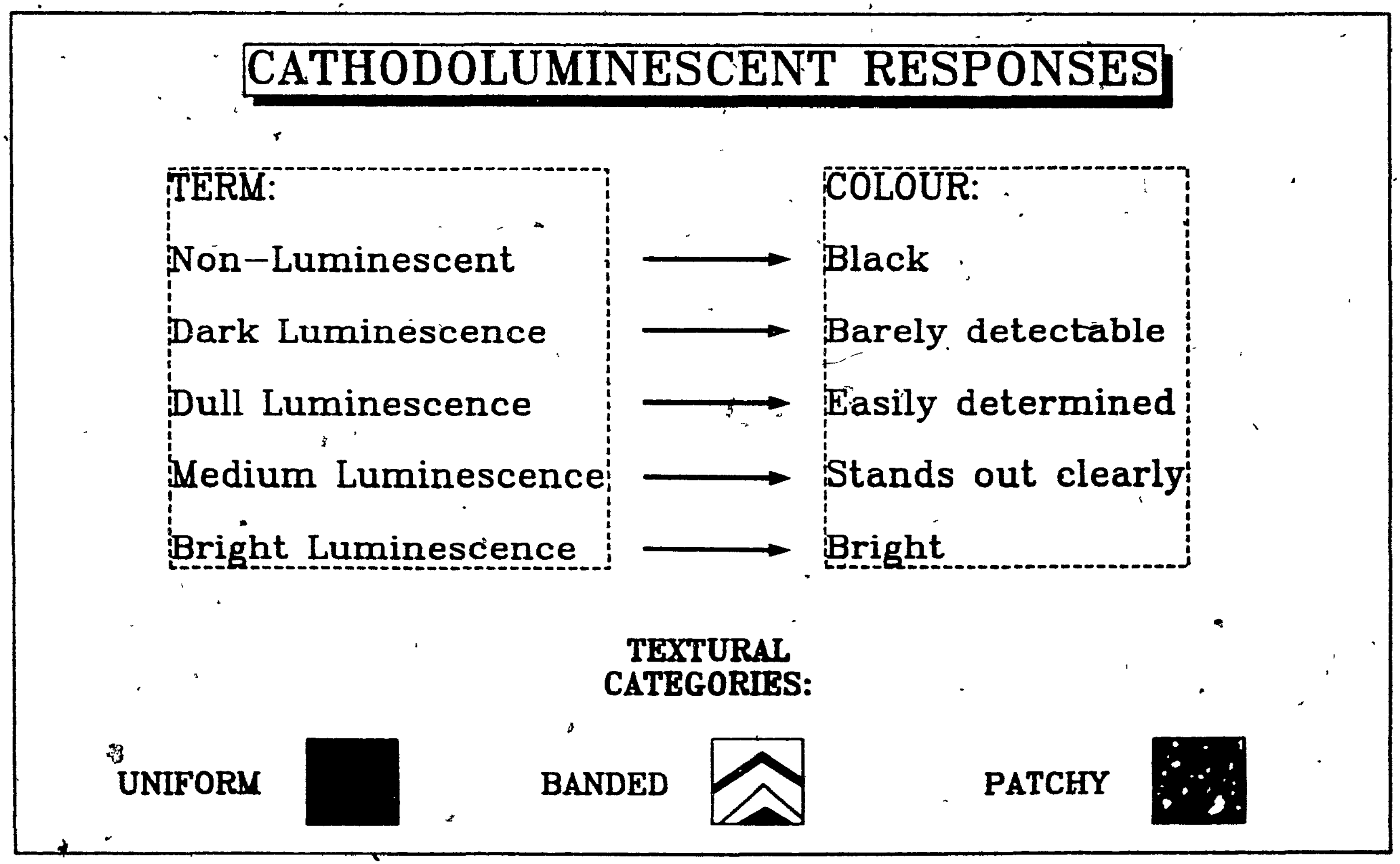

Figure 10: Types of cathodoluminescence recognized, see text for further explanation.

Plate 15

Cathodoluminescence

a. Non-luminescent brachiopod shell in uniform, dark red luminescing micrite. Note thin, darkly luminescing bands in shell. Costigan Member, Hummingbird Creek (#27). 1 mm scale bar.

b. Non-luminescent, euhedral pyrite crystals replacing uniformly dull luminescing micrite. Pyrite contains patches of micrite and uniformly medium luminescing early planar dolomite (which also occurs in the micrite). Alpine (#24) 0.5 mm scale bar.

c. Uniformly dull luminescing early planar dolomite <D> in burrow; micrite <M> is uniformly darkly luminescing. Oldman River (#06). 50 m above base of Palliser Formation. 0.1 mm scale bar.

d. Patchy, brightly luminescing nonplanar dolomite associated with sphalerite <S> replacing and/or cutting uniformly medium luminescing replacive nonplanar dolomite. Morro Member, Alpine (#24). 1 mm scale bar.

e. Cathodoluminescent banding in white sparry dolomite <W>, in cavity next to sphalerite <S> (dark to non-luminescent, with bright rims), in uniformly medium luminescing replacive nonplanar dolostone <R>. Morro Member, Alpine (#24). 0.5 mm scale bar.

f. Close-up of 15e, showing large white sparry dolomite rhomb <W> in plane polarized light for comparison. Replacive nonplanar dolomite <R>, sphalerite <S>. 0.5 mm scale bar.

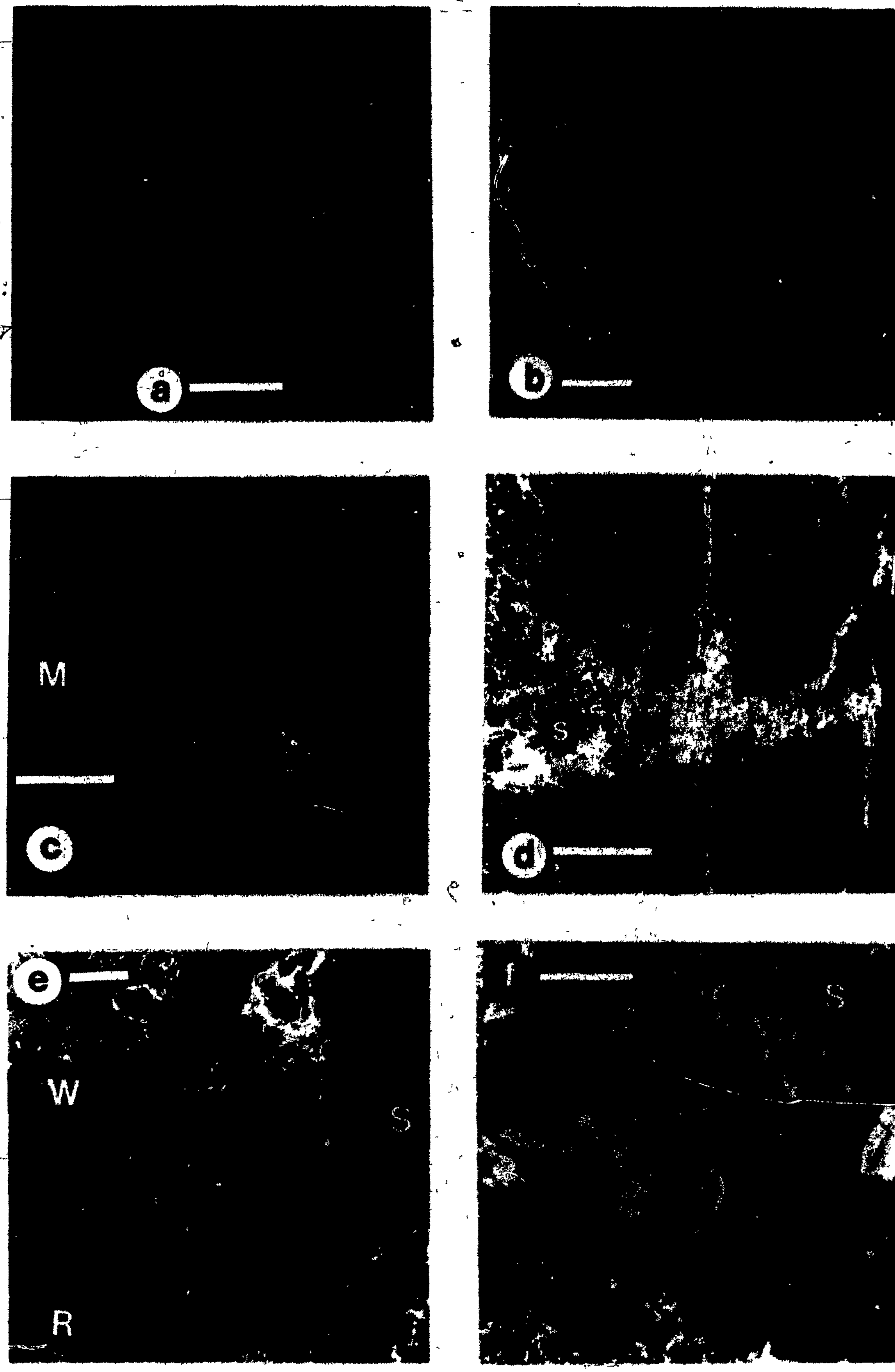

a
b
M
c
S
d
e
W
S
R
f
S

Plate 16

<u>Cathodoluminescence, continued</u>

a. Cathodoluminescent banded white sparry dolomite in peloidal wackestone, Morro Member, Crowsnest Pass. 5 m above base of Palliser Formation. 0.5 mm scale bar.

b. Mostly uniform, medium luminescing white sparry dolomite <D>, with thin bright rims, in shelter cavity beneath stromatoporoid (same sample as 4e), coarse blocky calcite <C> fills remaining pore space. Morro Member, Hummingbird Creek. 157 m above base. 0.5 mm scale bar.

c. Ferroan white sparry dolomite rhombs <D> displaying patchy medium/bright luminescence. Bright luminescing dolomite (nonferroan) appears to be replacing medium luminescing dolomite. Alizarin red-s stained calcite <C> is darkly luminescent. Oldman River (#06). 0.5 mm scale bar.

d. Medium luminescent, ferroan white sparry dolomite is syntaxially overgrown along fractures by nonferroan, brightly luminescing white sparry dolomite. Oldman River (#06). 0.5 mm scale bar.

e. Banded sample 14a in cathodoluminescent light. Galena <G> is non-luminescent; sphalerite <S> is non-luminescent with bright rims; lower, ferroan, white sparry dolomite band <W> in uniformly medium luminescing; white sparry dolomite that is mixed with sphalerite displays patchy, medium/bright luminescence, brightly luminescing dolomite is nonferroan. Oldman River (#06). 0.5 mm scale bar.

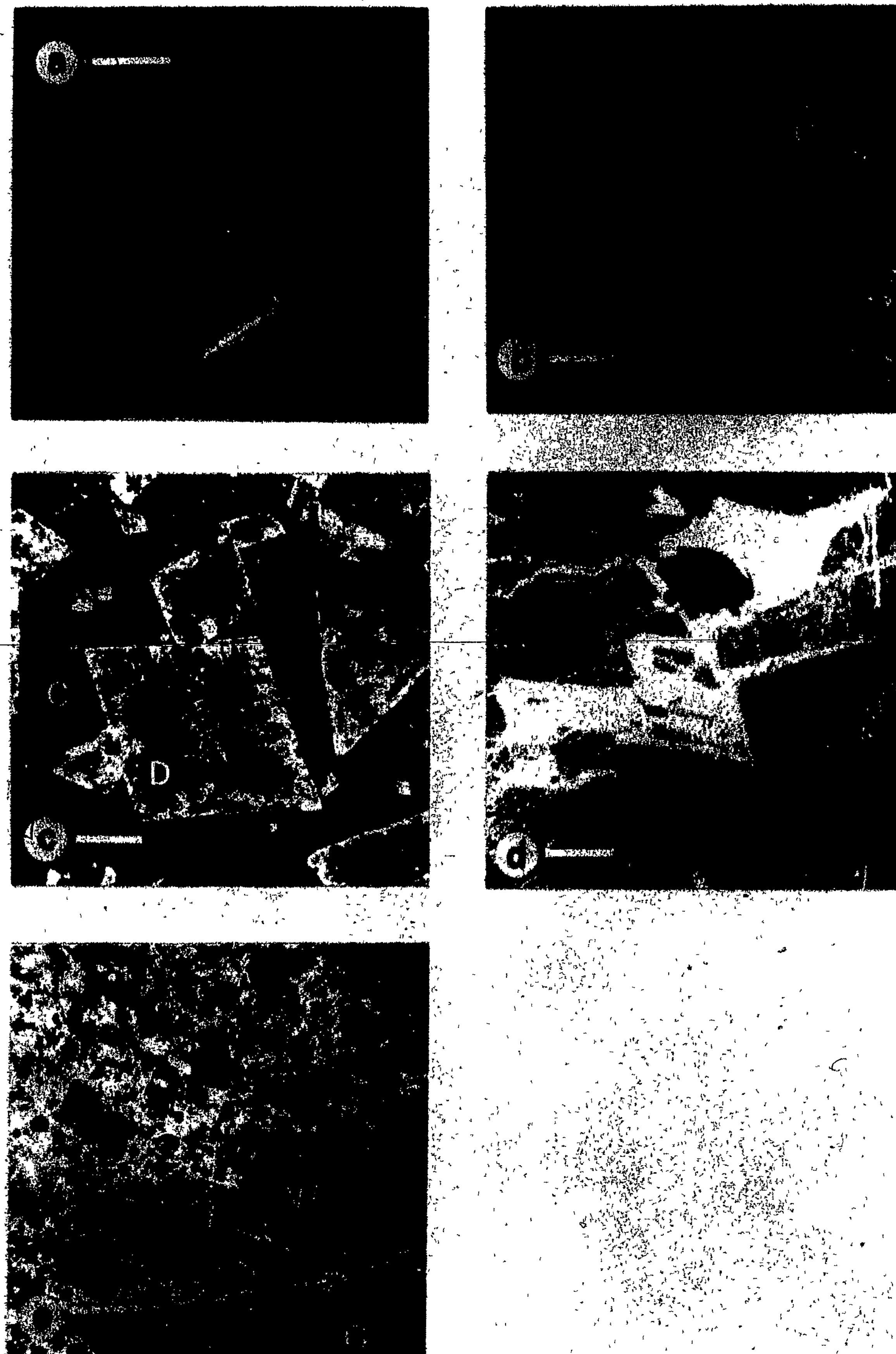
C
D

3.4.3 Calcium and Magnesium

Six dolomite samples were analyzed by x-ray fluorescence (XRF) in part to determine their calcium/magnesium ratios (Table 3). Three samples of early planar dolomites had Ca/Mg ratios of 1.143 to 1.193 (or mole% Ca of 53.34 to 54.39) while three nonplanar dolomite samples (1 replacive nonplanar, 1 mixture of white sparry and replacive nonplanar dolomite, and 1 white sparry dolomite) had ratios of 1.060 to 1.112 (or mole% Ca of 51.46 to 52.90). Although six samples is a statistically small population, and the range is not large, nonplanar dolomites are less calcian than early planar dolomite. This may represent a retention by early planar dolomites of originally high calcium contents from precursor early proto-dolomites which formed on or near the sea floor or during shallow burial. Later, nonplanar dolomite formed under deeper burial conditions with lower calcium values (Ca/Mg ratios closer to the ideal of 1:1). Alternatively, coarser crystalline nonplanar dolomites may have lost calcium relative to precursor planar dolomites during neomorphism.

Table 3
Calcium and Magnesium in some Dolomites

sample number	mol%Ca	Ca/Mg	sample type
HC 33	54.39	1.193	early planar dolomite
CN 10	53.76	1.162	early planar dolomite
HC 44	53.34	1.143	early planar dolomite
OLD 7	52.80	1.112	white sparry dolomite
OLD 2	52.63	1.111	white sparry dolomite
MAB 45	51.46	1.060	replacive nonplanar dolomite

3.4.4 Stable Isotopes of Carbon and Oxygen

Carbon and oxygen isotope data for 32 dolomite and 20 calcite analyses are listed in Appendix Two. Statistics for these data have been calculated by phase type (Tables 4 and 5). All results of carbon and oxygen isotope analyses are expressed as δ ('delta') values, in parts per thousand (per mil) relative to the PDB standard.

Figure 11 shows the stable isotope data for all analyzed carbonates, and Figure 12 the dolomite samples. Four groups of dolomites are distinguished; 1) saddle dolomites (white sparry) that occur in limestones, 2) saddle dolomites (white sparry) that occur in dolostones, 3) replacive nonplanar dolomites, and 5) early planar dolomites.

Most nonplanar dolomites (Figure 12: white sparry dolomites in dolostones and replacive nonplanar) have a similar narrow range of $\delta^{13}C$ (+0.4 to -1.3) and a wide range of $\delta^{18}O$ (-9.3 to -14.9) that overlap and are indistinguishable from each other solely on the basis of stable isotopes. The nonplanar samples which do not overlap the others are saddle dolomites in limestones, which overlap early planar dolomites at lower ($\delta^{18}O$) values. The $\delta^{13}C$ of dolomites are close to zero (except for three anomalously negative analyses).

Considerable variation occurs in the $\delta^{18}O$ values of the various phases. Early planar dolomites have the lowest $\delta^{18}O$ values, ranging from -3.4 to -6.6 and averaging -5.1. This range partially overlaps early (penecontemporaneous?) sabkha-type dolomites from the subsurface Wabamun Group, with $\delta^{18}O$ ranging from -3.4 to -4.1 and averaging -3.7 (Halim-Dihardja 1986). Replacive nonplanar dolomites range from -10.0 to -13.9 $\delta^{18}O$ and average -11.8. White sparry dolomites have a broad distribution of $\delta^{18}O$ and also display some anomalously negative $\delta^{13}C$ values. Even when the three anomalous points are ignored, white sparry dolomites range from -5.2 to -14.9 ($\delta^{18}O$).

Table 4
Dolomite Isotope Statistics

SAMPLE TYPE	n	C/O	MAX/MIN (RANGE)		$\bar{x}$	MEDIAN VALUE	σ	WITH OUT:
SADDLE in LIMESTONE	3	$\delta^{13}C$	+1.4	-1.0	-0.1	-0.7	1.3	
		$\delta^{18}O$	-5.2	-7.2	-6.0	-5.8	1.0	
WHITE SPARRY DOL in DOLOSTONE	12	$\delta^{13}C$	+0.4	-15.2	-2.9	-0.6	5.5	
		$\delta^{18}O$	-9.3	-18.2	-12.9	-11.7	2.6	
	9	$\delta^{13}C$	+0.4	-1.3	-0.2	0.0	0.7	*
		$\delta^{18}O$	-9.3	-14.9	-12.6	-13.3	2.3	*
ALL WHITE SPARRY DOLOMITE	15	$\delta^{13}C$	+1.4	-15.2	-2.4	-0.7	5.1	
		$\delta^{18}O$	-5.2	-18.2	-11.5	-11.6	3.7	
	12	$\delta^{13}C$	+1.4	-1.3	-0.3	-0.3	0.7	*
		$\delta^{18}O$	-5.2	-14.9	-11.0	-11.6	3.6	*
REPLACIVE NONPLANAR	8	$\delta^{13}C$	+0.6	-1.1	-0.2	-0.1	0.6	
		$\delta^{18}O$	-10.0	-13.9	-11.8	-11.5	1.3	
ALL NONPLANAR (WSD + RNpD)	23	$\delta^{13}C$	+1.4	-15.2	-1.6	-0.6	4.2	
		$\delta^{18}O$	-5.2	-18.2	-11.6	-11.6	3.0	
	20	$\delta^{13}C$	+1.4	-1.3	-0.3	-0.3	0.7	*
		$\delta^{18}O$	-5.2	-14.9	-11.3	-11.6	2.9	*
EARLY PLANAR	8	$\delta^{13}C$	+1.1	-0.1	+0.3	+0.2	0.4	
		$\delta^{18}O$	-3.4	-6.6	-5.1	-4.6	1.3	
ALL DOLOMITE (PLANAR + NONPLANAR)	31	$\delta^{13}C$	+1.4	-15.2	-1.1	-0.1	3.7	
		$\delta^{18}O$	-3.4	-18.2	-10.0	-11.3	4.0	
	28	$\delta^{13}C$	+1.4	-1.3	-0.1	0.0	0.7	*
		$\delta^{18}O$	-3.4	-14.9	-9.5	-10.0	3.8	*

Abbreviations used in Tables 4 and 5:

$\bar{x}$ - average value.
n - number of samples.
σ - standard deviation.
* - two (Munroe-Alpine-Boivin) very light carbon and one (Oldman River) very light oxygen saddle dolomite analyses not included in statistics, Table 4.
** - one (Hummingbird Creek) light oxygen micrite analysis not included in statistics, Table 5.
RNpD - replacive nonplanar dolomite.
WSD - white sparry dolomite.

Table 5
Calcites Isotope Statistics

SAMPLE TYPE	n	C/O	MAX/MIN (RANGE)		$\bar{x}$	MEDIAN VALUE	σ	WITH OUT:
BRACHIOPOD SHELLS	3	$\delta^{13}C$	+1.3	+0.3	+0.9	+1.1	0.5	
		$\delta^{18}O$	-7.2	-8.4	-7.8	-7.9	0.6	
MICRITE	4	$\delta^{13}C$	+1.4	-1.1	+0.2	+0.7	1.1	
		$\delta^{18}O$	-6.2	-12.5	-8.7	-7.8	2.7	
	3	$\delta^{13}C$	+1.4	-0.1	+0.7	+0.7	0.8	**
		$\delta^{18}O$	-6.2	-8.1	-7.4	-7.8	1.0	**
BRACHIOPOD SHELLS & MICRITE	7	$\delta^{13}C$	+1.4	-1.1	+0.5	+0.7	1.1	
		$\delta^{18}O$	-6.2	-12.5	-8.3	-7.9	2.0	
	6	$\delta^{13}C$	+1.4	-0.1	+0.8	+1.1	0.6	**
		$\delta^{18}O$	-6.2	-8.4	-7.6	-7.8	0.8	**
FRACTURE FILLING	8	$\delta^{13}C$	-0.2	-3.5	-1.8	-1.7	1.2	
		$\delta^{18}O$	-11.5	-19.7	-16.2	-16.7	3.3	
ALL SPARRY	12	$\delta^{13}C$	+1.1	-3.5	-1.1	-0.8	1.6	
		$\delta^{18}O$	-6.8	-19.7	-12.8	-12.6	4.7	
ALL CALCITE	20	$\delta^{13}C$	+1.4	-3.5	-0.6	-0.2	1.6	
		$\delta^{18}O$	-6.2	-19.7	-11.6	-8.6	4.7	

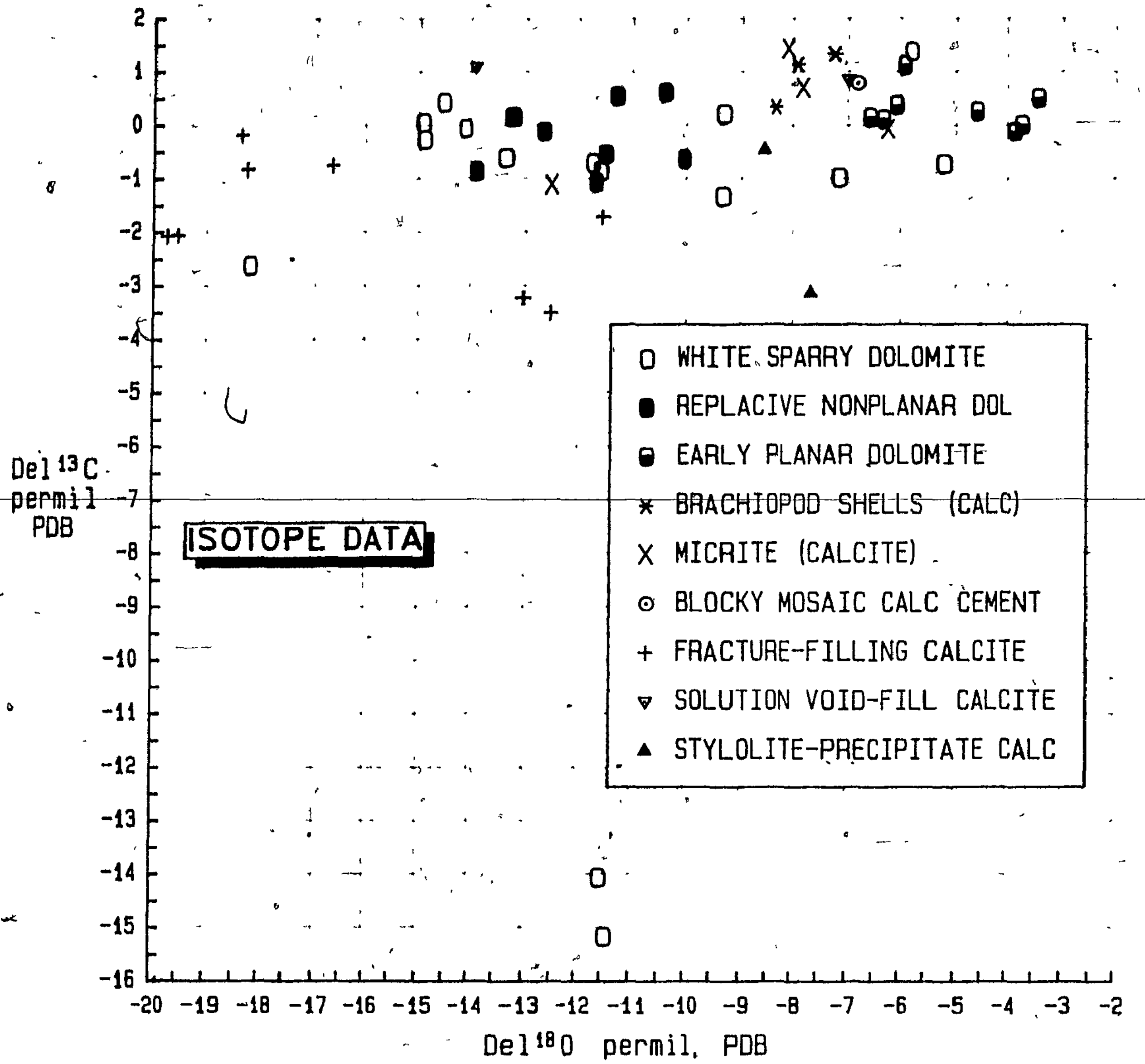

__Figure 11:__ All stable carbon and oxygen isotope data obtained from samples analyzed for this study. $\delta^{13}C$ versus $\delta^{18}O$.

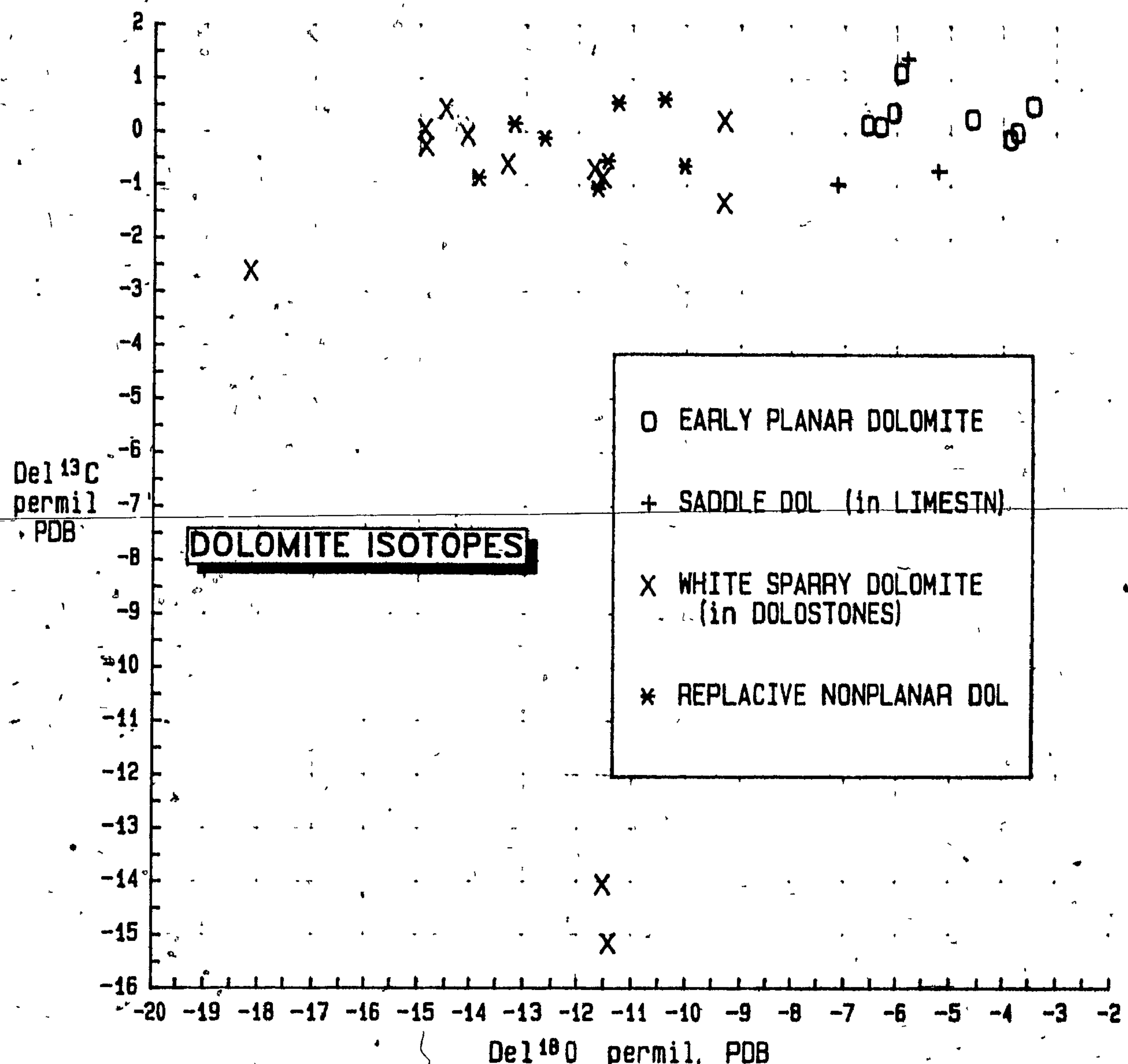

<u>Figure 12:</u> Stable carbon and oxygen isotope data for dolomite phases. White sparry dolomites are subdivided into limestone and dolostone occurrences. $\delta^{13}C$ versus $\delta^{18}O$.

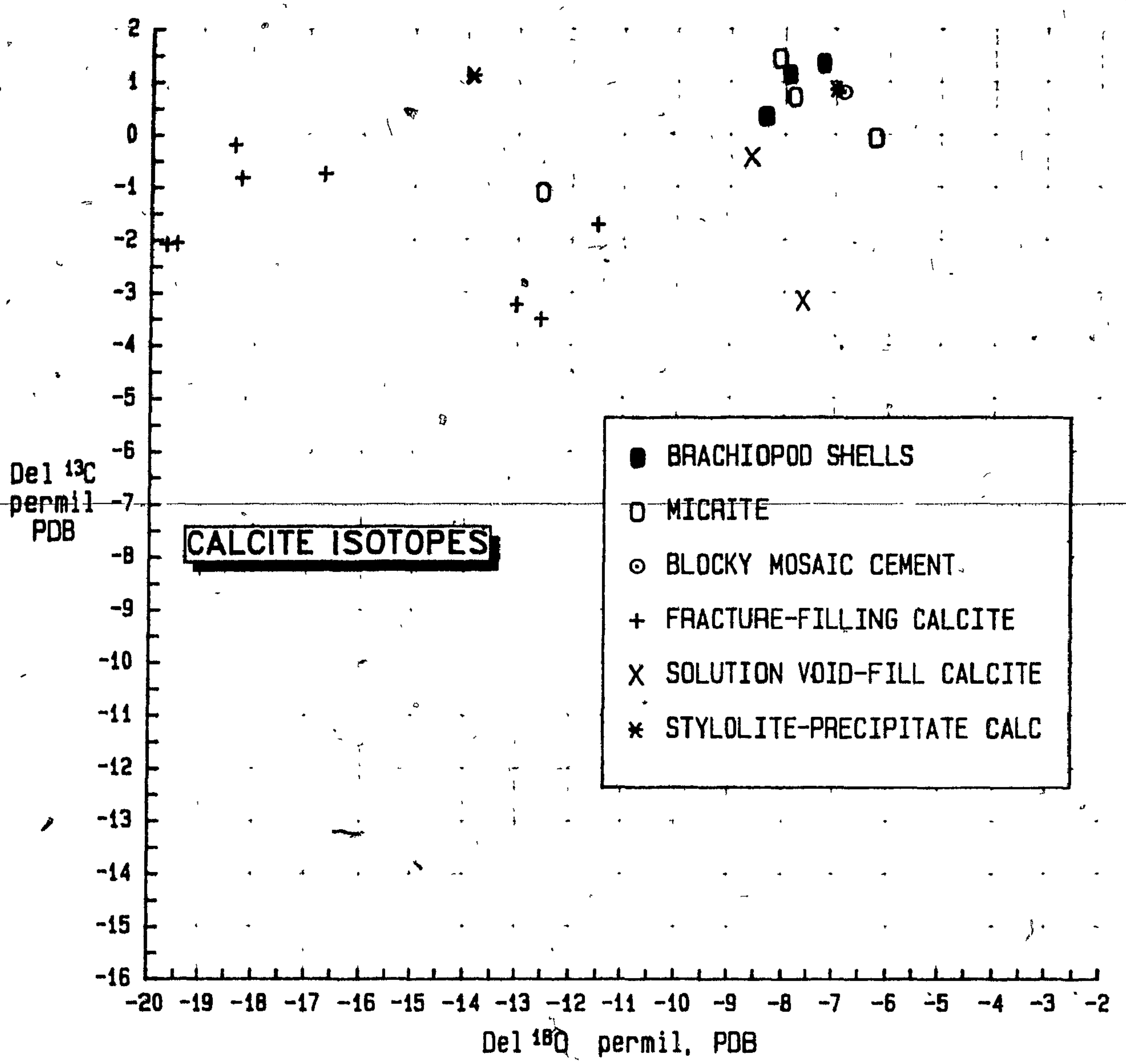

Figure 13: Stable carbon and oxygen isotope data for calcite phases. $\delta^{13}C$ versus $\delta^{18}O$.

The least negative $\delta^{18}O$ values were obtained from saddle dolomites in limestones, which fill solution and/or primary (e.g., shelter) voids and constitute a distinct subcategory of white sparry dolomites. Saddle dolomites in limestones have a range of -5.2 to -7.2 ($\delta^{18}O$), averaging -6.0, while all other white sparry dolomites range from -9.3 to -14.9, averaging -12.3.

Figure 13 is a plot of δ values for calcite components. Table 5 lists the statistics for the isotopes of calcite components. Analyses on three brachiopod shells gave values of -7.2 to -8.4 $\delta^{18}O$, averaging -7.8. $\delta^{13}C$ ranged from +0.3 to +1.4, suggesting that they have not been affected by meteoric waters. The shells were non-cathodoluminescent with some thin darkly luminescent bands (the faintest category after non-luminescent), and had well preserved multi-layered, fibrous-parallel, punctate or pseudopunctate shell structure. Micrites have a $\delta^{18}O$ of -6.2 to -8.1 and $\delta^{13}C$ of -0.1 to +1.4. Together, brachiopod shells and micrite range from -6.2 to -8.4 and average -7.6 $\delta^{18}O$.

From the Tangent oil field in the subsurface Wabamun Group, Halim-Dihardja (1986) reported a value of $\delta^{18}O$ = -7.6 for a non-luminescent brachiopod shell and -6.0 to -7.3 for micrites and calcite allochems. Five brachiopods from the top of the Palliser in Maligne Canyon, Jasper National Park, averaged -6.8 $\delta^{18}O$ and +0.3 $\delta^{13}C$ (E.W. Mountjoy, personal communication, 1988).

Gonzalez and Lohmann (1985) suggested that marine cements have the heaviest oxygen values, and are therefore the best estimate of the original marine isotopic conditions, however, no marine cements were recognized during this study. Popp et al. (1986) plotted (their Figure 7, p.1266) $\delta^{18}O$ values of -5.5 to -6.5 for Famennian marine carbonate cements (not from the Palliser Formation), taken from Lohmann and Walker (1984). Based on analyses of fibrous marine calcite cements from the Frasnian and Famennian of the Canning Basin, Australia, Wallace

(1987) estimated that Late Devonian, low-magnesium marine calcites should have a $\delta^{18}O$ of approximately -6.4. Combining the results from marine calcites analyzed for this study with published Famennian data gives a range of approximately -6 to -8 $\delta^{18}O$ for the possible value of the least fractionated marine carbonates (following Popp et al. 1986, Al-Aasm and Veizer 1982, and Gonzalez and Lohmann 1985). The heaviest value is the best with which to estimate the isotopic composition ('SMOW') of the Famennian sea (see Appendix Two).

The $\delta^{18}O$ isotope relationship among inorganically precipitated calcite, water, and temperature has been investigated for the range of 0-500°C (O'Neil et al. 1969). The relationship is described by the equations:

$$10^3 \ln a_{(C-W)} = 2.78\times10^6\times T^{-2} - 2.89$$

$$a_{(C-W)} = \frac{1000 + \delta^{18}O_{(C)}}{1000 + \delta^{18}O_{(W)}}$$

where a is the isotopic fractionation factor, T is the water temperature in °K, c refers to calcite and w to water.

Although brachiopods, and possibly micrite as well, represent organically controlled precipitation, brachiopod shells precipitate at isotopic equilibrium with sea water, are not highly fractionated, and commonly are not strongly altered diagenetically because they precipitated as low-magnesium calcite (Al-Aasm and Veizer 1982, Popp et al. 1986).

As the micrites have an isotopic range similar to the brachiopods (Figure 13), they are included together as 'marine calcite'. Also, Anderson and Arthur (1983) indicated that at low temperatures, there is little difference in the degree of fractionation between some organic and inorganic calcite precipitation (Figure 14), although there is some difference between various minerals (e.g., aragonite, low-Mg calcite, high-Mg calcite).

$\delta^{18}O$ values are converted from PDB$_{(calcite)}$ to SMOW$_{(water)}$ using the relationship:

$$\delta^{18}O_{(C\ vs.\ SMOW)} = 1.03086 \times \delta^{18}O_{(C\ vs.\ PDB)} + 30.86$$

(Friedman and O'Neil 1977)

Choosing 22°C (295.15°K) as the water temperature and $\delta^{18}O = -6$ (+24.7 SMOW) as the heaviest (least altered?) value for marine calcite, the 'SMOW' for shallow, warm Famennian ocean water is calculated from the above equation to be -4.2 $\delta^{18}O$ (PDB).

Figure 15 is a cross-plot of temperature versus $\delta^{18}O$ of various ocean water (SMOW) with lines for the $\delta^{18}O$ of dolomite. Choosing -4 (PDB) as an approximate value for the Famennian ocean (as calculated above) allows plotting of $\delta^{18}O$ values for various phases (assuming that they precipitated from unmodified sea water). Although 'higher temperature' values have been plotted relative to $\delta^{18}O = -4$, they likely precipitated from fluids with different ('evolved') isotopic compositions. In a simple model, the effect of progressive burial and diagenesis on pore fluids is to increase the salinity and enrich the ^{18}O content, i.e., to give the fluid a more positive $\delta^{18}O$ value (Choquette and James 1987). Therefore, the temperatures calculated for nonplanar dolomites are probably minimum temperatures. However, subsurface fluids may have complex origins, so that this need not be true in every case.

Early planar dolomites ($\delta^{18}O = -3.4$ to -6.6) have a temperature of formation range of 33-48°C (Figure 15). Nonplanar dolomites in dolostones (replacive nonplanar and white sparry dolomites: $\delta^{18}O = -9.3$ to -14.9), have a range of 63 to >100°C.

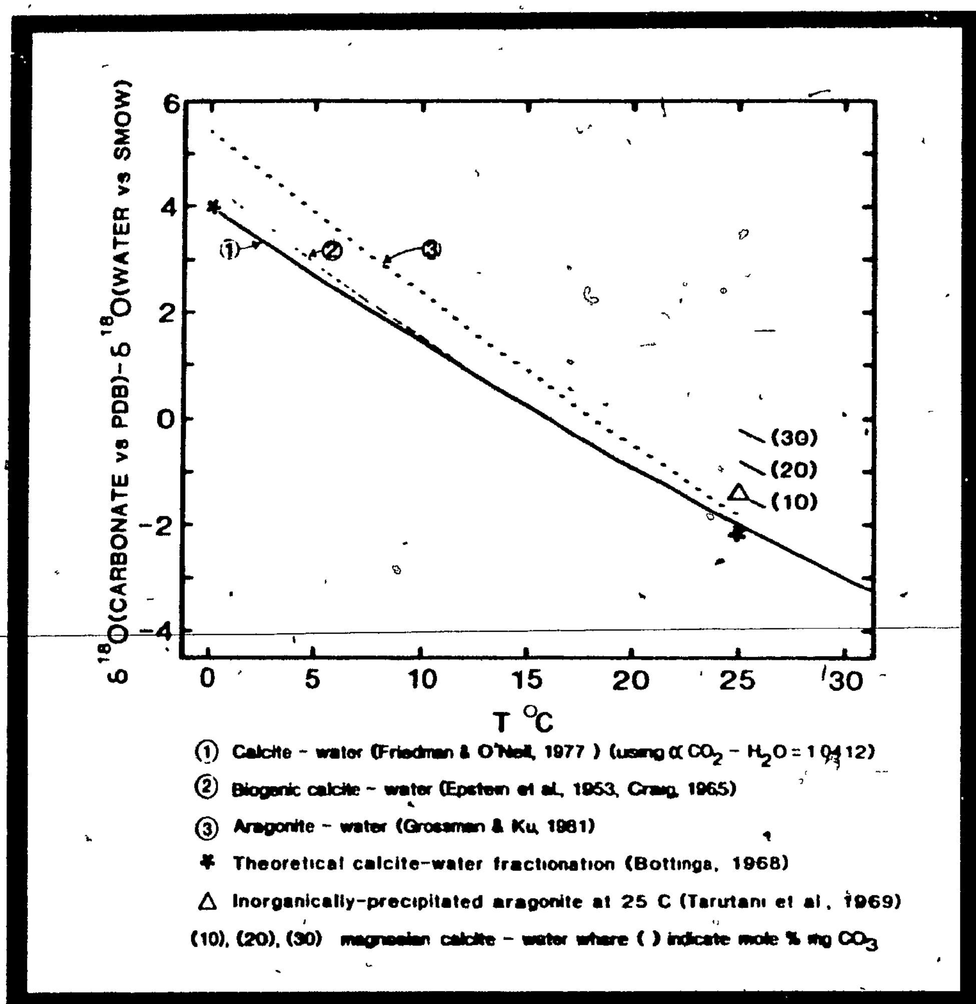

Figure 14: Oxygen isotopic fractionation between $CaCO_3$ and H_2O at sedimentary temperatures, from Anderson and Arthur (1983).

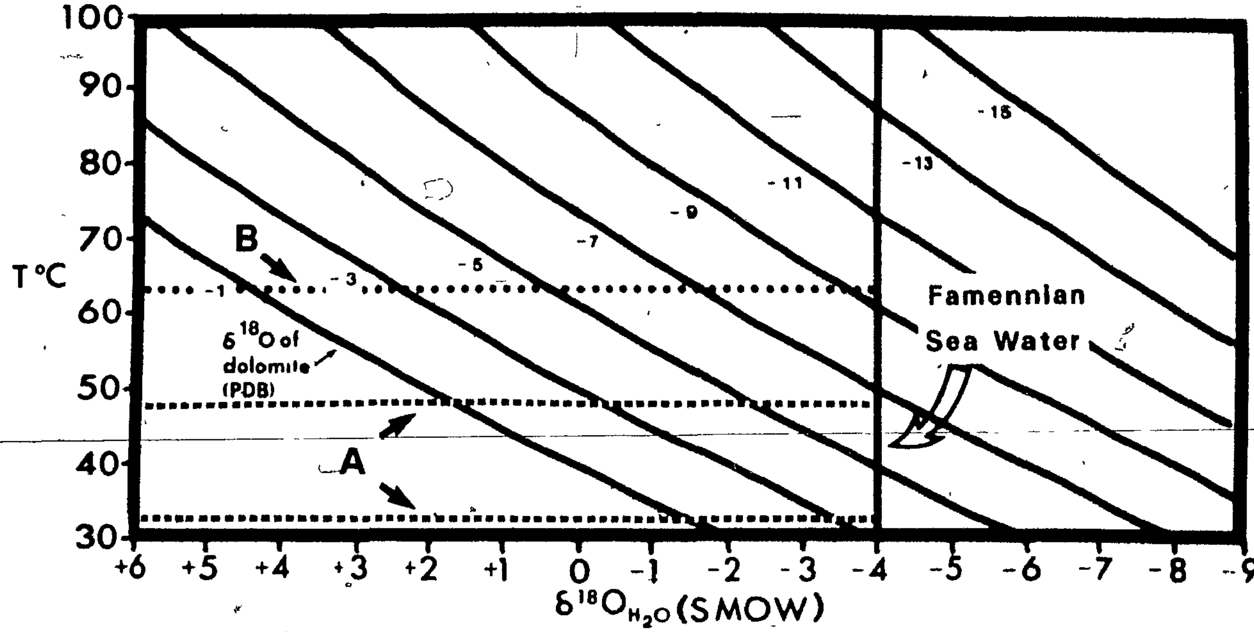

<u>Figure 15:</u> Plot of temperature versus $\delta^{18}O$ of water (SMOW) with cross-lines for the $\delta^{18}O$ of dolomite phases (PDB). Famennian sea water is assumed to have a $\delta^{18}O$ = -4 (SMOW). Modified from Woronick & Land (1985).

A - Possible T_f (temperature of formation) determined using the maximum (-3.4) and minimum (-6.6) $\delta^{18}O$ of planar dolomites.

B - Possible T_f determined using the minimum (-9.3) $\delta^{18}O$ of nonplanar dolomites in dolostones. Maximum = -14.9.

Since there is a range of possible values for the Famennian 'SMOW', the temperatures calculated above would be lower if the 'SMOW' was more negative (i.e., $\delta^{18}O = -8$).

The average $\delta^{13}C \approx 0$ for all dolomite and calcite samples is close to the overall average for Phanerozoic marine carbonates (Veizer and Hoefs 1976).

Calcite components show a wide distribution of δ values (both ^{18}O and ^{13}C), which is in part related to their geographic distribution. Figure 13 shows two groupings of fracture-filling calcites. The group at -11 to -13 $\delta^{18}O$ represent samples from the tectonic fractures associated with the mineralization at Oldman River. A second group at -16.5 to -20 represents late fractures at Hummingbird Creek and Munroe-Alpine-Boivin. At Munroe-Alpine-Boivin, a calcite-filled fracture with a $\delta^{18}O = -16.7$ (and associated with native sulphur) was reopened and filled by a younger generation of fracture-filling calcite (without sulphur) that has a $\delta^{18}O = -18.4$, which may represent higher temperature precipitation. These very negative $\delta^{18}O$ values are unusual when compared to other published isotope data for the Upper Devonian. Halim-Dihardja (1986) reported $\delta^{18}O$ values of -9.6 to -12.0 for late, coarse, fracture-filling calcite in the Wabamun, Tangent oil field. Mattes and Mountjoy (1980) determined $\delta^{18}O$ values of approximately -7 to -12 for late, sparry calcites associated with brecciation in the Frasnian Miette buildup. Walls et al. (1979) reported that late stage sparry calcites from the Upper Devonian Golden Spike reef had $\delta^{18}O$ values of -11.6 to -14.5.

Two analyses of calcite precipitated along stylolites in a fenestral mudstone from Hummingbird Creek (from the same hand sample) yielded very different $\delta^{18}O$ values (-7.0 vs. -13.9), but similar $\delta^{13}C$ values (+0.8 vs. +1.1) and may represent two different stages of stylolite formation. A blocky mosaic calcite cement analysis from the same sample yielded a $\delta^{18}O$ virtually identical to the heavier stylo-precipitate calcite.

Ch. 4 DISCUSSION and SUMMARY of DIAGENESIS

4.1 ENVIRONMENTS of DOLOMITIZATION

What are the physical and chemical conditions under which dolomite can form in significant quantities? This is one of the major questions to be answered in the search for a solution to the 'dolomite problem'. Morrow (1982a) suggested that dolomite formation would be kinetically favoured by 1) low Ca^{2+}/Mg^{2+}, 2) low Ca^{2+}/CO_3^{2-}, 3) low salinities, and 4) increased temperature. Machel and Mountjoy (1986) discussed kinetic and thermodynamic factors and suggested that high salinities (as well as low) are conducive to dolomite formation.

The supply of Mg^{2+} (plus some CO_3^{2-}) would be the limiting factor in dolomitizing a carbonate unit as there is already a supply of Ca^{2+} and CO_3^{2-}. Input of Mg^{2+} is dependent upon a source, and a hydrologic model to deliver enough of it to the "construction site" (Morrow 1982a).

Machel and Mountjoy (1986) suggested that the natural environments that are chemically capable of producing dolomite are: 1) any environments with salinities greater than the thermodynamic and kinetic dolomite saturation level; 2) alkaline environments caused by bacterial reduction and/or fermentation, or continental groundwater flow; and 3) hydrothermal and/or burial environments at elevated temperatures. Machel and Mountjoy (1986) reviewed the most often invoked dolomitization models and concluded that some would not be effective in producing the massive replacement dolostones that are so common in the geologic record. Specifically, the sabkha with reflux (e.g., Patterson and Kinsman 1981,1982) and fresh water/sea water mixing zone (e.g., Land 1973) models have not been proven to be capable of producing anything more than small amounts of dolomites that are often textural distinctive cements, with lesser amounts of disseminated replacive dolomites. Machel and Mountjoy (1986) suggested that moderately to highly saline shallow subtidal environments and burial environments at elevated temperatures are the most likely settings in which to form massive replacement dolostones.

Shallow subtidal dolomite (or protodolomite) has been described by Behrens and Land (1973) from Holocene carbonate sands in the slightly hypersaline Baffin Bay, Texas. More recently, Sass and Katz (1982) described the massive dolostones of the Cretaceous Soreq Formation, Israel. They suggested that these dolostones formed penecontemporaneously in hypersaline, shallow subtidal sea water on a carbonate platform based on strong petrographic and geochemical evidence. Bien and Land (1983) similarly argued that the Permian San Andres Formation was dolomitized by compositionally evolved fluids of marine origin in a shallow subtidal environment.

A number of examples of subsurface dolomitization have been reported in the literature. Mattes and Mountjoy (1980) suggested that fluids compacted from basinal sediments caused peripheral dolomitization of the Upper Devonian Miette buildup, Alberta. Illing (1959) and Jodry (1969) had earlier proposed similar models for the Devonian Leduc reefs, subsurface of Alberta, and the Silurian reefs, subsurface of Michigan, respectively, but had not petrographically documented the timing relationships. Morrow (1982b) and Land (1985) considered subsurface fluids to be insufficiently Mg^{2+}-rich to form massive dolostones. However, the three studies mentioned above invoke the focussing or concentration of Mg^{2+}-bearing fluids (derived from a sufficiently large area) through a relatively small area of carbonate rock. Mechanisms for channeling fluids include faults (Jones 1980) and porous and permeable (aquifer) units bounded by impermeable layers (Gregg 1985).

Garven and Freeze (1984a, 1984b) and Garven (1985) proposed an elegant model for gravity-driven fluid flow over large distances in sedimentary basins. A topographically-high recharge area provides a source of groundwater. The gravity-driven flow model has been applied to the Mississippi Valley-type sulfide deposits (and associated dolomitization) of the Viburnum Trend, Missouri (Gregg 1985), and extended to include much of the Ozark region of Missouri, Arkansas, Kansas, and Oklahoma (Leach and Rowan 1986).

One important aspect of the gravity-driven flow model is that temperatures in the discharge area (down flow) may be elevated over that expected from heating due to the thermal gradient. Forced convective heat transport can lead to near surface temperatures of 50-95°C for a 300 km long, wedge-shaped basin (Garven and Freeze 1984b). Larger basins may develop higher temperatures.

Another model, suggested by Oliver (1986), has fluids being expelled from compacting sediments caught in convergent plate margins. As each thrust sheet is emplaced, fluids are driven towards the continental interior. All of the above models may have important implications for the study of dolomitization, base metal mineralization, hydrocarbon migration, faulting, and fracturing.

Figure 16 shows a representative burial history plot for the Palliser Formation in the Lewis thrust, although most sections probably have similar burial histories. Deep burial diagenesis occurs at depths of ≈600 m, as this is the depth at which stylolites begin to form (Dunnington 1967). The steep slopes during the Cretaceous represent the shedding of a thick clastic wedge from the rising Cordillera, the emplacement of thrust sheets from the west, and finally, uplift (in a thrust sheet) and erosional unroofing. The temperature scale is based solely on an assumed geothermal gradient of 30°C/km. Gravity-driven flow might have strongly influenced the thermal history of the Palliser Formation any time during or after the Cretaceous.

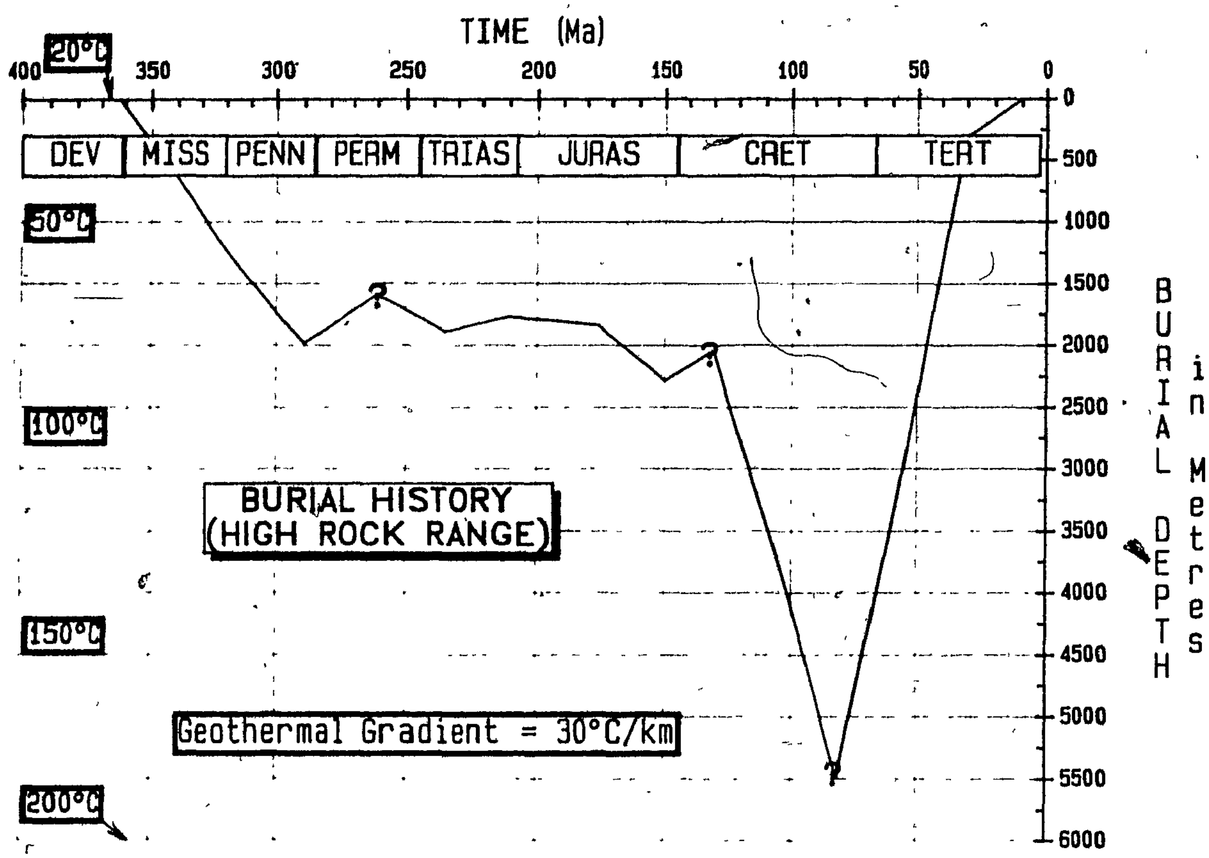

Figure 16: Burial history plot for the Palliser Formation in the High Rock Range (especially for sections 4-16 in the Lewis thrust sheet, including Oldman River). Thicknesses from McCrossan and Glaister (1964), and Norris (1958).

4.2 ENVIRONMENTS of DIAGENESIS

The paragenetic sequence for the Palliser Formation is summarized in Figure 17. This diagram was derived from petrographic observations and based on textural fabrics such as cross-cutting relationships with fractures and stylolites or successive stages of growth, as with cements. Questions marks indicate uncertainty in the placement of the onset and termination of a given phase or process. Uncertainties are numerous because not all diagenetic phases were observed 'in contact', so their relative timing is in doubt. Some phases (e.g., Pb-Zn mineralization) were observed only locally.

Diagenesis is interpreted to have occurred in three broad regimes; (1) shallow burial, including sea floor processes, (2) deep burial, and (3) uplift, including near surface telogenetic processes.

Shallow burial is the regime of near surface diagenesis, dominated by fluids of sea water, or modified sea water composition. Mechanical compaction was dominant over chemical compaction. The deep burial diagenetic regime is dominated by chemical compaction, fracturing and pervasive dolomitization. Features which are syn- to post-microstylolitization and/or stylolitization are considered to have occurred in the deep burial environment. Carbonate sediments were isolated from 'near surface' phenomena, e.g., no direct downward percolation of surface fluids. Aqueous substances were transported in regional flow patterns or were derived from mineralogical transformations occurring deeper in the basin or in laterally equivalent strata. Subsurface brines, or mixtures of brines, are the diagenetic fluids. Fracturing may have played an important role in forming conduit systems for fluid movement.

Uplift refers to the regime dominated by compressional tectonics, thrust sheet emplacement, erosional unroofing, fracturing, and, probably, gravity-driven flow. Near surface processes such as vadose fresh water input were of minor importance (e.g., Recent silt in porosity in outcrops).

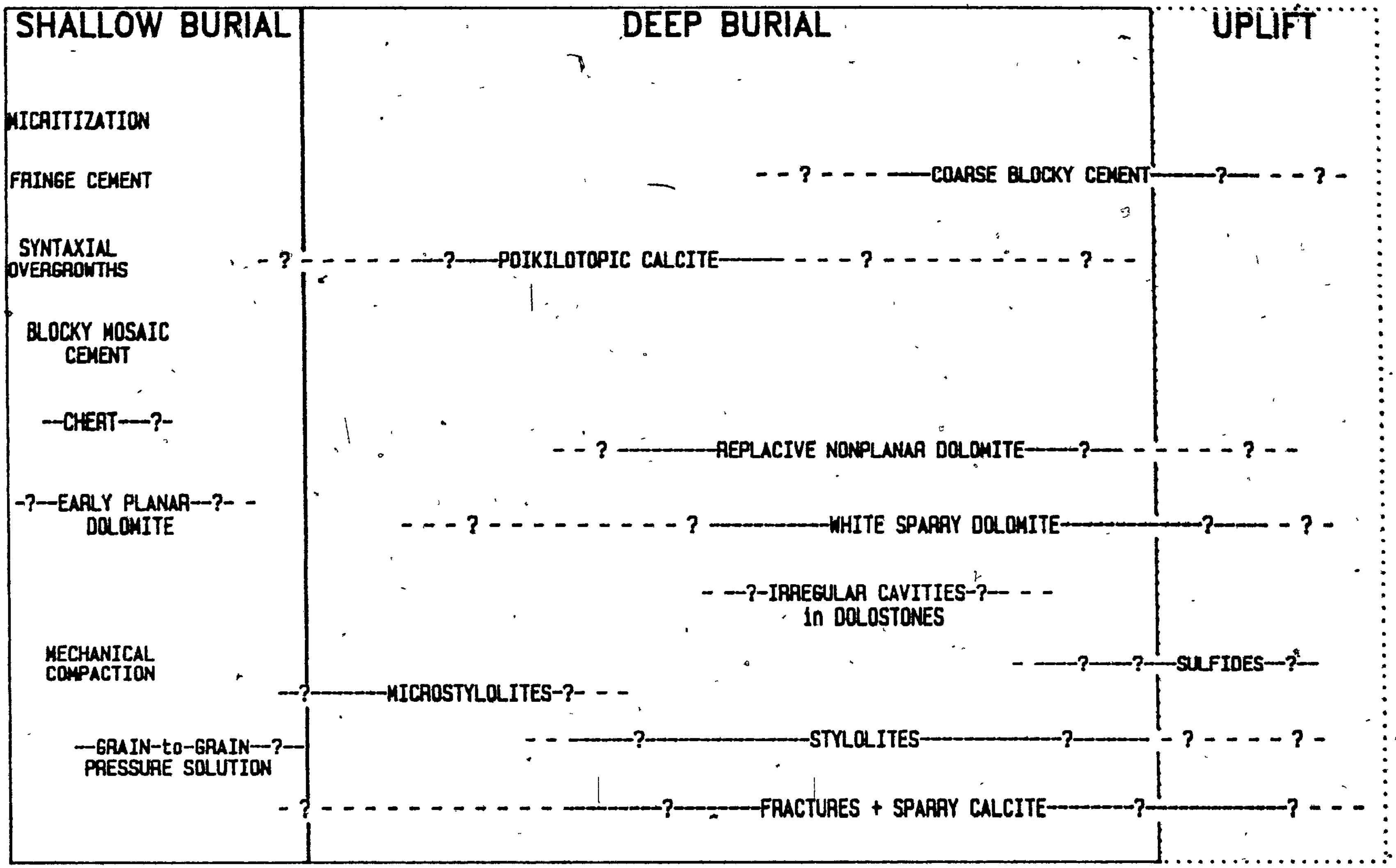

Figure 17: Overall paragenetic sequence for the Palliser Formation.

4.3 SHALLOW BURIAL DIAGENESIS

Most calcite diagenesis, with the exception of fracture-filling calcite, occurred relatively early in the diagenetic history. Mechanical compaction, grain-to-grain pressure solution, micritization, and formation of fenestral porosity occurred penecontemporaneously, or soon after, deposition.

4.3.1 Calcite Cements

Fringe calcite and syntaxial overgrowth cements are mutually exclusive and occur as the first cements on grains (always an echinoderm fragment in the case of syntaxial overgrowths), but do not occur together. The next cement to form was blocky mosaic calcite cement, which occluded the majority of the pore space. Distinct, faintly cathodoluminescent bands in a grainstone from Hummingbird Creek suggest that some blocky mosaic calcite may have precipitated in several stages. However, most examples of this phase are homogeneous, with uniform cathodoluminescence.

Calcite cements, such as fringe, syntaxial overgrowth, and blocky mosaic formed early, indurating grainy sediments, likely causing the cessation of mechanical compaction and grain-to-grain pressure solution. Stress would then be accommodated by the onset of fracturing and pervasive pressure solution, i.e., microstylolite, and eventually, through-going stylolite formation in the deeper burial environment.

4.3.2 Early Planar Dolomite

Early planar dolomites, or a precursor phase, probably began forming soon after deposition of the sediment, and continued in the shallow burial environment, as previously suggested by R de Wit (cited in Fox 1951) and Beales (1953).

Evidence for the timing is varied. Early planar dolomite is fabric selective and follows 'sedimentary features' such as burrows and bedding. It does not replace any diagenetic phase (e.g., calcite cements) and is cross-cut by fractures and stylolites. Early planar dolomite does not replace fossils, although rhombs locally cut their exterior boundaries. Evenly disseminated early planar dolomites occur in early-formed chert nodules. In the surrounding limestone, early planar dolomite is concentrated along microstylolites. Microstylolites do not occur in the chert nodules. This indicates that early planar dolomites formed before chert and microstylolites. No evidence for submarine reworking of dolomite (e.g., clasts) was found.

If permeability was a major control on the dolomite distribution, than replacement of peloids in grainstones must have occurred before blocky mosaic calcite completely occluded porosity. Similarly, growth of early planar dolomite in some early-formed micritic nodules probably occurred before induration of these nodules was complete. The early planar dolomite rhombs which surround burrows in mudstones and wackestones likely formed while sufficient permeability existed to allow dolomitizing fluids to move out of the burrows and into the micrite. Sea water is the most likely source of magnesium, either moving downward into the burrowing, or flowing out of adjacent compacting sediments and funneling upward through the burrow.

Relative to nonplanar dolomites, early planar dolomites are characterized by higher Ca/Mg ratios, less negative $\delta^{18}O$ values, and uniform cathodoluminescence.

Excess calcium (over the ideal 1:1) may have been retained in the lattice of these dolomites, suggesting precipitation at or near the sea floor as a disordered protodolomite (sensu Graf and Goldsmith 1956).

A temperature of formation for planar dolomite can be estimated from the oxygen isotopic composition (assuming that sea water was the dolomitizing fluid), yielding a range of 33-48°C, when a value of $\delta^{18}O = -4$ is used for the Famennian 'SMOW'. This temperature range would then represent the sea floor or, more likely, the shallow burial conditions of formation of planar dolomite or its precursor (protodolomite?).

The range of $\delta^{18}O$ values for early planar dolomites (-3.4 to -6.6) may record the subsequent diagenesis undergone by protodolomites as they neomorphosed to early planar dolomite with increasing burial. Continued diagenesis may have caused isotopic exchange at elevated temperatures in fluids of differing isotopic compositions leaving a spectrum of $\delta^{18}O$ values from least altered (heaviest) to most altered (lightest).

The uniformity of the cathodoluminescence of early planar dolomites suggests precipitation from a fluid of relatively constant composition. Sea water, representing a very large reservoir, could maintain such a constant composition, as could subsurface brines under certain conditions. Thin, brighter luminescing rims locally displayed by early planar dolomite may represent a later stage of burial dolomite which precipitated in a different chemical environment.

Kendall (1977) studied the dolomitic mottling of limestones in the Ordovician Yeoman and lower Red River formations of Saskatchewan and Manitoba. He noted the control over dolomitization exerted by burrows and bedding planes but suggested that this did not imply penecontemporaneous dolomite formation. Kendall (1977) speculated that the permeability difference between the burrows and their host sediment might have been preserved, or even enhanced by early diagenetic processes. This is certainly possible, however, in the Palliser, the presence of early micrite-replacive dolomite surrounding the burrows suggests early formation. Although coarse-grained sediments, such as burrow-fillings, may have porosity and permeability created and destroyed almost at random during diagenesis, the early diagenetic history of micrite is usually more straightforward. Micrite generally undergoes a unidirectional loss of porosity and permeability, both through physical compaction and de-watering, and precipitation of micritic cement (Shinn and Robbin 1983; and others). The permeability of micrite is not likely to be enhanced by early diagenetic processes, although it may be preserved. This should also hold true for peloids and micritic nodules.

Dolomitization by downward diffusion of Mg^{2+} from sea water into relatively permeable back-fills in burrow has been suggested by Morrow (1978) for the mottled limestones of the upper Ordovician Irene Bay - Thumb Mountain formations, Canadian Arctic Archipelago. Morrow (1978) envisaged successive stages of dolomitization, starting with "micron-sized seed nuclei" of dolomite acting as loci for later growth of diagenetic dolomite. He suggested that later growth of dolomite may have been aided by the release of Mg^{2+} from organic matter and/or clay minerals contained in the burrows. A continuous spectrum of stages of dolomitization are preserved in these limestones, from the more calcium-rich, idiotopic "seed nuclei" dolomite, to the coarser, more stoichiometric, xenotopic dolomite.

The importance of permeability in some cases of early dolomitization was suggested by a study of Recent carbonate sediments from the Florida Keys (Shinn 1968b). Sand-sized fillings in desiccation cracks were preferentially dolomitized over the surrounding, relatively impermeable, mud polygons.

Of even greater relevance to the problem of dolomitic mottling in the Palliser is the study done by Brown and Farrow (1978). They described nodules of predominantly dolomite mineralogy forming around thalassinidean burrows in the Recent clastic sediments of Loch Sunart, off the west coast of Scotland. This dolomite has formed at the sea floor, since these sediments have never been buried; therefore, the only possibly dolomitizing fluid is sea water. Meadows and Anderson (1975), cited in Brown and Farrow (1978), found that sulfate-reducing bacteria were most concentrated in and around these burrows. Brown and Farrow (1978) suggested that bacterial activity might have locally raised alkalinities high enough to, first, promote calcite precipitation, and then, the dolomitization of this calcite.

Under certain circumstances, burrows may act as a micro-environment favourable to the formation of dolomite (or protodolomite). This would help explain the recurrence, throughout the Paleozoic in particular, of dolomite-mottled (burrowed) shelf carbonates (see Appendix One for more examples of dolomitic mottling in carbonates).

4.4 DEEP BURIAL DIAGENESIS

During deep burial (depths of ≈600 m or more), pervasive, through-going pressure solution processes were dominant, forming microstylolites and stylolites. Carbonate removed by pressure solution may have been re-precipitated as cement. Poikilotopic and fracture-filling calcite, and nonplanar dolomite may have originated in this way. Fractures both cut, and are cut by, stylolites, indicating both phases may have occurred over extended ranges.

4.4.1 Nonplanar Dolomite

Pervasive, replacement dolomite (replacive nonplanar) began to form after the major period of microstylolite formation had ceased, preserving previously formed pressure seams as ghost textures. Pore-filling dolomites (white sparry dolomites) formed penecontemporaneously with, or after, the replacive dolomites. Nonplanar dolomites were observed in contact with planar dolomites only where fractures or solution voids containing nonplanar dolomites cut limestones. In these instances, the planar dolomite clearly predates the nonplanar dolomite.

The relatively light $\delta^{18}O$ values for most nonplanar dolomites (except saddle dolomites in limestones) probably indicate precipitation (or neomorphism) at higher temperatures, in the deep burial diagenetic environment.

Saddle dolomites that occur in limestones form a group distinct from other white sparry dolomites, both through occurrence (i.e., not in dolostones) and heavier $\delta^{18}O$ values which coincide with part of the range for early planar dolomites. These $\delta^{18}O$ values may indicate relatively low temperature precipitation, or retention of the dissolving carbonate's (limestone or early planar dolomite) heavy isotopic composition through cannibalization of CO_2, or both.

Early formation of saddle dolomites has been proposed for the Upper Devonian Swan Hills oil field, central Alberta (Viau and Oldershaw 1984). Iron-zoned saddle dolomites occur in fractures that are present only below a chronostratigraphic marker one third of the way up into the buildup. On this basis, Viau and Oldershaw (1984) suggested that these fractures, and the saddle dolomite, are synsedimentary and formed while the Swan Hills buildup was at sea level. The saddle dolomites also occur in the underlying carbonate platform. However, Viau and Oldershaw (1984) did not discuss the possibility that the fractures may be synsedimentary, while the saddle dolomite is not, having precipitated later during burial.

One of the three limestone samples containing saddle dolomite shows no evidence of limestone dissolution or neomorphism (from Hummingbird Creek), while in the two other samples (from Munroe-Alpine-Boivin and Hummingbird Creek), saddle dolomite lines the walls of solution-enlarged pores in lime wackestones, suggesting that induration of micrite and a change to pore fluids undersaturated with respect to $CaCO_3$ occurred before or during dolomite precipitation. This fact, along with the relatively high temperatures generally suggested for saddle dolomite precipitation (e.g., Radke and Mathis 1980, 60-150°C; Gregg and Sibley 1984, >50°C) suggest that saddle dolomites in limestones likely precipitated at higher temperatures than the approximately 42-53°C temperatures that would have been yielded if their $\delta^{18}O$ values had been plotted on Figure 15. The subsurface fluids from which they precipitated may have had a heavy oxygen isotopic composition due to dissolution of relatively heavy limestone components. The precipitating dolomite would further fractionate (incorporate) the heavy oxygen, resulting in relatively less negative $\delta^{18}O$ values. Saddle dolomite (or any white sparry dolomite) in dolostones have much lighter oxygen compositions which do not record strong interaction with limestones.

The similarity in isotopic composition between white sparry and replacive nonplanar dolomites might suggest that they formed together from one fluid, at or above the critical roughening temperature (Gregg and Sibley 1987), in the deep burial environment. However, just as saddle dolomites in limestones may have acquired an isotopic signature from the surrounding rock (through cannibalization of carbonate), saddle dolomites in dolostones might have acquired their isotopic compositions from the replacive nonplanar dolomites, even if they precipitated much later.

The most negative $\delta^{18}O$ (= -18.2) value, for a ferroan saddle dolomite (in dolostone) from the fault gouge at Oldman River, might represent very high temperature precipitation, however, no general correlation between ferrous iron content of dolomite and its isotopic composition could be demonstrated from the data.

Two saddle dolomite (in dolostone) samples from Munroe-Alpine-Boivin yielded anomalously negative (-14 to -15) $\delta^{13}C$ values. Petrographically, these saddle dolomites are identical to others from the same section, and they have similar cathodoluminescence and $\delta^{18}O$ values. Very negative $\delta^{13}C$ values may be due to bacterial reduction of sulfate and/or thermal decarboxylation (Hudson 1977; Irwin et al. 1977; Land 1980). Very light $\delta^{13}C$ values do not imply elevated temperature as the $\delta^{13}C$ of carbonates is relatively insensitive to temperature changes (Anderson and Arthur 1983).

Ch. 5 CONCLUSIONS

The Famennian Palliser Formation was deposited as a carbonate ramp in a shallow subtidal setting. The Morro Member is less fossiliferous, less argillaceous, and thicker-bedded than the overlying Costigan Member, which suggests somewhat deeper-water depositional environments for the Costigan. The dominant lithologies are bioturbated mudstones and wackestones. Burrowing is ubiquitous, and the differential weathering of the dolomite in burrows versus the limestones gives a rough texture to outcrops. Locally, several other facies were deposited under varying conditions. Peloidal, echinodermal, and intraclastic grainstones and packstones may indicate an increase in the water energy. Peloids are the most common allochem in the study area. Peloids may have originated as algal precipitates, fecal pellets, micritized echinoderm fragments, and as rounded micrite intraclasts.

At Hummingbird Creek, a mud-flat facies caps tabular stromatoporoid mounds (above 150 m, Figure A3-3, Appendix Three), indicating that sedimentation locally built up to sea level, suggesting subaerial exposure. Casts of evaporitic minerals, mud-cracks, rip-up clasts, and a restricted fauna indicate elevated salinities and periodic desiccation.

The distribution of lithotypes (more fine-grained to the west) indicates a general westward deepening of depositional environments.

Calcite cements are volumetrically minor, but occlude all the available pore space; interparticle in grainstones, intrafossil and fenestral in micritic rocks. Equant to prismatic isopachous fringe or syntaxial overgrowths on echinoderm fragments are the first cements, followed by blocky, equant mosaic calcite, which occludes the majority of pore space in limestones. These phases occurred before pervasive pressure solution. The remaining calcite phases precipitated after pressure solution. Poikilotopic calcite occurs in planar and nonplanar dolostones. Locally, a coarse blocky calcite cement occurs in brecciated rocks and solution enlarged voids. Calcite-filled fractures formed both before and after stylolites. Stylolites can begin forming after only 600 m of burial (Dunnington 1967) and probably continued to from during burial and possibly uplift, as did fractures.

Dolomitization occurred in at least three stages. Early planar dolomite began forming in limestones soon after deposition of the sediment. Sea water, or early compactional fluids, supplied the magnesium to the site of dolomitization, often burrows other relatively permeable zones in micrites. Early planar dolomite probably formed as a calcian protodolomite and then underwent neomorphism during burial diagenesis. This type of dolomitization has been referred to as the shallow subtidal model (Machel and Mountjoy 1986) and could have occurred mainly during mechanical compaction.

Consideration of the isotopic composition of brachiopod shells and micrite suggests that the shallow warm Famennian ocean had an isotopic composition of -4 ($\delta^{18}O$) relative to SMOW. Assuming that early planar dolomite precipitated from fluids of near sea water composition suggests that they formed between 33 and 48°C.

After microstylolite formation, pervasive replacive nonplanar dolomitization occurred. Ghost textures of sedimentary structures, fossils and microstylolites are preserved in the dolostones. The dolomitizing fluid probably was a modified subsurface brine of unknown origin in the deep burial environment. Replacive nonplanar dolomite probably accounts for less than five percent of the Palliser Formation, and was not found in limestones.

White sparry nonplanar dolomites precipitated both before and after stylolitization, and occur as a volumetrically minor phase in replacive nonplanar dolostones and limestones. In limestones, white sparry dolomites occur in primary and solution-enlarged voids and have relatively heavy oxygen isotope compositions. In dolostones, they occur in fractures and solution enlarged porosity and are lighter in oxygen. The similarities between white sparry dolomite and its host rock suggests that the dolomite forms by cannibalizing carbonate liberated through solution of the surrounding rock.

There is no evidence to indicate that planar and nonplanar dolomites are part of a continuous spectrum of dolomitization. Petrographic and isotopic data indicate that planar and nonplanar dolomites formed at different times and are unrelated. Planar dolomites are fabric destructive, do not replace fossils,and are controlled by primary sedimentary structures, or are modified by later diagenesis. Nonplanar dolomites commonly preserve textures (including fossils) and crosscut both sedimentary and early diagenetic features.

Sulfide mineralization occurs at two sections, Oldman River and Munroe-Alpine-Boivin, in association with nonplanar dolomitization. Sulfides precipitated with or after replacive nonplanar dolomite and with or before white sparry dolomite. Fracture-filling or poikilotopic calcite are commonly the last phases to precipitate. At Oldman River, the sulfides are localized around two tear faults in the Lewis thrust sheet, suggesting that they formed after thrusting and uplift had begun. At Munroe-Alpine-Boivin, mineralization may have occurred earlier in the diagenetic history (before thrusting?). The sphalerite is confined to replacive dolostone units, most of which are cross-cut by faults.

Models of regional subsurface flow, such as those proposed by Garven and Freeze (1984a, 1984b), Garven (1985), Gregg (1985), and Oliver (1986), may be applicable to the nonplanar dolomitization and sulfide mineralization in the Palliser Formation. Large-scale flow of brines, directed along faults or other conduits, might have provided sufficient numbers of pore-volumes of fluids to cause the observed dolomitization. However, more data on the regional distribution and continuity of the various dolomite types is required before a definitive statement is made on the source of the nonplanar dolomites.

REFERENCES

AL-AASM, I.S., & VEIZER, J., 1982, Chemical stabilization of low-Mg calcite: an example of brachiopods; Journal of Sedimentary Petrology, v.52(4), p.1101-1109.

AL-HASHIMI, W.S., & HEMINGWAY, J.E., 1973, Recent dolomitization and the origin of the rusty crusts of Northumberland; Journal of Sedimentary Petrology, v.43(1), p.82-91.

ANDERSON, T.F., & ARTHUR, M.A., 1983, Stable isotopes of oxygen and carbon and their applications to sedimentologic and paleoenvironmental problems; in ARTHUR, M.A. (Ed.), Stable isotopes in sedimentary geology; Society of Economic Paleontologists and Mineralogists Short Course No. 10, p.1-1 - 1-151.

ANDRICHUK, J.M., 1960, Facies analysis of Upper Devonian Wabamun Group in west-central Alberta, Canada; American Association of Petroleum Geologists Bulletin, v.44(10), p.1651-1681.

ARCHIBALD, D.A., GLOVER, J.K., PRICE, R.A., FARRAR, E., & CARMICHAEL, D.M., 1983, Geochronology and tectonic implications of magmatism and metamorphism, southern Kootenay Arc and neighbouring regions, southeastern British Columbia. Part I: Jurassic to mid-Cretaceous; Canadian Journal of Earth Sciences, v.20(12), p.1891-1913.

BACK, W., HANSHAW, B.B., PLUMMER, L.N., RAHN, P.H., RIGHTMIRE, C.T., & RUBIN, M., 1981, Process and rate of dedolomitization: mass transfer and ^{14}C dating in a regional aquifer; Geological Society of America Bulletin, v.94(12), p.1415-1429.

BATHURST, R.G.C., 1966, Boring algae, micrite envelopes and lithification of molluscan biosparites; Geological Journal, v.5, p.15-32.

------, 1975, Carbonate sediments and their diagenesis, Developments in Sedimentology 12; 2nd ed., Elsevier, Amsterdam, 620 pp.

------, 1980, Stromatactis - Origin related to submarine-cemented crusts in Paleozoic mud mounds; Geology, v.8, p.131-134.

------, 1982, Genesis of stromatactis cavities between submarine crusts in Paleozoic carbonate mud buildups; Journal of the Geological Society of London, v.139, p.165-181.

BEACH, H.H., 1943, Moose Mountain and Morley map-areas, Alberta; Geological Survey of Canada Memoir 236, 74 pp.

BEALES, F.W., 1953, Dolomitic mottling in Palliser (Devonian) limestone, Banff and Jasper National Parks, Alberta; American Association of Petroleum Geologists Bulletin, v.37(10), p.2281-2293.

------, 1954, Palliser banks in the late Devonian seas of southwestern Alberta; Alberta Society of Petroleum Geologists Bulletin, v.2(10), p.1-5.

------, 1956, Conditions of deposition of Palliser (Devonian) limestone of southwestern Alberta; American Association of Petroleum Geologists Bulletin, v.40(5), p.848-870.

------, 1958, Ancient sediments of Bahaman type; American Association of Petroleum Geologists Bulletin, v.42(8), p.1815-1880.

BEHRENS, E.W., & LAND, L.S., 1972, Subtidal Holocene dolomite, Baffin Bay, Texas; Journal of Sedimentary Petrology, v.42(1), p.155-161.

BIEN, A., & LAND, L.S., 1983, Carbonate sedimentation and diagenesis associated with Mg-Ca-chloride brines: the Permian San Andres Formation in the Texas Panhandle: Journal of Sedimentary Petrology, v.53(1), p.243-260.

BELYEA, H.R., 1955, Cross-sections through the Devonian System of the Alberta Plains; Geological Survey of Canada Paper 55-3, 29 pp.

------, 1964, Ch.6 - Upper Devonian, Part 2; in McCROSSAN, R.G., & GLAISTER, R.P. (Eds.), Geologic history of western Canada; Alberta Society of Petroleum Geologists, Calgary, p.66-88.

------, & McLAREN, D.J., 1956, Devonian sediments of Bow Valley and adjacent areas; in Fox, F.G. (Ed.), 6th Annual Field Conference Guidebook; Alberta Society of Petroleum Geologists, Calgary, p.66-91.

BOTTINGA, Y., 1968, Calculation of fractionation factors for carbon and oxygen isotopic exchange in the system calcite-carbon dioxide-water; Journal of Physical Chemistry, v.72(3), p.800-808.

BOURQUE, P.-A., & GIGNAC, H., 1983, Sponge-constructed stromatactis mud mounds, Silurian of Gaspé, Québec; Journal of Sedimentary Petrology, v.53(2), p.521-532.

BROWN, B.J., & FARROW, G.E., 1978, Recent dolomitic concretions of crustacean burrow origin from Loch Sunart, west coast of Scotland; Journal of Sedimentary Petrology, v.48(3), p.825-834.

BUDAI, J.M., LOHMANN, K.C., & WILSON, J.L., 1987, Dolomitization of the Madison Group, Wyoming and Utah Overthrust belt; American Association of Petroleum Geologists Bulletin, v.71(8), p.909-924.

BUDD, D.A., & PERKINS, R.D., 1980, Bathymetric zonation and paleoecological significance of microborings in Puerto Rican shelf and slope sediments; Journal of Sedimentary Petrology, v.50(3), p.881-904.

CHANDA, S.K., BHATTACHARYYA, A., & SARKAR, S., 1983, Compaction in limestones: a reappraisal; Journal of the Geological Society of India, v.24(2), p.73-92.

CHOQUETTE, P.W., & JAMES, N.P., 1987, Diagenesis #12. Diagenesis in limestones - 3. The deep burial environment; Geoscience Canada, v.14(1), p.3-35.

CRAIG, H., 1957, Isotopic standards for carbon and oxygen and correction factors for mass-spectrometric analysis of carbon dioxide; Geochimica et Cosmochimica Acta, v.12(1), p.133-149.

------, 1965, The measurement of oxygen isotope paleotemperatures; in TONGIORGI, E. (Ed.), Stable isotopes in oceanographic studies and paleotemperatures; Consiglio Nazionale delle Richerche, Laboratorio de Geologia Nucleare, Pisa, p.161-182.

CRICKMAY, C.H., 1952, Discrimination of late Upper Devonian; Journal of Paleontology, v.26, p.589-609.

------, 1956, The Palliser-Exshaw contact; in FOX, F.G. (Ed.), 6th Annual Field Conference Guidebook; Alberta Society of Petroleum Geologists, Calgary, p.56-58.

de GROOT, K., 1967, Experimental dedolomitization; Journal of Sedimentary Petrology, v.37(4), p.1216-1220.

de WIT, R., & McLAREN, D.J., 1950, Devonian sections in the Rocky Mountains between Crowsnest Pass and Jasper, Alberta; Geological Survey of Canada Paper 50-23, 66 pp.

DUNHAM, R.J., 1962, Classification of carbonate rocks according to depositional textures; in HAM, W.E. (Ed.), Classification of carbonate rocks; American Association of Petroleum Geologists Memoir 1, p.108-121.

DUNNINGTON, H.V., 1967, Aspects of diagenesis and shape change in stylolitic limestone reservoirs; Seventh World Petroleum Congress, Mexico, Proceedings, v.2, p.339-352.

EKDALE, A.A., BROMLEY, R.G., & PEMBERTON, S.G., 1984, Ichnology - Trace fossils in sedimentology and stratigraphy; Society of Economic Paleontologists and Mineralogists Short Course No. 15, 317 pp.

ELIUK, L. & HUNTER, D.F., Wabamun Group structural thrust fault fields: The Limestone-Burnt Timber example; in KRAUSE, F.F., & BURROWES, O.G. (Eds.), Devonian lithofacies and reservoir styles in Alberta, Second International Symposium on the Devonian System, Calgary; Canadian Society of Petroleum Geologists, p.39-62.

EPSTEIN, S., BUCHSBAUM, R., LOWENSTAM, H.A., & UREY, H.C., 1953, Revised carbonate-water isotopic temperature scale; Geological Society of America Bulletin, v.64(11), p.1315-1326.

EVAMY, B.D., 1963, The application of a chemical staining technique to a study of dedolomitization; Sedimentology, v.2, p.164-170.

FOLK, R.L., 1965, Some aspects of recrystallization in ancient limestones; in PRAY, L.C., & MURRAY, R.C. (Eds.), Dolomitization and limestone diagenesis: a symposium; Society of Economic Paleontologists and Mineralogists Special Publication No. 13, p.14-48.

FOLKMAN, Y., 1969, Diagenetic dedolomitization in the Albian-Cenomian Yagur Dolomite on Mount Carmel (northern Israel); Journal of Sedimentary Petrology, v.39(1), p.380-385.

FOX, F.G., 1951, Devonian stratigraphy of Rocky Mountains and Foothills between Crowsnest Pass and Athabaska River, Alberta, Canada; American Association of Petroleum Geologists Bulletin, v.35(4), p.822-843.

-----, 1954, Devonian stratigraphy of Rocky Mountains and Foothills between Crowsnest Pass and Athabaska River, Alberta, Canada; in CLARK, L.M. (Ed.), Western Canada Sedimentary Basin: a symposium; American Association of Petroleum Geologists, p.109-130.

FLUGEL, E., 1982, Microfacies analysis of limestones; Springer-Verlag, New York-Heidelberg-Berlin, 630 pp.

FRANK, J.R., 1981, Dedolomitization in the Taum Sauk Limestone (Upper Cambrian), southeast Missouri; Journal of Sedimentary Petrology, v.51(1), p.7-18.

FRIEDMAN, G.M., GEBELEIN, C.D., & SANDERS, J.E., 1971, Micritic envelopes of carbonate grains are not exclusively of photosynthetic algal origin; Sedimentology, v.16(1), p.89-96.

FRIEDMAN, I., & O'NEIL, J.R., 1977, Compilation of stable isotope fractionation factors of geochemical interest; in FLEISCHER, M. (Ed.), Data of geochemistry, 6th ed.; U.S. Geological Survey Professional Paper, 440-K, 12 pp.

GARVEN, G., 1985, The role of regional fluid flow in the genesis of the Pine Point deposit, western Canada sedimentary basin; Economic Geology, v.80(2), p.307-324.

------, & FREEZE, R.A., 1984a, Theoretical analysis of the role of groundwater flow in the genesis of stratabound ore deposits. 1. Mathematical and numerical model; American Journal of Science, v.284(10), p.1085-1124.

------, & ------, 1984b, Theoretical analysis of the role of groundwater flow in the genesis of stratabound ore deposits. 2. Quantitative results; American Journal of Science, v.284(10), p.1125-1174.

GELDSETZER, H.H.J., 1982, Depositional history of the Devonian succession in the Rocky Mountains southwest of the Peace River Arch; in Current Research, Part C; Geological Survey of Canada Paper 82-1C, p.55-64.

------, de MILLE, G., SANGSTER, D.F., CHUNG, C.F., McDONALD, J.A., & JONASSON, I.R., 1986, The Upper Devonian Palliser Formation, Rocky Mountains, B.C. and Alberta: Geochemistry and general geology; Geological Survey of Canada Open File No. 1021, 50 pp.

GIBSON, G., 1981, Geology of the Munroe-Alpine-Boivin carbonate-hosted zinc occurrences, Rocky Mountain Front Ranges, southeastern British Columbia (NTS 82G/14E, 82J/3E); British Columbia Ministry of Energy, Mines & Petroleum Resources Preliminary Map 46.

GONZALEZ, L.A., & LOHMANN, K.C., 1985, Carbon and oxygen isotopic composition of Holocene reefal carbonates; Geology, v.13(11), p.811-814.

GRAF, D.L., & GOLDSMITH, J.R., 1956, Some hydrothermal syntheses of dolomite and protodolomite; Journal of Geology, v.64(2), p.173-186.

GREGG, J.M., 1985, Regional epigenetic dolomitization in the Bonterre Dolomite (Cambrian), southeastern Missouri; Geology, v.13(7), p.503-506.

GREGG, J.M., & SIBLEY, D.F., 1984, Epigenetic dolomitization and the origin of xenotopic dolomite texture; Journal of Sedimentary Petrology, v.54(3), p.908-931.

------, & ------, 1987, Classification of dolomite rock textures; Journal of Sedimentary Petrology, v.57(6), p.967-975.

GROSSMAN, E.L., & KU, T.-H., 1981, Aragonite-water isotopic paleotemperature scale based on the benthic foraminifer Hoeglundina elegans; Geological Society of America Abstracts with Programs, v.13(7), p.464.

HALBERTSMA, H.L., & MEIJER-DREES, N.C., 1987, Wabamun limestone sequence in north-central Alberta; in KRAUSE, F.F., & BURROWES, O.G. (Eds.), Devonian lithofacies and reservoir styles in Alberta, Second International Symposium on the Devonian System, Calgary; Canadian Society of Petroleum Geologists, p.21-38.

HALIM-DIHARDJA, M.K., 1986, Diagenesis and sedimentology of the Late Devonian (Famennian) Wabamun Group in the Tangent, Normandville, and Eaglesham fields, north-central Alberta; Unpublished M.Sc. thesis, McGill University, Montréal, 173 pp.

HARKER, P., & McLAREN, D.J., 1958, The Devonian-Mississippian boundary in the Alberta Rocky Mountains; in GOODMAN, A.J. (Ed.), Jurassic and Carboniferous of western Canada; American Association of Petroleum Geologists, p.244-259.

HOLTER, M.E., 1977, The Oldman River lead-zinc occurrence, southwestern Alberta; Bulletin of Canadian Petroleum Geology, v.25(1), p.92-109.

HONJO, S., FISCHER, A.G., & GARRISON, R., 1965, Geopetal pyrite in fine-grained limestones; Journal of Sedimentary Petrology, v.35(2), p.480-488.

HÖY, T., & van der HEYDEN, P., 1988, Geochemistry, geochronology, and tectonic implications of two quartz monzonite intrusions, Purcell Mountains, southeastern British Columbia; Canadian Journal of Earth Sciences, v.25(1), p.106-115.

HUDSON, J.D., 1977, Stable isotopes and limestone lithification; Journal of the Geological Society of London, v.133, p.637-660.

ILLING, L.V., 1954, Bahaman calcareous sands; American Association of Petroleum Geologists Bulletin, v.38, p.1-95.

ILLING, L.V., 1959, Deposition and diagenesis of some Upper Paleozoic carbonate sediments in western Canada; Fifth World Petroleum Congress, New York, N.Y., Proceedings, section 1, p.23-52.

IRWIN, H., CURTIS, C., & COLEMAN, M., 1977, Isotopic evidence for source of diagenetic carbonates formed during burial of organic-rich sediments; Nature, v.269, p.209-213.

JODRY, R.L., 1969, Growth and dolomitization of Silurian reefs, St. Clair County, Michigan; American Association of Petroleum Geologists Bulletin, v.53(4), p.957-981.

JONES, R.M.P., 1980, Basinal isostatic adjustment faults and their petroleum significance; Bulletin of Canadian Petroleum Geology, v.28( ), p.211-251.

KATZ, A., 1971, Zoned dolomite crystals; Journal of Geology, v.79, p.38-51.

KENDALL, A.C., 1977, Origin of dolomite mottling in Ordovician limestones from Saskatchewan and Manitoba; Bulletin of Canadian Petroleum Geology, v.25(3), p.480-504.

KOBLUK, D.R., & KAHLE, C.F., 1978, Geologic significance of boring and cavity dwelling marine algae; Bulletin of Canadian Petroleum Geology, v.26(3), p.362-379.

KUTNEY, E., 1960, Palliser Formation; in HARGREAVES, G.E., HUNT, A.D., de WIT, R., & WORKMAN, L.E. (Eds.), Lexicon of geologic names in the Western Canada Sedimentary Basin and Arctic Archipelago; Alberta Society of Petroleum Geologists, Calgary, p.121-122.

LAND, L.S., 1973, Holocene meteoric dolomitization of Pleistocene limestones, North Jamaica; Sedimentology, v.20(3), p.411-424.

------, 1980, The isotopic and trace element geochemistry of dolomite: the state of the art; in ZENGER, D.H., DUNHAM, J.B., & ETHINGTON, R.L. (Eds.), Concepts and models of dolomitization; Society of Economic Paleontologists and Mineralogists Special Publication No. 28, p.87-110.

------, 1985, The origin of massive dolomite; Journal of Geological Education, v.33, p.112-125.

LEACH, D.L., & ROWAN, E.L., 1986, Genetic link between Ouachita foldbelt tectonism and the Mississippi Valley-type lead-zinc deposits of the Ozarks; Geology, v.14(11), p.931-935.

LESLIE, G.A., 1955, A comparison of the diagenetic and diagnostic features of the Sturgeon Lake, Normandville, and Clairmont reef complexes: Unpublished M. Sc. thesis, University of Alberta, Edmonton, 77 pp.

LETHIERS, F., 1981, Ostracodes du Dévonien terminal de l'ouest du Canada: Systématique, biostratigraphie et paléoécologie; Géobios, Mémoire Spécial 5, Lyon, 236 pp.

LOHMANN, K.C., & MEYERS, W.J., 1977, Microdolomite inclusions in cloudy prismatic calcites: a proposed criterion for former high-magnesian calcites; Journal of Sedimentary Petrology, v.47(3), p.1078-1088.

------, **& WALKER, J.C.G.,** 1984, Secular variations in $\delta^{13}C$ and $\delta^{18}O$ composition of Phanerozoic oceans; Geological Society of America Abstracts with Programs, v.16(6), p.578.

MACHEL, H.-G., 1986, Cathodoluminescence in calcite and dolomite and its chemical interpretation; Geoscience Canada, v.12(4), p.139-147.

------, **& MOUNTJOY, E.W.,** 1986, Chemistry and environments of dolomitization - a reappraisal; Earth-Science Reviews, v.23(3), p.175-222.

MACINTYRE, I.G., 1985, Submarine cements - The peloidal question; in SCHNEIDERMANN, N., & HARRIS, P.M. (Eds.), Carbonate cements; Society of Economic Paleontologists and Mineralogists Special Publication No. 36, p.109-116.

MACQUEEN, R.W., & SANDBERG, C.A., 1970, Stratigraphy, age, and interregional correlation of the Exshaw Formation, Alberta Rocky Mountains; Bulletin of Canadian Petroleum Geology, v.18(1), p.32-66.

MARSZALEK, D.S., 1975, Calcisphere ultrastructure and skeletal aragonite from the alga Acetabularia antillana; Journal of Sedimentary Petrology, v.45(1), p.266-271.

MATTES, B.W., & MOUNTJOY, E.W., 1980, Burial dolomitization of the Upper Devonian Miette buildup, Jasper National Park, Alberta; Society of Economic Paleontologists and Mineralogists Special Publication No. 28, p.259-297.

MAURIN, A.F., 1972, Laminites et stromatolites algaires du Famennien des Montagnes Rocheuse, Alberta; (Abstract) Twenty-fourth International Geological Congress, Montréal, section 7, p.586.

MAURIN, A.F, 1982, Famennian reefs in the Palliser of the Rocky Mountains (Alberta); (Abstract) International Association of Sedimentologists, Eleventh International Congress on Sedimentology, Hamilton, p.117-118.

McCLAY, K.R., & INSLEY, M.W., 1986, Duplex structures in the Lewis thrust sheet, Crowsnest Pass, Rocky Mountains, Alberta, Canada; Bulletin of Canadian Petroleum Geology, v.8(8), p.911-922.

McCROSSAN, R.G., & GLAISTER, R.P., 1964, (Eds.), Geologic history of western Canada; Alberta Society of Petroleum Geologists, Calgary, 232 pp.

McLAREN, D.J., 1955, Devonian formations in the Alberta Rocky Mountains between Bow and Athabasca Rivers; Geological Survey of Canada Bulletin 35, 59 pp.

------, **& MOUNTJOY, E.W.**, 1962, Alexo equivalents in the Jasper region, Alberta; Geological Survey of Canada Paper 62-23, 36 pp.

MEADOWS, P.S., & ANDERSON, J.S., 1975, Chemical and biotic differences between mud; (Abstract) Estuarine and Brackish Water Sciences Association Bulletin, No. 12, p.8.

MEYERS, W.J., 1974, Carbonate cement stratigraphy of the Lake Valley Formation (Mississippian) Sacremento Mountains, New Mexico; Journal of Sedimentary Petrology, v.44, p.837-861.

MORROW, D.W., 1978, Dolomitization of lower Paleozoic burrow-fillings; Journal of Sedimentary Petrology, v.48(1), p.295-306.

------, 1982a, Diagenesis 1. Dolomite - part 1: The chemistry of dolomitization and dolomite precipitation; Geoscience Canada, v.9(1), p.5-13.

------, 1982b, Diagenesis 1. Dolomite - part 2: Dolomitization models and ancient dolostones; Geoscience Canada, v.9(2), p.57-76.

MOUNTJOY, E.W., 1960, Structure and stratigraphy of the Miette and adjacent areas, eastern Jasper National Park, Alberta; Unpublished Ph.D. thesis, University of Toronto, Toronto, 249 pp.

------, 1965, Stratigraphy of the Devonian Miette reef complex and associated strata, eastern Jasper National Park, Alberta; Geological Survey of Canada Bulletin 110, 132 pp.

MOUNTJOY, E.W., 1967, Factors governing the development of the Frasnian Miette and Ancient Wall reef complexes (banks and biostromes), Alberta; in OSWALD, D.H. (Ed.), International Symposium on the Devonian System, Calgary; Alberta Society of Petroleum Geologists, part 2, p.387-408.

------, & GELDSETZER, H.H.J., 1981, Devonian stratigraphy and sedimentation, southern Rocky Mountains; in Guidebook 13, Geological Association of Canada, Mineralogical Association of Canada & Canadian Geophysical Union, Joint Annual Meeting, Calgary, p.195-224.

NISHIDA, D.K., 1987, A Famennian stromatoporoid patch reef in the Wabamun Group, west-central Alberta, Canada; in KRAUSE, F.F., & BURROWES, O.G. (Eds.), Devonian lithofacies and reservoir styles in Alberta, Second International Symposium on the Devonian System, Calgary; Canadian Society of Petroleum Geologists, p.63-72.

------, MURRAY, W., & STEARN, C.W., 1985, Stromatoporoid-algal facies hydrocarbon traps in the late Devonian (Famennian) Wabamun Group, north-central Alberta, Canada; (Abstract) American Association of Petroleum Geologists Bulletin, v.69(2), p.293.

NORRIS, D.K., 1958, Beehive Mountain, Alberta and British Columbia; Geological Survey of Canada Paper 58-5, 22 pp.

OLIVER, J., 1986, Fluids expelled tectonically from orogenic belts: their role in hydrocarbon migration and other geologic phenomena; Geology, v.14(2), p.99-102.

O'NEIL, J.R., CLAYTON, R.N., & MAYEDA, T.K., 1969, Oxygen isotope fractionation in divalent metal carbonates; Journal of Chemical Physics, v.51(12), p.5547-5558.

PATTERSON, R.J., & KINSMAN, D.J.J., 1981, Hydrologic framework of a sabkha along Arabian Gulf, American Association of Petroleum Geologists Bulletin, v.65(8), p.1457-1475.

------, & ------, 1982, Formation of diagenetic dolomite in coastal sabkha along Arabian (Persian) Gulf, American Association of Petroleum Geologists Bulletin, v.66(1), p.28-43.

PERKINS, R.D., 1985, Timing of syntaxial cement; (Abstract) American Association of Petroleum Geologists Bulletin, v.69(2), p.295.

POPP, B.N., ANDERSON, T.F., & SANDBERG, P.A., 1986, Brachiopods as indicators of original isotopic compositions in some Paleozoic limestones; Geological Society of America Bulletin, v.97(10), p.1262-1269.

RAASCH, G.O., 1987, Devonian Famennian faunal zones in western Canada and their chronostratigraphic significance; (Abstract) Subcommission on Devonian Stratigraphy Newsletter No. 3, p.7.

RADKE, B.M., & MATHIS, R.L., 1980, On the formation and occurrence of saddle dolomite; Journal of Sedimentary Petrology, v.50(4), p.1149-1168.

REESOR, J.E., 1973, Geology of the Lardeau map-area, east-half, British Columbia; Geological Survey of Canada Memoir 369, 129 pp.

RUPP, A., 1967, Origin, structure, and environmental significance of Recent and fossil calcispheres; (Abstract) Geological Society of America Special Paper 101, p.186.

SARTENAER, P., 1969, Late Upper Devonian (Famennian) rhynochellid brachiopods from western Canada; Geological Survey of Canada Bulletin 169, 269 pp.

SASS, E., & KATZ, A., 1982, The origin of platform dolomites: new evidence; American Journal of Science, v.282(8), p.1184-1213.

SCHMIDT, V., 1964, Facies, diagenesis, and related reservoir properties in the Gigas beds (Upper Jurassic), northwestern Germany; in PRAY, L.C., & MURRAY, R.C. (Eds.), Dolomitization and limestone diagenesis: a symposium; Society of Economic Paleontologists and Mineralogists Special Publication No. 13, p.124-168.

SHINN, E.A., 1968a, Practical significance of birdseye structures in carbonate rocks; Journal of Sedimentary Petrology, v.38(1), p.215-223.

------, 1968b, Selective dolomitization of Recent sedimentary structures; Journal of Sedimentary Petrology, v.38(2), p.612-616.

------, 1983, Birdseyes, fenestrae, shrinkage pores, and loferites: a reevaluation; Journal of Sedimentary Petrology, v.53(2), p.619-628.

------, & ROBBIN, D.M., 1983, Mechanical and chemical compaction in fine-grained shallow-water limestones; Journal of Sedimentary Petrology, v.53(2), p.595-618.

SONNENFELD, P., 1964, Famennian reefs in Alberta, Canada; (Abstract) American Association of Petroleum Geologists Bulletin, v.48(4), p.548.

SPRY, I.M., 1963, The Palliser Expedition; Macmillan, Toronto, 310 pp.

STEARN, C.W., 1987, Effect of the Frasnian-Famennian extinction event on the stromatoporoids; Geology, v.15(7), p.677-679.

------, **HALIM-DIHARDJA, M.K., & NISHIDA, D.K.**, 1987, An oil-producing stromatoporoid patch reef in the Famennian (Devonian) Wabamun Formation, Normandville field, Alberta; Palaios, v.2(6), p.560-570.

STEWART, D.O., 1960, Palliser Formation; in HARGREAVES, G.E., HUNT, A.D., de WIT, R., & WORKMAN, L.E. (Eds.), Lexicon of geologic names in the Western Canada Sedimentary Basin and Arctic Archipelago; Alberta Society of Petroleum Geologists, Calgary, p.265.

STOAKES, F.A., 1987, Fault controlled dolomitization of the Wabamun Group, Tangent field, Peace River Arch, Alberta; in KRAUSE, F.F., & BURROWES, O.G. (Eds.), Devonian lithofacies and reservoir styles in Alberta, Second International Symposium on the Devonian System, Calgary; Canadian Society of Petroleum Geologists, p.73-85.

STYAN, W., 1984, Jura Creek field trip - Palliser/Wabamun Formation; in RICHARDS, B., STYAN, W., & HARRISON, R., Paleozoic carbonate reservoir units and facies distribution; Canadian Society of Petroleum Geologists & Canadian Society of Exploration Geophysicists, field trip guidebook B-1, Exploration Update'84, Calgary, p.1-14.

SUTTERLIN, P.Q., 1958, Uppermost Devonian (post-Woodbend) studies in southern Alberta; Unpublished Ph.D. thesis, Northwestern University, Evanston, Illinois, 108 pp.

SWINCHATT, J.P., 1969, Algal boring: a possible depth indicator in carbonate rocks and sediments; Geological Society of America Bulletin, v.80(7), p.1391-1396.

TARUTANI, T., CLAYTON, R.N., & MAYEDA, T.K., 1969, The effect of polymorphism and magnesium substitution on oxygen isotope fractionation between calcium carbonate and water; Geochimica et Cosmochimica Acta, v.33(8), p.987-996.

TOOMEY, D.F., MOUNTJOY, E.W., & MacKENZIE, W.S., 1970, Upper Devonian (Frasnian) algae and foraminifera from the Ancient Wall carbonate complex, Jasper National Park, Alberta, Canada; Canadian Journal of Earth Sciences, v.7(3), p.946-981.

VEIZER, J., & HOEFS, J., 1976, The nature of $^{18}O/^{16}O$ and $^{13}C/^{12}C$ secular trends in sedimentary carbonate rocks; Geochimica et Cosmochimica Acta, v.40, p.1387-1395.

VIAU, C.A., & OLDERSHAW, A.E., 1984, Structural controls on sedimentation and dolomite cementation in the Swan Hills Formation, Swan Hills field, central Alberta; in ELIUK, L. (Ed.), Carbonates in subsurface and outcrop; Canadian Society of Petroleum Geologists Core Conference, Calgary, p.101-131.

VON MORLOTT, A., 1847, Über Dolomit und seine künstliche Darstellung aus Kalkstein; Naturwissenschaftliche Abhandlungen, gesammelt und durch Subscription hrsg. von Wilhelm Haidinger, v.1, p.305-315.

WALLACE, M.W., 1987, Sedimentology and diagenesis of Upper Devonian carbonates, Canning Basin, western Australia: Unpublished Ph.D. thesis, University of Tasmania, Australia, 172 pp.

WALLS, R.A., MOUNTJOY, E.W., & FRITZ, P., 1979, Isotopic composition and diagenetic history of carbonate cements in Devonian Golden Spike reef, Alberta, Canada; Geological Society of America Bulletin, part I, v.90(10), p.963-982.

WANLESS, H.R., 1979, Limestone response to stress: Pressure solution and dolomitization; Journal of Sedimentary Petrology, v.49(2), p.437-462.

WARREN, P.S., 1937, Age of the Exshaw shale in the Canadian Rockies; American Journal of Science, v.233, p.454-457.

------, & STELCK, C.R., 1950, Succession of Devonian faunas in western Canada; Transactions of the Royal Society of Canada, series 3, v.44(4), p.61-78.

WONFOR, J.S., & ANDRICHUK, J.M., 1956, The Wabamun Group in the Stettler area, Alberta; Journal of the Alberta Society of Petroleum Geologists, v.4(5), p.99-111.

WORKUM, R.H., 1978, Cripple Creek, and leeward Leduc reef margin; in McILREATH, I.A., & JACKSON, P.C. (Eds.), The Fairholme carbonate complex at Hummingbird and Cripple Creek; Canadian Society of Petroleum Geologists, Calgary, p.74-87.

WORONICK, R.E., & LAND, L.S., 1985, Late burial diagenesis, Lower Cretaceous Pearsall and lower Glen Rose Formations, South Texas; <u>in</u> SCHNEIDERMANN, N., & HARRIS, P.M. (Eds.), Carbonate cements; Society of Economic Paleontologists and Mineralogists Special Publication No. 36, p.265-275.

APPENDIX ONE

The control of dolomitization by sedimentary structures.

There are numerous Recent and ancient examples of dolomite localized in burrows and other 'sedimentary structures' described. Ancient examples are summarized by order of their chronological appearance in the literature, followed by some studies on Recent sediments.

Van Tuyl (1916), in his classic paper, "The origin of dolomite", described dolomitic mottling "apparently following fucoid markings in the limestone" from the Lower Ordovician (Canadian Series) Tribes Hill Formation in New York State. Fisher (1954) also studied the Tribes Hill and described extensive, dolomitized fucoidal mottling which he attributed to penecontemporaneous dolomitization by magnesium-enriched sea water. He suggested that the magnesium came from the decomposition of seaweed, giving rise to conditions that locally favoured dolomitization.

Older studies often used the term fucoid to refer to the remains of marine algae or other plants. The term's meaning has evolved to identify trace fossils and now is loosely used to mean "any indefinite tunnel-like sedimentary structure identified as a trace fossil" (Gary <u>et al.</u> 1972), that is, a burrow. In photographs (especially Plates XX, XXI and XXII from Van Tuyl 1916), the Tribes Hill "fucoids" strongly resemble dolomite-filled burrows. In their study of the Tribes Hill Formation in New York, Braun and Friedman (1969) described dolomitic mottling and suggested that the dolomite followed burrows and trails in the mudstones. They further suggested that these biogenic traces may have provided more permeable pathways for dolomitizing fluids.

Griffin (1942) described dolomitic mottling from the Middle Ordovician (Champlainian Series) Platteville limestone of Minnesota. The mottling formed anastomosing "pipe-like"structures and "tongue-like extensions" from shaly partings. Griffin (1942) suggested that connate, magnesiumbearing brines caused dolomitization of the sediment "between the time of its lithification and that of jointing". Byers and Stasko (1978) studied the McGregor member of the Platteville Formation in Wisconsin. They concluded that dolomitization was controlled by the distribution of burrows, particularly Chondrites, due to a permeability difference between these burrows and the host rock. Dathe's (1983) work on the Platteville Group of northern Illinois described similar features and suggested that the permeability difference persisted until "late diagenetic, [dolomitizing] fluids" could exploit it. The Platteville's mottling was first reported by Leonard (1905) from outcrops in Iowa.

Fox (1951 and 1954) related a personal communication from R. de Wit in which it is suggested that dolomite bodies in the Upper Devonian Palliser Formation might be related to pre-lithification movement of fluids through zones of greater permeability formed by "algal colonies".

Beales (1953 and 1956) also studied the micrite- and peloid-rich Palliser Formation, and compared its depositional environment with that of the present-day Bahama Bank sediments. Beales (1953) expanded on the ideas of de Wit (in Fox 1951) and attributed the conspicuous dolomitic mottling to localization of dolomitizing fluids along zones of "effective diffusion porosity". The dolomitization spread from these more permeable "bedding laminae" and "worm burrows" to other parts of the rock. The magnesium was supplied by diffusion downward from the overlying sea water into the more permeable sediments soon after deposition. Beales (1953) also suggested that the presence of organic matter in the burrows may have encouraged the selective dolomitization.

Another peloidal carbonate, the Ordovician Camp Nelson Limestone of Kentucky, was studied by Fisher (1970), who concluded, similarly to Beales (1953), that the conspicuous mottling present in this unit represented the dolomitization of permeable burrow-fillings during early diagenesis.

Shourd and Levin (1976) studied the Ordovician upper Plattin subgroup of eastern Missouri (Van Tuyl 1916, also briefly discussed mottling in the Plattin). This unit is described as a non-porous biomicrite which they interpreted to have accumulated in an "offshore, level bottom environment". They noted Chondrites burrows filled with a light brown, fine grained dolomite. No timing relationships were suggested.

In a study of the limestones in the Ordovician Yeoman and lower Red River formations of Saskatchewan and Manitoba, Kendall (1977) noted the control of dolomitization by burrows and bedding planes and concluded that this did not necessarily imply penecontemporaneity of formation. He suggested that the dolomitization was related to the permeability contrasts between burrows and their host sediments, but this difference may have been preserved, or even enhanced, by early diagenetic processes.

The upper Ordovician Irene Bay - Thumb Mountain formations in the Canadian Arctic Archipelago is a sequence of medium- to thick-bedded fossiliferous and pelletal wackestones deposited in a shelf lagoon. Dolomite is localized in burrows, giving rise to a mottled fabric. Morrow (1978) recognized different stages of dolomitization. The earliest dolomitization resulted from magnesium flux from overlying sea water into the burrows which were presumably more permeable than the surrounding micrite.

Morrow (1978) interpreted the burrow-filling dolomite as having originated as penecontemporaneous "micron-sized seed nuclei" crystals which acted as loci for continued dolomite growth during "late diagenesis", perhaps aided by the release of magnesium from organic matter and/or clay minerals contained in the burrows. Progressive growth stages of dolomite are preserved in the burrows. These stages range from idiotopic (sensu Friedman 1965) fabrics where the dolomite contains 3 to 4.5 mole% excess $CaCO_3$ with preserved intercrystalline calcite mud to xenotopic (sensu Friedman 1965) dolomite containing 0 to

3 mole% excess $CaCO_3$ with no lime mud. The idiotopic, more calcian dolomite represents an earlier stage of dolomite growth (on the "seed nuclei"). As growth proceeded from more and more dilute solutions, the newly formed dolomites became increasingly more stoichiometric and larger in size. This led to the development of dolomite with a xenotopic fabric and lower strontium and sodium values.

Morrow (1978) cited chemical data to support early (penecontemporaneous), micron-sized dolomitization by sea water with lowered salinities and relatively low magnesium/calcium ratios. The lowered salinity may have resulted from seasonal increases in the amount of runoff from rain water, causing freshening, in a wet, tropical climate similar to that of Florida Bay. The supportive chemical data from the early dolomites are: high bulk strontium contents of about 150 ppm and sodium contents of 200 to 1000 ppm. Modern marine-derived dolomites contain 500 to 1000 ppm strontium (Morrow 1978) and 1010 to 3050 ppm of sodium (Land and Hoops 1973).

Morrow (1978) found that his burrow-dolomite was relatively enriched in strontium over associated calcite, suggesting that the dolomite has retained some marine-derived strontium. In addition, the sodium contents of his dolomites decrease with increasing crystal size and stoichiometry, perhaps indicating progressive loss with continued growth during late diagenesis.

Morrow (1978) noted that the bioturbated sediment between burrows should have contained "impurities", such as organics and/or clays, just as he postulates for the well-defined burrows (see above), and therefore should have also undergone at least partial dolomitization. However, there is no matrix dolomitization in the Irene Bay - Thumb Mountain sequence. The Palliser Formation, on the other hand, does contain matrix dolomite (early planar, section 3.2.1.1) and clays, and may lend support to the idea that such impurities may help promote somewhat later diagenetic dolomitization (at least in the Palliser).

In addition, using Morrow's (1978) model, it might be expected that a greater degree of dolomitization would have taken place towards the tops of the burrows since the source of magnesium was the overlying sea water. Morrow (1978) did not report this texture from his study area. However, in at least two Palliser localities (Hummingbird Creek and Crowsnest Pass sections), burrows that coarsen towards their tops were noted. This is essentially a geopetal texture, and the facing directions were corroborated by geopetal sediment in-fillings in shells. This coarsening seems to support a downward moving source of dolomitizing fluids. This coarsening is a relatively rare feature as most burrow dolomite shows no systematic variation in crystallinity.

Morrow (1978, p.304) suggested that the porosity difference between the burrows and the host sediment is the most important factor in controlling the distribution of the dolomitization, but he evidently meant that the permeability contrast exerts the major influence. Morrow (1978) estimated figures of 60% porosity for the pre-dolomitization burrow-fill and 20% for the surrounding "stiff lime mud". This 20% figure would be too low for an uncemented mud as Shinn and Robbin (1983) gave figures of 65 to 75% porosity for recent carbonate sediments (mudstones and wackestones). They conducted compaction experiments on subtidal muds and found a reduction in porosity of only 30% after a 50% thickness reduction. Clearly, a lime mud at the sea floor, having undergone little or no compaction, should have much more than 20% porosity. Submarine cementation may quickly reduce the porosity of lime muds although Morrow (1978) made no mention of submarine cementation, hardgrounds or similar features. However, this does not seriously affect this model as permeability differences between a mud and a relatively coarse-grained burrow back-fill should be quite large, regardless of initial porosities.

Delgado (1980) studied the Ordovician Galena Group in the Mississippi Valley. He found finely crystalline dolomite filling burrows at hardground surfaces. Abrasion of dolomite crystals in burrows by scouring and of crystals at the edges of intraclasts suggests that dolomitization occurred on the sea floor. In his brief study of the Galena in Iowa, Van Tuyl (1916) suggested that the mottling was of the "inorganic type", i.e., not related to the presence of fucoids (or burrows).

Shinn (1968) suggested that permeability controls the distribution of Recent dolomitization in the intertidal and supratidal zones of the Florida Keys. Sand-sized fillings in desiccation cracks are preferentially dolomitized over the surrounding, relatively impermeable mud polygons.

Brown and Farrow (1978) described nodules (predominantly dolomite) forming around thalassinidean (crustacean) burrows in the Recent sediments of Loch Sunart, off the west coast of Scotland. These concretions form in modern clastic muds at temperate latitudes in waters of 50 to 70 m depth (subtidal). This is a good example of dolomite, associated with burrows, forming at the sea floor as there has been virtually no burial of these modern concretions. Brown and Farrow (1978) suggested that dolomitization had been aided by the presence of disseminated organic matter in the concretions. Meadows and Anderson (1975), cited in Brown and Farrow (1978), found that sulfate-reducing bacteria were more concentrated around burrows than in the surrounding mud. Brown and Farrow (1978) suggested that this could cause alkalinities to rise high enough to promote dolomitization in and around the burrows. The initial deposition of calcium carbonate (later dolomitized) is also aided by the rise in alkalinity. After enough calcium ions are removed from the water, dolomite will begin to form, with sea water as the source of magnesium. Perhaps burrows can act as micro-environments favourable to the formation of dolomite.

REFERENCES

BEALES, F.W., 1953, Dolomitic mottling in Palliser (Devonian) limestone, Banff and Jasper National Parks, Alberta; American Association of Petroleum Geologists Bulletin, v.37(10), p.2281-2293.

------, 1956, Conditions of deposition of Palliser (Devonian) limestone of southwestern Alberta; American Association of Petroleum Geologists Bulletin, v.40(5), p.848-870.

BRAUN, M., & FRIEDMAN, G.M., 1969, Carbonate lithofacies and environments of the Tribes Hill Formation (Lower Ordovician) of the Mohawk Valley, New York; Journal of Sedimentary Petrology, v.39(1), p.113-135.

BROWN, B.J., & FARROW, G.E., 1978, Recent dolomitic concretions of crustacean burrow origin from Loch Sunart, west coast of Scotland; Journal of Sedimentary Petrology, v.48(3), p.825-834.

BYERS, C.W., & STASKO, L.E., 1978, Trace fossils and sedimentologic interpretation - McGregor Member of Platteville Formation (Ordovician) of Wisconsin; Journal of Sedimentary Petrology, v.48(4), p.1303-1310.

DATHE, D.B., 1983, The origin of mottled dolomitic limestones in the Platteville Group (Ordovician) of northern Illinois; Geological Society of America Abstracts with Programs, v.15(4), p.255.

DELGADO, D.J., 1980, Submarine diagenesis (aragonite dissolution, cementation by calcite, and dolomitization) in Ordovician Galena Group, upper Mississippi Valley; (Abstract) American Association of Petroleum Geologists Bulletin, v.64(5), p.697.

EKDALE, A.A., BROMLEY, R.G., & PEMBERTON, S.G., 1984, Ichnology - Trace fossils in sedimentology and stratigraphy; Society of Economic Paleontologists and Mineralogists Short Course No. 15, 317 pp.

FISHER, D.W., 1954, Lower Ordovician (Canadian) stratigraphy of the Mohawk Valley, New York; Geological Society of America Bulletin, v.65(1), p.71-96.

FISHER, I.S., 1970, Origin of small irregular dolomite bodies in the pelletal Camp Nelson Limestone (Ordovician) of central Kentucky; Southeastern Geology, v.12(2), p.115-120.

FOX, F.G., 1951, Devonian stratigraphy of Rocky Mountains and Foothills between Crowsnest Pass and Athabaska River, Alberta, Canada; American Association of Petroleum Geologists Bulletin, v.35(4), p.822-843.

------, 1954, Devonian stratigraphy of Rocky Mountains and Foothills between Crowsnest Pass and Athabaska River, Alberta, Canada; in CLARK, L.M. (Ed.), Western Canada Sedimentary Basin: a symposium; American Association of Petroleum Geologists, p.109-130.

FRIEDMAN, G.M., 1965, Terminology of crystallization textures and fabrics in sedimentary rocks; Journal of Sedimentary Petrology, v.35(3), p.643-655.

GARY, M., McAFEE Jr., R., & WOLF, C.L., 1972, (Eds.), Glossary of geology; American Geological Institute, Washington, 905 pp.

GRIFFIN, R.H., 1942, Dolomitic mottling in the Platteville limestone; Journal of Sedimentary Petrology, v.12(2), p.67-76.

KENDALL, A.C., 1977, Origin of dolomite mottling in Ordovician limestones from Saskatchewan and Manitoba; Bulletin of Canadian Petroleum Geology, v.25(3), p.480-504.

LEONARD, A.G., 1905, Geology of Clayton County; Iowa Geological Survey, v.XIV, p.213-318.

MEADOWS, P.S., & ANDERSON, J.S., 1975, Chemical and biotic differences between mud; (Abstract) Estuarine and Brackish Water Sciences Association Bulletin, No. 12, p.8.

MORROW, D.W., 1978, Dolomitization of lower Paleozoic burrow-fillings; Journal of Sedimentary Petrology, v.48(1), p.295-306.

SHINN, E.A., 1968, Selective dolomitization of Recent sedimentary structures; Journal of Sedimentary Petrology, v. 38(2), p.612-616.

------, & ROBBIN, D.M., 1983, Mechanical and chemical compaction in fine-grained shallow-water limestones; Journal of Sedimentary Petrology, v.53(2), p.595-618.

SHOURD, M.L., & LEVIN, H.L., 1976, Chondrites in the upper Plattin subgroup (middle Ordovician) of eastern Missouri; Journal of Paleontology, v.50(2), p.260-268.

VAN TUYL, F.M., 1916, The origin of dolomite; Iowa Geological Survey, v.XXV, p.251-421.

APPENDIX TWO
Geochemistry

Staining

All thin sections and hand samples were stained following the method suggested by Dickson (1966). Samples were partially immersed in a mixture of alizarin red-S and potassium ferricyanide dissolved in a dilute hydrochloric acid solution (0.5 to 2.5%) for 30 to 120 seconds. Alizarin red-S principally distinguishes calcite from dolomite while potassium ferricyanide detects the presence of sufficient amounts of ferrous iron in the carbonates (Dickson 1966). Dickson (1966) suggested that greater than 1% $FeCO_3$ in solid solution with $CaCO_3$ will be detected. Although no estimate of the lower limit of detectability of iron in dolomite was made, Dickson (1966) pointed out that for a given acidity of the staining solution, dolomite will be less reactive than calcite, suggesting that dolomite will only stain at higher concentrations of Fe^{2+}.

Cathodoluminescence

Cathodoluminescence (CL) is the emission of light by minerals excited by a beam of electrons. Since Smith and Stenstrom (1965) published their results, CL has become commonplace in sedimentologic and diagenetic studies.

The following discussion is summarized from Machel's (1986) review paper. Carbonate mineral luminescence usually results from trace or minor elements present within the crystal lattice in solid solution. Certain elements act as activators while others act as sensitizers or quenchers. Electrons in the outer shells of activator elements absorb energy during electron bombardment and release it in the form of light (luminescence). Sensitizer elements similarly absorb energy but then transmit some or all of it to an activator element, thereby increasing the activator's response to excitation. A sensitizer may or may not be an activator as well. Quenchers are elements which dampen or eliminate luminescence by absorbing the available excitation energy without luminescing themselves.

Numerous workers (e.g., Smith and Stenstrom 1965; Meyers 1974; Pierson 1981; Amieux 1982; Machel 1986; Mason 1987) have long recognized that Mn^{2+} is the main activator and Fe^{2+} is the main quencher of luminescence in calcite and dolomite. However, Machel (1986) pointed out that these are not the only important elements to be considered. On the basis of data collected from many sources, Machel (1986) indicated that, for calcite and dolomite, the main activators are; Mn^{2+}, Pb^{2+}, several rare earth elements (REE), Cu^{2+}, Zn^{2+}, Ag^{+}, Bi^{+}, and possibly Mg^{2+}. The main sensitizers are; Pb^{2+}, Ce^{2+}, Ce^{4+}, and several REE. The main quenchers are; Fe^{2+}, Ni^{2+}, and Co^{2+}.

CL Operating Conditions

All CL observations were made on a Nuclide Corporation Luminoscope model ELM-2B (with a cold cathode-type gun) mounted on a Zeiss binocular microscope. The beam energy was 14 to 16 kilovolts and the beam current was 0.8 to 1.0 milliamperes under a vacuum pressure of 60 to 150 millitorrs (either helium or residual gas). A Pentax K1000 35mm camera body was mounted on the microscope for photography. Kodak Recording Film 2475 (ASA 1000) was used for black and white prints, Kodak VR1000 (ASA 1000) for colour prints, and Kodak Professional Slide Film (ASA 1600/3200) for colour slides. Correct exposure times ranged from 20 to 120 seconds, depending on the brightness of the luminescence and the ASA of the film. The reporting of the operating conditions follows the suggestions of Marshall (1978).

Stable Carbon and Oxygen Isotopes

Both carbon and oxygen have more than one naturally occurring stable (non-radioactive) isotope. Carbon has two stable isotopes, one with 12 (^{12}C) and one with 13 (^{13}C)

neutrons in its nucleus (along with 12 protons in each case). Oxygen has three stable isotopes; ^{16}O, ^{17}O, and ^{18}O, all with 16 protons. The ratio of these isotopes can be measured, allowing for comparison among various naturally occurring substances. The ratios used are $^{13}C/^{12}C$ and $^{18}O/^{16}O$ which are reported relative to a standard. The 'δ' (delta) value is the relative difference in the ratios between a sample and the standard, expressed as parts per thousand or per mil. Positive δ values indicate a sample with a ratio greater than the standard and <u>vice versa</u> for a negative value. The more negative a δ value, the greater the proportion of the light (^{16}O or ^{12}C) isotope in the sample.

Anderson and Arthur (1983) listed the international standards most commonly used to report results. For carbon and oxygen, it is a Cretaceous belemnite from the Peedee Formation of South Carolina, called the PDB standard. There is also a standard based on the isotopic composition of a hypothetical average modern sea water called Standard Mean Ocean Water (SMOW) which is often used as a reference point from which to measure ancient or modified modern water compositions.

In this study, all carbon and oxygen isotope results from rock component analyses are expressed as δ values, in parts per thousand (per mil), and relative to the PDB standard.

Carbon and oxygen isotopes can be used to help identify or trace the depositional and diagenetic conditions that a carbonate phase has experienced. Most physical and chemical processes will fractionate the various isotopes in a predictable manner.

Isotopic compositions can be affected by numerous processes. For example, evaporation will fractionate the lighter isotopes into the gaseous phase, leaving the fluid with more positive (a greater proportion of the heavier isotope) δ values. An increase in the temperature of precipitation (e.g., with burial) will lead to more negative δ values in the carbonate phase, at least with respect to oxygen ($\delta^{18}O$), as carbon ($\delta^{13}C$) is not highly affected by temperature. The subsurface mixing of different fluids will alter the evolution of their isotopic compositions.

Even the precipitation of mineral species (e.g., carbonates) will preferentially remove the heavier isotope species. The carbonate should be more positive (heavier) than the fluid. However, biologic and/or disequilibrium effects may complicate this process. Anderson and Arthur (1983) suggested that; (1) the isotopic composition of the fluid, (2) the temperature, and (3) the rate of precipitation are the leading factors influencing the actual isotopic of carbonate phases. For instance, high rates of precipitation can lead to disequilibrium values which differ from those predicted by consideration of fluid composition and temperature only. Gonzalez and Lohmann (1985) discussed biologic and kinetic fractionation and suggested that both cause isotopic disequilibrium compositions which are not as heavy as those expected under equilibrium conditions.

Problems related to associating isotopic signatures with specific processes or environments are further complicated by the probability that the precipitating fluid (ocean water or subsurface brine) had a SMOW value different from that of today's ocean (defined as zero), so modern analogues must be used with caution.

From a study of Holocene reefal components, Gonzalez and Lohmann (1985) have suggested that marine cements be used to determine the original marine isotopic composition as they show the heaviest oxygen values and therefore were less fractionated than other components. Popp _et al._ (1986) suggested that the non-luminescent portions of low-magnesium calcite (LMC) brachiopods have undergone little diagenetic alteration and are therefore the best indicators of original isotopic compositions in limestone. Popp _et al._ (1986) also suggested that because modern brachiopods precipitate their shells at or near isotopic equilibrium, it is not unreasonable to assume that many (but maybe not all) ancient forms did likewise. Al-Aasm and Veizer (1982) studied the distribution of Na and Mg in LMC brachiopods and also suggested that these components have undergone relatively little (<20%) diagenetic alteration.

The oxygen isotope fractionation between carbonates and water is in part temperature dependent. Attempts have been made to use this relationship to determine temperatures of crystallization of various phases. Unfortunately, the effects of a change in the isotopic composition of the fluid may be indistinguishable from a simple temperature increase.

Land (1980, 1985) suggested that dolomite and calcite co-precipitating in equilibrium will fractionate isotopes differently. The δ^{18}Oxygen of dolomite will be 3 to 6 per mil (PDB) heavier at 25°C, plus 0.8 per mil for a further fractionation effect during acid treatment to liberate CO_2 for analysis, giving values heavier by 4 to 7 per mil. However, very few if any proven examples of co-precipitated dolomite-calcite pairs have been demonstrated to exist (Land 1980).

Carbon and oxygen isotope analyses were performed at the University of Michigan. Powdered samples weighing 0.3 to 0.5 mg were taken from polished rock slabs using drill bits with diameters of 20 to 500 μm. To remove organic matter, samples were roasted in a vacuum at 380°C for 10 minutes (calcite) or 60 minutes (dolomite). The samples were then reacted in anhydrous phosphoric acid at 55°C in a vessel connected to an on-line gas-extraction system and a VG 602E Micromass ratio mass spectrometer. The results were converted to PDB and corrected for ^{17}O using the method of Craig (1957). The powdered calcite standard NBS-20 was run for calibration. Precision was maintained at better than 0.1 per mil.

TABLE A2-1
STABLE ISOTOPE ANALYSES RESULTS, BY SECTION

SECTION NAME	SAMPLE NUMBER	DESCRIPTION	$\delta^{18}O$ (per mil,PDB)	$\delta^{13}C$ (per mil,PDB)
OLDMAN	1	FRACTURE-FILL CALCITE	-12.6	-3.5
RIVER	3	WHITE SPARRY DOLOMITE (F)	-14.9	0.0
(OLD)	7A	WHITE SPARRY DOLOMITE (F)	-11.7	-0.7
	7B	FRACTURE-FILL CALCITE	-13.0	-3.2
	8A	R Np DOLOMITE (F)	-11.5	-0.6
*	8B	WHITE SPARRY DOLOMITE (F)	-18.2	-2.6
	9A	W SPARRY DOLOMITE (F, CG)	-14.9	-0.3
	9B	W SPARRY DOLOMITE (F, FG)	-13.3	-0.6
	10A	R Np DOLOMITE (F)	-11.7	-1.1
	10B	WHITE SPARRY DOLOMITE (F)	-11.6	-0.9
	10C	FRACTURE-FILL CALCITE	-11.5	-1.7
	22A	EARLY PLANAR DOLOMITE	-6.1	+0.4
	22B	EARLY PLANAR DOLOMITE	-6.6	+0.2
CROWSNEST	10A	EARLY PLANAR DOLOMITE	-3.4	+0.5
PASS (CN)	10B	MICRITE (Cc, CONTAMINATED)	-6.2	-0.1
MUNROE-	13A	SOLN VOID-FILL CALCITE	-8.6	-0.4
ALPINE-	13B	WHITE SPARRY DOLOMITE (Ls)	-7.2	-1.0
BOIVIN	19A	WHITE SPARRY DOLOMITE	-9.3	+0.2
(MAB)	19B	R Np DOLOMITE (DARK GREY)	-10.0	-0.6
	20A	WHITE SPARRY DOLOMITE	-14.5	+0.4
	20B	R Np DOLOMITE (GREY)	-13.9	-0.9
	20C	R Np DOLOMITE (DARK BROWN)	-13.2	+0.2
*	21A	WHITE SPARRY DOLOMITE	-11.5	-14.1
	21B	R Np DOLOMITE (BLACK)	-10.4	+0.6
	21C	R Np DOLOMITE (DARK GREY)	-11.3	+0.6
*	22	WHITE SPARRY DOLOMITE	-11.4	-15.2
LATER	34A	FRAC CALCITE (With SULPHUR)	-18.4	-0.2
EARLIER	34B	FRAC CALC (Without SULPHUR)	-16.7	-0.8
	39	WHITE SPARRY DOLOMITE	-9.3	-1.3
	40A	R Np DOLOMITE (GREY)	-14.1	-0.1
	40B	R Np DOLOMITE (BLACK)	-12.7	-0.1

TABLE A2-1, continued

SECTION NAME	SAMPLE NUMBER	DESCRIPTION	$\delta^{18}O$ (per mil,PDB)	$\delta^{13}C$ (per mil,PDB)
HUMMINGBIRD	8	BRACHIOPOD SHELL (CALCITE)	-8.4	+0.3
CREEK (HC)	10A	EARLY PLANAR DOLOMITE	-6.3	+0.1
	10B	E P DOLOMITE (CONTAMINATED)	-7.0	-0.6
	12	WHITE SPARRY DOLOMITE (Ls)	-5.2	-0.7
	17	WHITE SPARRY DOLOMITE (Ls)	-5.8	+1.4
	21A	MICRITE (CALCITE)	-8.1	+1.4
	21B	BLOCKY MOSAIC Cc (FENESTRA)	-6.8	+0.8
	21C	WHITE STYLO-CALCITE	-7.0	+0.8
	21D	WHITE STYLO-CALCITE	-13.9	+1.1
	33A	EARLY PLANAR DOLOMITE	-5.9	+1.1
	33B	MICRITE (CALCITE)	-7.8	+0.7
	36	FRACTURE-FILL CALCITE	-18.3	-0.8
	41A	FRACTURE-FILL CALCITE	-19.7	-2.1
**	41B	MICRITE (CALCITE)	-12.5	-1.1
	44A	EARLY PLANAR DOLOMITE	-3.7	+0.0
	44B	EARLY PLANAR DOLOMITE	-3.9	-0.1
	44C	SOLN VOID-FILL CALCITE	-7.6	-3.2
	45A	BRACHIOPOD SHELL (CALCITE)	-7.2	+1.3
	45B	BRACHIOPOD SHELL (CALCITE)	-7.9	+1.1
	46	EARLY PLANAR DOLOMITE	-4.6	+0.3
	50	FRACTURE-FILL CALCITE	-19.5	-2.1

Abbreviations used in Table A2-1

AVE - average; BRACH - brachiopod shell; Cc - calcite; CG - coarse grained; F - ferroan; FG - fine grained; Ls - in limestones; SOLN - solution; STYLO - stylolite; W - white.

E P - early planar dolomite.
R Np - replacive nonplanar dolomite.
*, ** - analyses that are not included in group statistics, shown in Tables 4 and 5.

TABLE A2-2
X-RAY FLUORESCENCE RESULTS

Samp #	SiO_2	Al_2O_3	P_2O_5	TiO_2	Fe_2O_3	CaO	SrO	MgO	Na_2O	K_2O	SO_3	BaO	MnO	Zn	L.O.I.	TOTAL
CN 10	1.48	0.44	0.01	0.02	0.13	31.29	74	19.34	<0.01	0.05	0.03	37	0.01	46	47.21	99.99
HC 33	1.02	0.26	0.01	0.02	0.10	32.01	79	19.29	<0.01	0.01	0.01	<10	0.01	59	47.29	100.04
HC 44	1.55	0.35	0.01	0.02	0.15	31.03	159	19.51	<0.01	0.11	0.04	39	0.01	31	47.36	100.16
MAB 45	0.61	0.24	0.02	0.02	0.11	30.63	73	20.77	<0.01	0.07	<0.01	12	0.03	23	47.39	99.97
OLD 2	0.60	0.19	0.01	0.01	1.41	30.75	74	19.89	<0.01	0.04	0.10	20	0.15	11	46.56	99.71
OLD 7	5.22	0.66	0.02	0.05	3.16	28.77	118	18.43	<0.01	0.38	1.23	<10	0.17	3279	41.34	99.77
OLD 1	<0.01	0.13	0.01	<0.01	0.03	55.79	554	0.33	<0.01	<0.01	0.02	21	0.02	<10	43.80	100.19

	mol%Ca	Ca/Mg	
CN 10	53.76	1.162	(early planar dolomite)
HC 33	54.39	1.193	(early planar dolomite)
HC 44	53.34	1.143	(early planar dolomite)
MAB 45	51.46	1.060	(replacive nonplanar dolomite)
OLD 2	52.63	1.111	(white sparry dolomite)
OLD 7	52.80	1.112	(white sparry dolomite)
OLD 1			(fracture-filling calcite)

Note: Detection limit for major elements is 0.01%, for others, it is 10 ppm.
All Analyses done on fused beads prepared from ignited samples.
All the iron present in a sample has been recalculated as Fe_2O_3.

References

AL-AASM, I.S., & VEIZER, J., 1982, Chemical stabilization of low-Mg calcite: an example of brachiopods; Journal of Sedimentary Petrology, v.52(4), p.1101-1109.

AMIEUX, P., 1982, La cathodoluminescence: méthode d'étude sédimentologique des carbonates; Bulletin des Centres de Récherches Exploration-Production Elf-Aquitaine, v.6(2), p.437-483.

ANDERSON, T.F., & ARTHUR, M.A., 1983, Stable isotopes of oxygen and carbon and their applications to sedimentologic and paleoenvironmental problems; in ARTHUR, M.A. (Ed.), Stable isotopes in sedimentary geology; Society of Economic Paleontologists and Mineralogists Short Course No. 10, p.1-1 - 1-151.

DICKSON, J.A.D., 1966, Carbonate identification and genesis as revealed by staining; Journal of Sedimentary Petrology, v.36(2), p.491-505.

GONZALEZ, L.A., & LOHMANN, K.C., 1985, Carbon and oxygen isotopic composition of Holocene reefal carbonates; Geology, v.13(11), p.811-814.

LAND, L.S., 1980, The isotopic and trace element geochemistry of dolomite: the state of the art; in ZENGER, D.H., DUNHAM, J.B., & ETHINGTON, R.L. (Eds.), Concepts and models of dolomitization; Society of Economic Paleontologists and Mineralogists Special Publication No. 28, p.87-110.

------, 1985, The origin of massive dolomite; Journal of Geological Education, v.33, p.112-125.

MACHEL, H.-G., 1986, Cathodoluminescence in calcite and dolomite and its chemical interpretation; Geoscience Canada, v.12(4), p.139-147.

MARSHALL, D.J., 1978, Suggested standards for the reporting of cathodoluminescence results; Journal of Sedimentary Petrology, v.48(2), p.651-653.

MASON, R.A., 1987, Ion microprobe analysis of trace elements in calcite with an application to the cathodoluminescence zonation of limestone cements from the Lower Carboniferous of South Wales, U.K.; Chemical Geology, v.64, p.209-224.

PIERSON, B.J., 1981, The control of cathodoluminescence in dolomite by iron and manganese; Sedimentology, v.28, p.601-610.

POPP, B.N., ANDERSON, T.F., & SANDBERG, P.A., 1986, Brachiopods as indicators of original isotopic compositions in some Paleozoic limestones; Geological Society of America Bulletin, v.97(10), p.1262-1269.

SMITH, J.V., & STENSTROM, R.C., 1965, Electron-excited luminescence as a petrologic tool; Journal of Geology, v.73, p.627-635.

APPENDIX THREE

Table A3-1 contains the names and locations of the twenty-seven stratigraphic sections plotted in Figure 2 (Chapter One). Sections sampled by Esso Minerals Canada (#1-23) are indicated by 'EMC'. 'NTS' are the National Topographic System map numbers. 'UTM' are the Universal Transverse Mercator map coordinates (easting and northing).

Figures A3-1, A3-2, and A3-3 are columnar representations of three sections measured by the author. These sections are plotted at a scale of 1000 : 1.

Table A3-2 contains thin section descriptions of samples from the twenty-three EMC sections, listed in double columns. The numbers on each line refer to the distance, in metres, above the base or below the top of the exposed Palliser Formation, and are based on sampling and measurements by Esso field parties. Allochems are listed in their order of abundance.

TABLE A3-1
Names and Locations of EMC Sections

SECTION NUMBER	SECTION NAME	NTS	UTM EASTING	UTM NORTHING
79 EMC 01	WHITEMAN GAP	82 O 03	611400	5658400
79 EMC 02	LODER PEAK	82 O 03	630080	5661000
79 EMC 03	MT. HEAD	82 J 07	666650	5591100
79 EMC 04	MT. FARQUHAR	82 J 02	661800	5564500
79 EMC 05	LOST CREEK	82 J 02	662500	5562200
79 EMC 06	OLDMAN RIVER	82 J 02	663000	5554800
79 EMC 07	MT. LYALL	82 J 02	665200	5552000
79 EMC 08	CACHE CREEK	82 J 02	668500	5544000
79 EMC 09	MT. ERRIS	82 G 15	667700	5528800
79 EMC 10	RACEHORSE	82 G 15	671000	5519000
79 EMC 11	CROWSNEST PASS	82 G 10	670400	5499800
79 EMC 12	MT. COULTHARD	82 G 10	676000	5491400
79 EMC 13	PEECHEE	82 G 07	675000	5483000
79 EMC 14	MT. DARRAH	82 G 07	674000	5478500
79 EMC 15	MT. BORSATO	82 G 07	675000	5474500
79 EMC 16	FLATHEAD	82 G 07	675600	5464600
79 EMC 17	CHINA WALL	82 G 06	644000	5459450
79 EMC 18	THREE SISTERS	82 G 11	635000	5493600
79 EMC 19	MT. FRAYN	82 G 11	635000	5493600
79 EMC 20	PHILLIPS PEAK	82 G 14	640800	5538500
80 EMC 21	SPRAY LAKES	82 J 14	618200	5649200
80 EMC 22	BULL RIVER	82 G 06	617800	5480000
79 EMC 23	WARDNER	82 G 06	614600	5473400
# 24	MUNROE-ALPINE-BOIVIN	82 J 03	637800	5547000
# 25	MT. INDEFATIGABLE	82 J 11	630200	5612200
# 26	MT. MURRAY	82 J 14	621500	5623600
# 27	HUMMINGBIRD CREEK	83 C 01	552700	5769500

Symbols for Figures A3-1 to A3-3

∇ - brachiopod
- burrow
¤ - calcisphere
▲ - chert
CG - coated grain
CI - covered interval
☆ - echinoderm fragment
fos - fossil
frag - fragment
gast - gastropod
INTBD - interbedded

= - laminated
≈ - laminated, wavy
lt - light
med - medium
- ostracod
pel - peloid
Q - quartz silt
∼ - shell
- stromatoporoid
weath - weathering

Figure A3-1: CROWSNEST PASS (#11)

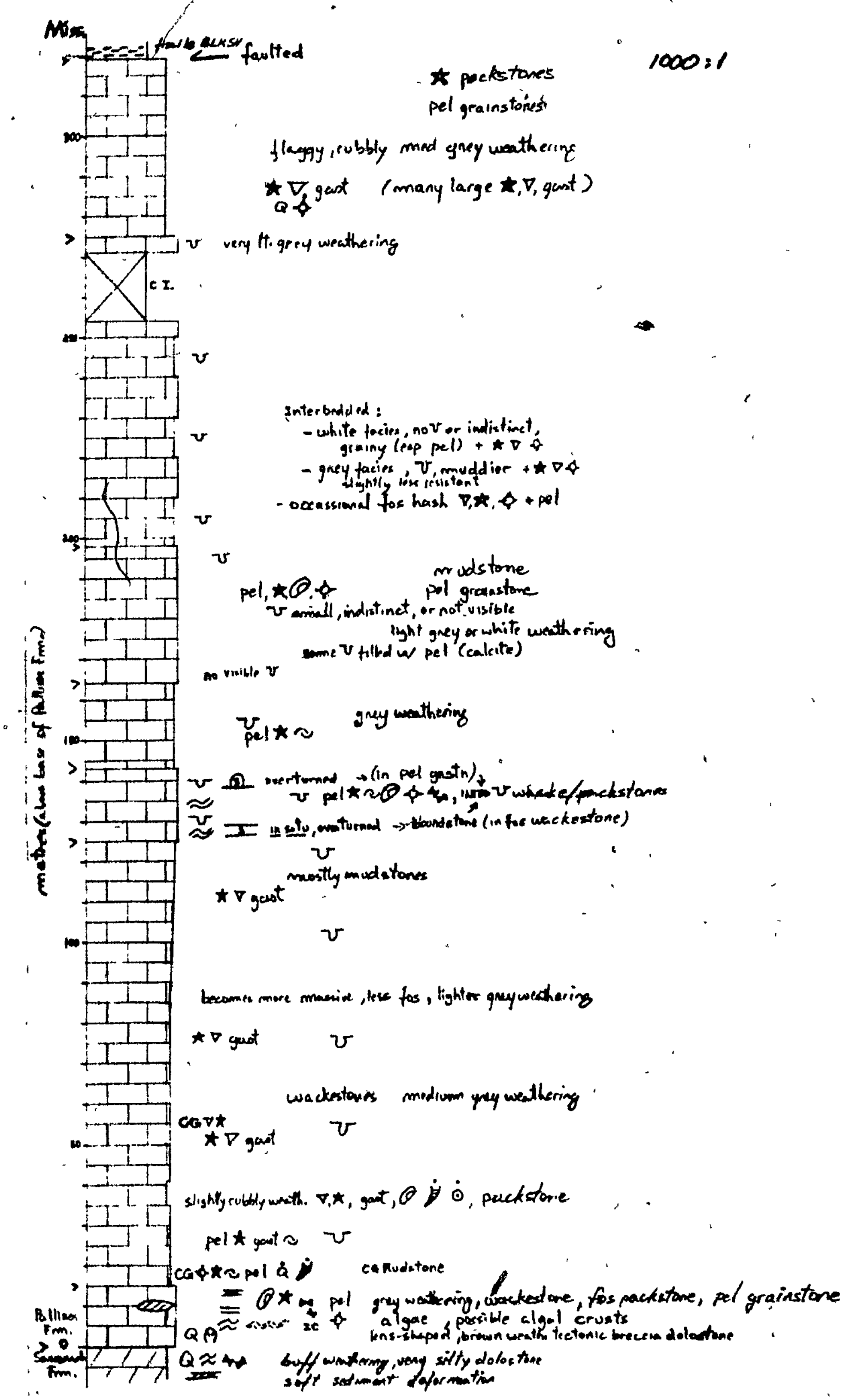

Figure A3-2: Mt. INDEFATIGABLE (#25)

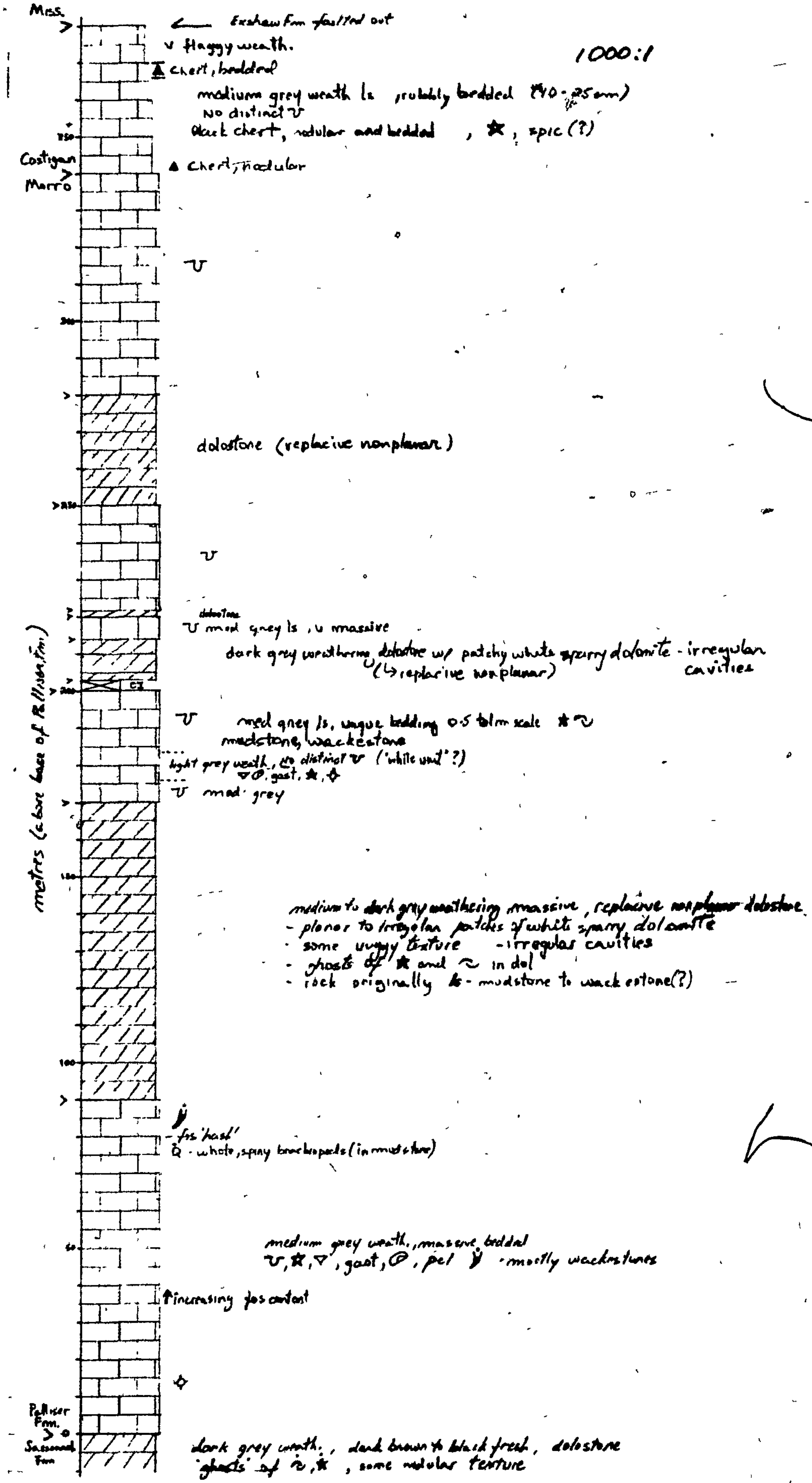

5

Figure A3-3: HUMMINGBIRD CREEK (#27)

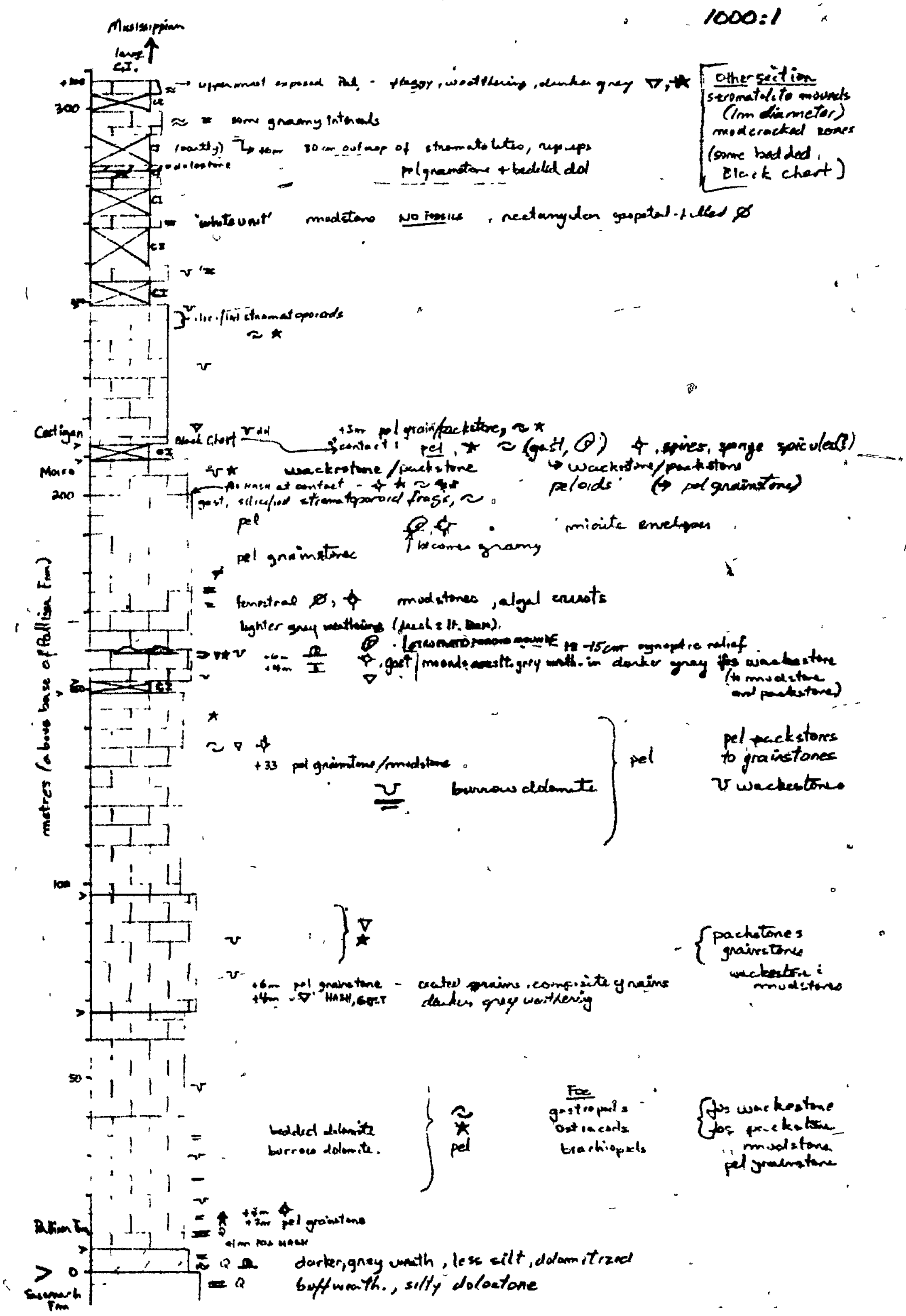

TABLE A3-2
Thin Section Descriptions from EMC Sections

Symbols

A - algae; ▼ - brachiopod shell; B - bryozoan;
C - calcisphere; ▲ - chert; E - echinoderm;
f - foraminiferid; F - fossil fragment; G - gastropod;
I - intraclast; O - ostracod; P - peloid; Q - quartz silt;
S - shell; SP - spine or spicule; $ - stromatoporoid.

WHITEMAN GAP (01)

EXSHAW		
224	packstone	E P O ▼
208	mudstone	P E O
168	wackestone	E P O
160	wackestone	E P C
136	mudstone	E
112	mudstone	E ▼
88	packstone	P E O
64	wackestone	E S G
48	grainstone	P E O
40	packstone	E P SP G ▼
16	wackestone	E P
ALEXO		

LODER PEAK (02)

EXSHAW		
128	grainstone	P I E S
120	grainstone	P E
112	grainstone	P I E S
104	wackestone	P E
96	wackestone	E P S O
88	wackestone	P E S
80	packstone	P E I
72	grainstone	P
64	mudstone	E
48	packstone	P I E S C
32	grainstone	P I C S
24	wackestone	E P O
8	wackestone	P E O
4	wackestone	E P S
ALEXO		

MOUNT HEAD (03)

EXSHAW		
4	grainstone	P E
8	dolostone	Q
16	dolostone	
19	evaporites	
21	evaporites	
23	evaporites	
26	mudstone	Q
32	grainstone	P
40	wackestone	P E
48	grainstone	P I
56	mudstone	P E
64	dolostone	
72	wackestone	P E S
80	wackestone	E P O C
≈≈≈≈≈≈≈≈≈≈≈≈≈≈≈≈≈≈≈≈		
THRUST		

MOUNT FARQUHAR (04)

EXSHAW

4	grainstone	P E
8	wackestone	E S
16	wackestone	E S
24	wackestone	E SP
32	wackestone	E
40	packstone	E P S
48	wackestone	E P O S
56	wackestone	E
64	wackestone	E P S
72	wackestone	E P
80	packstone	E P S
88	wackestone	E P O Q
96	packstone	E P O
104	grainstone	P E I
112	wackestone	P E
120	mudstone	E C
125	wackestone	P E

≈≈≈≈≈≈≈≈≈≈≈≈≈≈≈≈≈≈≈≈≈≈≈≈≈≈≈≈≈≈

THRUST

LOST CREEK (05)

EXSHAW

56	wackestone	E P SP
48	packstone	E S
40	wackestone	E P SP
32	packstone	E O S SP
24	packstone	E
16	wackestone	E S
8	wackestone	E S
4	packstone	E P I

≈≈≈≈≈≈≈≈≈≈≈≈≈≈≈≈≈≈≈≈≈≈≈≈≈≈≈≈≈≈

THRUST

OLDMAN RIVER (06)

EXSHAW

176	wackestone	E P
168	wackestone	E
160	mudstone	
152	wackestone	E P
144	mudstone	E
136	wackestone	E ▼ G P
128	mudstone	E P
120	mudstone	E
112	mudstone	E
104	mudstone	E S
96	mudstone	E S
88	wackestone	E P
80	grainstone	P E C
72	wackestone	P E
64	grainstone	P E C
56	wackestone	E P
48	packstone	E P
40	packstone	E P
32	wackestone	E S P
24	packstone	E S
16	packstone	P E SP
8	packstone	E S B SP
4	packstone	E P SP

≈≈≈≈≈≈≈≈≈≈≈≈≈≈≈≈≈≈≈≈≈≈≈≈≈≈≈≈≈≈

THRUST

MOUNT LYALL (07)

EXSHAW

4	packstone	E ▼ S
8	wackestone	E S Q
16	wackestone	E S SP Q
24	packstone	E O SP
32	packstone	E SP O G
40	packstone	E P SP O G
48	wackestone	S ▼ O E G
56	packstone	E P C
64	grainstone	P I E
72	mudstone	C
80	mudstone	E
88	mudstone	E
96	mudstone	E
104	wackestone	E
112	mudstone	E P S
120	mudstone	C
128	wackestone	G E

THRUST

CACHE CREEK (08)

EXSHAW

4	packstone	E
8	mudstone	
16	wackestone	E
24	wackestone	E SP
32	wackestone	E S
40	wackestone	E S
48	wackestone	E S
56	wackestone	P E
64	mudstone	
72	grainstone	P E I
80	grainstone	P E I

THRUST

MOUNT ERRIS (09)

EXSHAW

4	wackestone	P E
8	wackestone	E P
16	wackestone	E P O S
24	wackestone	E
32	packstone	P E
40	packstone	P E

THRUST

RACEHORSE (10)

EXSHAW

4	wackestone	E O
8	packstone	E S
16	packstone	E S P
24	packstone	E S P Q
32	grainstone	P C S *f*
40	wackestone	E P
48	wackestone	E P S
56	wackestone	E P
64	grainstone	P I E S C
72	wackestone	P E C
80	mudstone	
88	wackestone	E S
96	wackestone	E S
104	wackestone	E P C
112	mudstone	E Q
120	mudstone	
128	mudstone	▼
136	mudstone	▼ P
144	mudstone	E ▼
152	wackestone	E P
160	wackestone	E P
168	wackestone	E P
176	wackestone	E P S
184	wackestone	E P G O
192	wackestone	P E
200	packstone	P E
208	grainstone	P E I

THRUST

CROWSNEST PASS (11)

EXSHAW

323	wackestone	E S
319	packstone	E P S
312	wackestone	E P S
304	wackestone	E S P
296	wackestone	E P S
280	packstone	P E S
272	grainstone	P E I
264	grainstone	P I E
256	mudstone	▼
248	mudstone	F
240	mudstone	E P O
232	wackestone	E S P
224	grainstone	P I E S
216	packstone	P E I S
208	packstone	P E I C
200	grainstone	P S E I
192	grainstone	P E O
184	mudstone	P E
176	mudstone	P
168	wackestone	E P S
160	wackestone	E P
152	mudstone	
144	packstone	E P I S
136	mudstone	P E
128	mudstone	S
120	wackestone	S E
112	wackestone	E
104	wackestone	E S P
96	wackestone	E P G
88	packstone	E P
80	packstone	P E
72	grainstone	P E O I
64	packstone	E P I S
56	packstone	E P I S
48	packstone	E P
40	packstone	E P G S
32	packstone	E P G O
24	grainstone	P C
16	grainstone	P C
8	grainstone	P C
4	grainstone	P I C

SASSENACH

MOUNT COULTHARD (12)

EXSHAW

4	dolostone	E
8	wackestone	E S
16	packstone	E P
24	wackestone	E P
32	grainstone	P E
40	grainstone	P E S
48	grainstone	P E S I
56	mudstone	P E
64	mudstone	
72	mudstone	
80	mudstone	
88	packstone	P E O
96	mudstone	P
104	mudstone	
112	packstone	P E O
120	packstone	P E
128	packstone	P E C O
136	packstone	P E C O
140	packstone	PE S C

ALEXO

PEECHEE (13)

EXSHAW

4	wackestone	E
16	packstone	E ▼ O
32	grainstone	P E
56	mudstone	E
72	packstone	E S
88	grainstone	P
96	grainstone	P S
112	dolostone	
136	packstone	E S
160	grainstone	P E A
184	packstone	E P ▼

ALEXO

MOUNT DARRAH (14)		
EXSHAW		
14	packstone	E P S G
24	packstone	E P O G
32	dolostone	S
40	wackestone	E S Q
48	wackestone	E S Q
56	grainstone	P E I
64	packstone	P E I
72	mudstone	P E
80	mudstone	
88	packstone	P E I C
96	grainstone	P E I G C
104	grainstone	P E I $
112	grainstone	P E I $
120	wackestone	P E $
128	mudstone	
136	wackestone	E P
144	mudstone	P
152	grainstone	P E I
160	wackestone	E
168	dolostone	
176	dolostone	
184	wackestone	E P S
192	packstone	P E S C
200	packstone	E P S
208	wackestone	P E
216	wackestone	E S
224	packstone	E O
ALEXO		

MOUNT BORSATO (15)		
EXSHAW		
4	packstone	E S G
8	wackestone	E
16	wackestone	E
24	packstone	E P
32	packstone	E P
40	wackestone	E S
48	packstone	P E
56	grainstone	P E I
64	grainstone	P E I
72	wackestone	E P
80	wackestone	P E
88	wackestone	E
96	wackestone	E P
104	mudstone	P
112	wackestone	E P
120	mudstone	E
128	mudstone	E
136	mudstone	E S
144	wackestone	E S
152	wackestone	E P
160	wackestone	E S
168	wackestone	E P S
176	wackestone	E P
184	wackestone	E P S
192	packstone	P E S G C
200	wackestone	E S
204	wackestone	E S O
ALEXO		

FLATHEAD (16)		
EXSHAW		
4	packstone	E P S
8	packstone	E P S O
16	packstone	E P S G
24	grainstone	P E I C
32	grainstone	P E I C
40	grainstone	P E I C
48	grainstone	P E S
56	grainstone	P E
64	grainstone	P E
72	grainstone	P I F C $
80	wackestone	E P S $
88	mudstone	E
96	wackestone	E S O P
104	wackestone	E P I O
112	wackestone	E P I C
128	packstone	P E
136	packstone	E P I O Q
144	packstone	P E O Q
ALEXO		

CHINA WALL (17)		
EXSHAW		
0	wackestone	E O Q
12	mudstone	E Q
16	mudstone	E S Q
24	packstone	E
32	packstone	E
40	packstone	E S
48	wackestone	E O
56	packstone	E P
64	packstone	P E S
72	grainstone	P I E S
80	mudstone	E S
88	mudstone	E S
96	mudstone	E
104	packstone	P I E
112	wackestone	E S I P
120	grainstone	P E I
128	grainstone	P E S
136	packstone	P E S O
144	mudstone	E
152	grainstone	P E I S
160	wackestone	P E
168	packstone	P E
176	packstone	P E O
184	grainstone	P E O C
192	packstone	P E I S
200	wackestone	E P S
208	packstone	E G O I
216	wackestone	E G O P
224	packstone	E O
232	packstone	E O
240	packstone	E P O
248	packstone	P E S C
256	grainstone	P I E
ALEXO		

THREE SISTERS (18)

EXSHAW		
4	grainstone	E SP P
8	grainstone	E SP P
16	grainstone	E Q
24	chert	
32	mudstone	Q F
40	mudstone	Q
48	mudstone	P F
61	mudstone	
64	mudstone	
86	mudstone	E F
104	mudstone	O C
112	mudstone	C E
120	mudstone	C
128	mudstone	C
136	mudstone	
144	mudstone	C
152	mudstone	Q
160	mudstone	P C
168	mudstone	
176	mudstone	C
184	mudstone	
192	mudstone	C
200	mudstone	C
208	mudstone	C
216	mudstone	P C S
224	mudstone	C
232	mudstone	C
240	mudstone	C
248	mudstone	C
256	mudstone	F
264	mudstone	
272	mudstone	C
ALEXO		

MOUNT FRAYN (19)

EXSHAW		
4	mudstone	
16	mudstone	F
32	wackestone	E Q
48	mudstone	
64	mudstone	E Q
80	mudstone	S
96	mudstone	E
104	mudstone	
144	grainstone	P E ▼
160	mudstone	E
176	mudstone	E
192	mudstone	F
208	mudstone	
224	mudstone	F
248	mudstone	
256	mudstone	E
272	mudstone	
288	mudstone	
304	mudstone	
336	grainstone	P E
352	mudstone	E
368	mudstone	
384	mudstone	E
408	wackestone	E
424	mudstone	E
440	mudstone	E
448	mudstone	S
BASE HIDDEN		

PHILLIPS PEAK (20)		
EXSHAW		
8	mudstone	SP Q
12	mudstone	SP
22	mudstone	SP
30	mudstone	
38	grainstone	E
46	mudstone	E S
54	packstone	E S Q
62	wackestone	E SP Q
70	packstone	E S
78	wackestone	E SP
93	mudstone	E
101	mudstone	
109	mudstone	E
117	mudstone	
125	mudstone	E
133	grainstone	P E
141	grainstone	P E O
157	mudstone	E O
165	mudstone	E
173	wackestone	E I
181	grainstone	P E
213	dolostone	
221	dolostone	
229	mudstone	E
245	mudstone	E
253	mudstone	E
261	mudstone	E O
256	mudstone	E
293	packstone	E O
301	wackestone	E O
309	packstone	E F
317	mudstone	E S Q
325	grainstone	P Q
333	packstone	P E S
341	wackestone	E S
349	grainstone	P E S Q
357	mudstone	E S
365	grainstone	P
373	mudstone	E
397	mudstone	P E S
405	wackestone	P E
≈≈≈≈≈≈≈≈≈≈≈≈≈≈≈≈≈≈≈≈≈≈≈≈≈≈≈≈		
THRUST		

SPRAY LAKES (21)		
EXSHAW		
263	packstone	E SP O S
240	packstone	P E
236	wackestone	E S
216	wackestone	E S
210	grainstone	P E
198	mudstone	
192	mudstone	E
184	mudstone	E
177	mudstone	E
169	wackestone	E S
163	packstone	E P O S
158	wackestone	E P S
154	wackestone	E G
148	mudstone	E O G
143	wackestone	E S P
137	wackestone	E P O
131	wackestone?	E P O
125	mudstone	E
120	mudstone	E
113	mudstone	E
111	wackestone	E P S
105	wackestone	P E S
100	wackestone	E P S
96	wackestone	E P
91	grainstone	P I E C
86	mudstone	O E SP
81	mudstone	E
77	mudstone	E
72	wackestone	E P SP S
68	wackestone	P E O
63	wackestone	P E O
59	wackestone	E P O ▼
54?	wackestone	E P S
49	grainstone	P E I S
40	packstone	E P O
33	wackestone	E S
31	grainstone	E P O
27	wackestone	E S
22	wackestone	E O P
17	wackestone	E S
13	wackestone	E S G SP
8	dolostone	
5	grainstone	P I E S
2	wackestone	P E S
ALEXO?		

BULL RIVER (22)

UNKNOWN CONTACT

217	mudstone	C? Q
208	mudstone	C? Q
189	mudstone	C? Q S
183	mudstone	Q
177	mudstone	Q
171	mudstone	Q F
165	mudstone	F Q
159	mudstone	Q F
153	mudstone	Q
147	wackestone	E S
140	mudstone	E S
130	mudstone	S F
118	mudstone	Q
106	packstone	SP C
94	mudstone	F Q
87	mudstone	F
81	mudstone	F
75	mudstone	F Q
69	mudstone	F Q
63	mudstone	F Q
57	mudstone	F
51	packstone	P E
45	wackestone	F E P
40	wackestone	E F ▲
34	mudstone	F
27	wackestone	E S
17	mudstone	E F
9	mudstone	E F S
0	mudstone	F E

UNKNOWN CONTACT

WARDNER (23)

UNKNOWN CONTACT

88	mudstone	Q
80	mudstone	Q E
72	mudstone	E S P Q
64	packstone	P E O S
56	packstone	P E S
48	packstone	P E S
40	packstone	P E O G
32	packstone	E G O
24	wackestone	E S
16	wackestone	O E
8	mudstone	E
0	dolostone	

UNKNOWN CONTACT